Title
Improving Saccharomyces cerevisiae as a biofuel production organism

Author
Davis Lopez, Stephanie Anne

Publication Date
2015

Peer reviewed|Thesis/dissertation

Improving *Saccharomyces cerevisiae* as a biofuel production organism

By

Stephanie Anne Davis López

A dissertation submitted in partial satisfaction of the

requirements for the degree of

Doctor of Philosophy

in

Chemistry

in the

Graduate Division

of the

University of California, Berkeley

Committee in charge:

Professor Danielle Tullman Ercek, Co-Chair
Professor David Savage, Co-Chair
Professor John Dueber
Professor Jamie Cate

Fall 2015

ABSTRACT

Improving *Saccharomyces cerevisiae* as a biofuel production organism

by

Stephanie Anne Davis López

Doctor of Philosophy in Chemistry

University of California, Berkeley

Professor Danielle Tullman-Ercek, Co-Chair
Professor David Savage, Co-Chair

It is widely accepted that using petroleum-based fuels and chemicals is unsustainable, both in terms of their limited supply and hazardous greenhouse gas emissions. One alternative is to replace petroleum-derived liquid fuels such as gasoline with biofuels. Biofuels are energy-dense compounds such as medium-chain alcohols or fatty acids produced by microbes from plant-based feedstocks. Replacing fossil fuels with biofuels will have multiple beneficial impacts on the environment and economy, including carbon sequestration, greenhouse gas reduction, and generation of a renewable industry.

Here, we engineer the model yeast *Saccharomyces cerevisiae* to enhance its potential for biofuel production. Yeast are promising host organisms for many reasons. A sophisticated genetic toolkit is available, which allows for simple manipulation of metabolic pathways and strain characteristics. Industrial fermentations are well-established: *S. cerevisiae* are currently used to produce a variety of compounds, including bioethanol, amino acids, and therapeutics. In order for yeasts to become commercially viable production organisms for a range of biofuels, some challenges, need to be overcome, from limited production to product toxicity. Here, we used protein engineering methods to address some of these challenges and improve *S. cerevisiae* as a production organism.

It is important to consider transport at the commodity scales relevant to fuel production. Biofuel efflux is particularly important because it drives production forward, reduces cellular toxicity, and is necessary for continuous process schemes. We therefore set out to understand how medium chain fatty acids exit the cell. We characterized the transporter Tpo1 for activity on the fatty acids octanoic and decanoic acid, and identified two fatty acid substrate binding residues. Moreover, we showed that the native promoter gives the optimal expression level for fatty acid efflux. We also found that localization to the plasma membrane is sufficient for fatty acid tolerance and vacuolar localization is not necessary. We anticipate that this transporter will make an excellent target for increasing efflux of desired non-native substrates such as butanol.

We also investigated the use of transporters to improve cytoplasmic acetyl-Coenzyme A A(AcCoA) levels. As many heterologous bioproducts are constructed from AcCoA by cytosolic enzymes, increasing cytoplasmic AcCoA concentrations should improve product titers. Our long-term goal is to use the AcCoA transporters AT-1 and YBR220C to transport AcCoA directly from the mitochondria into the cytoplasm. To this end, we found that the AT-1 transporter is active in yeast and draws AcCoA into the endoplasmic reticulum. We have designed a suite of mitochondrial targeting tags to direct the transporters to the mitochondria, and are currently testing their effectiveness. We anticipate that the mitochondrially-located transporters will raise cytoplasmic AcCoA levels, and concomitantly improve product titers.

Finally, to address potential issues from product toxicity, we explored the cellular effects of medium-chain alcohols on *S. cerevisiae*, and used protein engineering to reduce a toxicity response. Specifically, we found that medium chain alcohols, including *n*-pentanol, *n*-hexanol, and *n*-heptanol, inhibit translation initiation. Two mutations in translation initiation factors, Gcd1 D85E and Sui2 D77Y, both reduce inhibition of translation initiation, producing a stable, dominant medium chain alcohol tolerance phenotype. Interestingly, a range of mutations at positions 85 in Gcd1 and 77 in Sui2 improve medium chain alcohol tolerance. These findings will be important for generating efficient medium-chain alcohol production strains.

Through these projects, we have advanced the potential of *S. cerevisiae* for commodity-scale biofuel production.

TABLE OF CONTENTS

Chapter 1
Improving *S. cerevisiae* as a biofuel production organism

Yeast and Biofuels

Climate change and pollution are global issues and scientists world-wide are working on solutions. Fossil fuels are not a sustainable energy source, due to pollution from use, production of greenhouse gases, and limited global supply [1]. Dependence on fluctuating oil market prices and politics of producer nations are risks for national energy security [1-2]. Future population increases will increase energy demands, necessitating alternative energy sources [3]. Biofuels are one solution to these problems [1]. The use of biofuels can reduce greenhouse gases [5] and sequester carbon [4]. Additionally, biofuel usage is a way to invest in US technologies [5] and create new local industries [6]. Kopetz finds that biofuels can be used for up to a quarter of world energy [2]. In short, biofuels are promising new technologies that will become an important part of world energy usage.

There are many different molecules that can be produced in cells and used as biofuels. One example is alcohols, which have been well studied. Ethanol is commonly added to the fuel sold at gas stations, but it is corrosive and has a low energy density [7]. The major selling point to ethanol is its high production level, up to 18% v/v [8], which is more than 140 g/L. A medium-chain alcohol such as *n*-butanol has a much higher energy density, 22% more than ethanol, and is much less corrosive [9]. It can be added to gasoline directly and used with good results in cars on the road today. *n*-Butanol can be produced in *E. coli* at yields of 30 g/L using the *Clostridium* pathway [10]**.** Si *et al.* can produce 242 mg/L *n*-butanol in *S. cerevisiae* using Adh1 and an amino-acid dependent pathway [11]. These yields are still far below ethanol yields, and butanol is not currently a cost-effective fuel additive or stand-alone biofuel. Longer-chain alcohols such as *n*-pentanol and *n*-hexanol have even higher energy densities and are expected to be a next-generation biofuel. *n*-Pentanol can be produced in *E. coli* at 750 mg/L [12]; *n*-hexanol has been produced at 47 mg/L (along with 5 g/L butanol) [13]. While microbial production of medium-chain alcohols has been demonstrated, significant improvements are required before commercialization could be feasible.

Outside of alcohols, several other classes of potential biofuel molecules are being explored. One type is fatty acids, which can be chemically converted to fatty acid methyl esters (FAME) or fatty acid ethyl esters (FAEE) [9]. *Synechocysitis* can produce 197 mg/L fatty acids [14]. *E. coli* can even directly produce FAEE [15]. Terpenoids, such as farnesene, are also promising biofuel molecules. [16] Unsaturation (such as the multiple carbon-carbon double bonds in farnesene) is undesirable in fuels, but chemical conversion can improve fuel properties [10]. A variety of other terpenoids including limonene can be produced in cyanobacteria [17] or *E. coli* [18]. Even alkanes such as nonane and dodecane can be produced in cells [19]. The range of potential biofuels may be overwhelming, but this range makes it very likely that at least one compound can be produced at a cost-effective level.

For biofuels to replace petroleum as the major fuel source, many issues need to be addressed, through a combination of engineering the feedstocks, production pathways, production strains, and extraction processes. To keep costs low, high biofuel

titers and efficient extraction processes are required. Additionally, there is a need for biofuels that can be produced from marginal lands, to avoid competing with food supplies [2]. From the chassis side, the major roadblock to bioproduction of fuels is toxicity of the fuel molecules.

Many alcohol compounds have both general and specific toxic effects in the cell. For instance, membrane fluidity and corresponding function are affected by butanol [21]. Alcohols permeabilize cell membranes, which can deplete proton gradients and disrupt gradients of ions and other small molecules [22-24]. Ethanol can cause diffusion of water across the yeast membrane and inhibit active transport of water [25]. The terpenes ß-pinene and limonene have been shown to inhibit H^+ and K^+ translocation and respiration in yeast [26-27], likely due to membrane effects. In addition, solvents increase denaturant sensitivity and decrease thermotolerance of proteins, with effects proportional to carbon chain length [28]. These solvents can also specifically inhibit protein function. For example, *n*-butanol has been shown to inhibit the ATPase of *Clostridium acetobutylicum* [21] and more recently, *n*-butanol and *n*-hexanol were found to inhibit the multidrug resistance pump Pdr5 in yeast [29]. Understanding these effects is the first step toward engineering solutions to improve tolerance.

Biofuels can be produced in a variety of different organisms, each with advantages and disadvantages. *E. coli* are easy to engineer due to genetic tractability and a rapid doubling time. One major disadvantage of bacteria is susceptibility to phage infections, which seriously disrupt fermentations [30]. *Clostridia* naturally produce butanol and ethanol, though these organisms have limited genetic tools and are also susceptible to phage [30]. Cyanobacteria and algae are promising organisms, as they use carbon dioxide as a carbon source, eliminating the need for sugar or cellulosic feedstocks [20]. Inefficient growth and processing systems and somewhat limited genetic tools are holding back cyanobacterias and algae from becoming a feasible biofuels solution [20]. Yeasts such as *S. cerevisiae* are an excellent production organism, with sophisticated genetic toolkits and well-established industrial fermentation strategies. Longer doubling times and more complicated biology have delayed successes in engineering *S. cerevisaie* for biofuel production relative to *E. coli*, but these organisms are nonetheless most likely to produce the world's biofuels in the future.

S. cerevisiae can produce a variety of compounds, including commodity chemicals such as amino acids and lactic acid, and specialty compounds such as insulin and hydrocortisone [31-33]. In terms of biofuels, yeast are best known for ethanol production, with up to 2 M intracellular ethanol at the end of fermentations [33]. *S. cerevisiae* produces other biofuels such as farnesol [35], *n*-butanol [11, 36], and isobutanol [37]. Higher alcohol production in yeast is lagging behind *E. coli* production [38]. Even though *S. cerevisiae* has a higher *n*-butanol tolerance than *E. coli* (approximately 2% vs. 1% maximal concentration), toxicity is nonetheless preventing higher production levels in the yeast. With some metabolic and chassis engineering, this low yields and toxicity can be overcome.

In order for yeasts to become the preferred production organism, some challenges need to be addressed. Most importantly, low yields of biofuels are problematic, as low cost is important for commodity chemicals such as biofuels. The lower yields in *S. cerevisiae* are largely due to the toxicity from feedstock impurities [39], metabolic intermediates [40-41] and end-products [21-29] that inhibit cell growth and production

titers. In addition, metabolic flux is hindered by other processes and pathways in the cell. A metabolic sink is needed to enable increased yields even for nontoxic fuels, by driving reactions forward. Secretion to the extracellular space is desirable, as it simplifies extraction and allows for continuous processing while simultaneously providing a route to enhanced tolerance.

There are several strategies for improving tolerance to potential biofuels such as *n*-butanol and *n*-hexanol. One solution is to re-engineer the membrane for biofuel tolerance, since membrane toxicity is a limiting factor for biofuel production. Another method is to engineer transporters to directly remove biofuels from the cell, thereby reducing toxic concentrations and allowing for higher production. Finally, evolutions allow the cell to overcome specific mechanisms of toxicity, many of which are as yet unknown. Used alone or in conjunction, these approaches can reduce toxicity of biofuel molecules and improve yeasts as production organisms.

The Plasma Membrane

The plasma membrane and organelle membranes are an important part of yeast physiology. Nicalaou *et al.* note that in recent years, there has been widespread interest in increasing tolerance to fuel products by changing membrane composition [42]. As the interface and exchange site between the cell and the environment, the membrane often limits growth rates [43]. In the presence of toxic alcohols, membrane disruptions further limit growth rates. Concomitantly, changes in the membrane can affect activity or function of transporters in the membrane [27], which are required for cell health and proliferation. Understanding the plasma membrane's role in both transporter function and biofuel toxicity will be a crucial step for engineering the most effective transporters and optimizing biofuel tolerance.

The plasma membrane has been studied extensively, and many of the lessons learned are directly applicable to organellar membranes as well. Cyclohexane and ß-pinene have been shown to disrupt mitochondrial membranes [26,44]. It is known that the sterol composition of the plasma membrane is important for thermotolerance [45]. As higher temperatures increase membrane fluidity, increased sterol concentrations help to stabilize the membrane, so that it can function properly. The membrane is also affected by alcohols, which can easily enter and remain in the membrane. There, the alcohols can increase both fluidity [46] and permeability [22], which disrupts membrane function. Huffer *et al.* observed that *S. cerevisiae* maintain membrane fluidity even in toxic alcohol concentrations [46]. Surprisingly, lipid composition and rigidity do not directly correlate to alcohol tolerance [46]. While it is clear that membrane composition and properties are important, scientists have yet to deconvolute how membrane changes lead to tolerance (or lack thereof). In addition to membrane changes in response to alcohols, the cell wall increases in hydrophobicity when yeasts were subjected to hydrophobic solvents [47].

Transporters Drive the Efflux of Biofuels and Direct Precursors

A key problem of biofuel production in yeast is the undesirable retention of the fuel product within the cell. Most classes of biofuels, from alcohols to long-chain hydrocarbons, are toxic at industrially relevant levels. The exception seems to be terpenoids such as farnesene [16], which are produced at high titers. Notably, farnesene is secreted at high levels as well. Therefore, it is expected that active mechanisms for the secretion of fuel products from the cell can improve or solve a host of problems, including product toxicity, creating a metabolic sink, and allowing for continuous processing of extracellular fuels.

Yeasts have evolved a variety of secretion devices to expel compounds from the cytoplasm. Multidrug resistance efflux pumps are a major class of devices that actively secrete unwanted chemicals to the extracellular space (48). ABC (ATP Binding Cassette) transporters such as Pdr5 are well characterized, yet have the disadvantage of high basal activity, regardless of substrate availability. The PDR (Pleiotropic Drug Resistance) pumps are major ATP users; when inhibited, cellular ATP levels will increase [49]. Use of these pumps would direct significant ATP away from biofuel generation, reducing yields. Another type of multidrug resistance efflux pump, the major facilitator superfamily (MFS) pump, has a natural, often metabolic, substrate and also acts on drug molecules [50]. MFS pumps are antiporters powered by the proton motive force, pumping substrates out of the cell in acidic environments and taking up molecules in basic environments [50]. The mechanism is an alternating “rocker-switch” movement with a single substrate-binding site [51-52]. This is a simpler design compared to Pdr5, which is thought to have multiple binding sites [53]. Yeast have dozens of multidrug resistance pumps with varied substrate specificities, and scientist are still discovering new pumps and new functions of known pumps.

There are many examples of native pumps that act directly on biofuel molecules. For example, the *S. cerevisiae* drug:H+ antiporter Tpo1 effluxes octanoic and decanoic acids [54], (See Chapters 2 and 3). Snq2 and Pdr5 can efflux decane and undecane [55], and Pdr18 [8] and Fps1 [56] efflux ethanol. In *E. coli*, AcrB effluxes geraniol [57].

Despite the plethora of pumps in yeast and ever-expanding research, many potential biofuels do not have a known transporter. Since most production organisms are derived from laboratory model organisms, they are unlikely to encounter toxic biofuel-like molecules during their normal lifetimes. “Wild” organisms that are exposed to a variety of conditions and toxins may have specialized transporters for novel compounds. Environmental isolates are a valuable source of pumps not normally found in laboratory model organisms. Heterologously expressed transporters from *Salmonella enterica* MsbA can improve efflux of zeaxanthin [58], and the *Pseudomonas putida* transporters TtgB and MexF efflux α-pinene and farnesyl hexanoate [57]. Other yeasts and fungi, and even eukaryotes such as humans have a wide variety of transporters that can potentially be useful for *S. cerevisiae*. Chen *et al*. used the transporters Abc2 and Abc3 from *Yarrowia lipolytica* to improve *S. cerevisiae* tolerance to decane and undecane [59]. The use of heterologous transporters in yeasts for biofuel applications has great potential and remains an interesting direction for research.

When a natural transporter does not exist, one can be engineered. Fisher showed that AcrB can be engineered to efflux *n*-butanol and other short-chain alcohols [60]. AcrB has also been engineered to efflux *n*-octanol [61]. While examples of transporters

engineered for biofuels are scarce, transporters for other compounds including glutamate have been created [62]. Transporters have also been engineered to have reverse directionality [63] and to use different ion gradients as an energy source [64]. Transporter engineering is a growing field of research, one with the potential to make biofuel production a feasible alternative to conventional fuel sources.

Transport is not just important for recovery of product. Kell hypothesizes that transporters can significantly contribute to fluxes of metabolites and products [65]. Transporters can also fix problems caused by the biofuels. For example, alcohols disrupt K^+ and H^+ gradients in yeast cells [66]. Overexpressing the K^+ pump Trk1 and the H^+ pump Pma1 in the normal lab strain S288C corrects this problem, even improving ethanol production beyond that of industrial ethanol strains such as Ethanol Red [22]. On the flip side, transporters, particularly high-copy multi-substrate drug efflux pumps can impose huge metabolic and energy burdens on the cell. Such pumps include Pdr5 from *S. cerevisiae* [50] and AcrB from *E. coli* [60]. Knocking out these transporters can improve growth rates [60,67-68]. Unfortunately, this also means that the expression levels of beneficial transporters can only be increased to a certain limit. Clearly, optimization of transporters in the cell is crucial for achieving high biofuel titers.

Engineering Yeasts Strains via Evolution

While scientists have collectively amassed a staggering amount of knowledge about cell biology, there is even more that remains unknown. For example, many details of yeast cellular function are far from “solved”. Without all of the information, we cannot always make accurate predictions as to how a biofuel molecule affects the cell nor how to improve tolerance to the toxic biofuel. Compounding the situation, phenotypes such as tolerance are not the result of a single mutation or overexpressed transporter, but rather the synergistic effect of alterations to multiple genes, including efflux pumps, cell wall and cell membrane properties, metabolism and cell structure adaptations [22,42]. Yeasts do not normally encounter high concentrations of butanol or hexanol, so they do not naturally have a high tolerance toward it. However, yeasts are highly adaptable, so natural evolutions can be used to identify systems affected by biofuel molecules and improve tolerance.

The simplest way to evolve strains is to let them grow in increasing amounts of a given biofuel. Any naturally arising mutations that confer a fitness advantage will be enriched in the culture over time, as the faster growing strains out-compete the wild type. This method has been used to improve yeast strains for thermotolerance [45], xylose utilization [63], hydrolysate tolerance [69-70], and many other phenotypes. The downside to this method is that point mutations may not be sufficient to improve tolerance when more complex adaptations are required [71]. Strains with general fitness improvements, or reductions in genome size can also overtake the culture [72] even though these may not be useful in production strains. Sikkema points out that changes accrued during evolution may be part of an adaptive response and not necessarily improve tolerance [27]. When analyzing genomic or transcriptional changes post-evolution, it is important to re-create mutations in wild-type strains in order to prove that they are functional. Natural evolutions are a valuable tool for improving tolerance, often successful where modern technologies fail.

Even with a high success rate, sometimes natural evolutions alone cannot reach a desired phenotype. The native mutation rate is fairly low for *S. cerevisiae*, with 1.13-2.43 mutations per cell per 100 generations [45,73]. Increasing the number of mutations per cell can lead to faster evolution times. UV mutagenesis or chemical mutagenesis with nitroso-methyl guanidine (NTG) are commonly used [74]. Ethyl methane sulfonate (EMS) can also cause deletions and rearrangements [74], and is often used in conjunction with other mutagens for alternating rounds of mutagenesis. This method is problematic in that many non-tolerance enhancing mutations will be found in any tolerant cells, thus requiring a lot of post-evolution cloning to determine causative mutations. Stanley and colleagues used chemical and natural mutagenesis in parallel, and interestingly found that the spontaneous mutations improved ethanol tolerance more than the chemical mutations [75]. Despite accessing more sequence space than natural evolutions, the chemically-induced changes were less capable, for reasons that are not yet understood.

Other large-scale, untargetted methods have proved useful for finding genes for tolerance improvement. In *E. coli*, *n*-butanol tolerance has been improved via overexpression and deletion libraries [76]. In yeast, Hong *et al*. used a library of overexpressed genomic fragments and a plate-based selection to find genes responsible for isobutanol and ethanol tolerance [77]. Gene deletion libraries have been used to find genes necessary for *n*-butanol tolerance, including genes involved in protein degredation [78]. Transcriptomics studies and microarrays have also proven useful in looking at ethanol tolerance genes [79-80]. While such big data methods are undeniably useful, we cannot solely rely such broad studies to dissect all aspects of tolerance. Intricate mechanisms require elegant experiments to comprehend. For example, a genome-level experiment highlighted Fps1 as having a role in ethanol efflux, but it was the focused experiments that showed how the osmolarity-triggered pump only effluxed ethanol once sufficient sugar was consumed, thereby activating the transporter [56].

Despite thousands of years of domestication and ethanol production, simple laboratory evolutions continue to improve ethanol production in *S. cerevisiae* [75,81]. Such successes showcase how powerful evolution is as a tool for strain engineering. Recently, evolutions for butanol tolerance were also carried out. *E. coli* have been evolved for higher ethanol and isobutanol tolerance [82-83]. The Kao group has also reported an evolution of *E. coli* for improved *n*-butanol tolerance [76]. In *S. cerevisiae*, strains have been evolved for *n*-butanol tolerance, with the final OD_{660} about 0.2 for the wild-type and 0.5 for the evolved strains in 1.5% *n*-butanol [77]. This tolerance extends to *n*-butanol, 2-butanol, isobutanol, and propanol [77]. The genes identified as important for tolerance included Rpn4, a transcription factor that increases proteasome gene expression and Rtg1, another transcription factor involved in inter-organelle communication [77]. Another evolution of *S. cerevisiae* in 2-butanol showed that overexpression of glycerol-3-phosphatase improved 2-butanol tolerance [84]. This study also looked at expression level changes, and found that a majority of upregulated genes were associated with the mitochondria, likely because alcohol-induced membrane permeability decreases efficiency of energy production [84]. In 1.9% *n*-butanol, the final OD_{600} (at 38 hours) was ~0.35 for the wild type and ~0.6 for the evolved strain [84]. Such tiny improvements hint at the extreme toxicity of the molecule.

Along with multiple toxicity mechanisms come multiple tolerance mechanisms. Single mutations can drive a population to a local tolerance solution [74,85], which may be well below the global tolerance maximum. Each tolerance study seems to find a new piece of the puzzle, yet combinations of these diverse mutations have yet to be studied. Fortunately, yeast have excellent genetic tools available. Haploid yeasts with varying tolerance levels can be mated to produce tolerant diploids. These diploids can be sporulated, and daughter cells with tolerance genes from both parents can be selected. Genomes from set of somewhat tolerant diploids can be shuffled to generate more tolerant strains in this way. Genome shuffling has been successfully used to improve tolerance toward alternative feedstock medias [86].

Above, we outlined several methods for improving yeast strains for biofuel production. Using transporters, fuel products can be actively removed from the cell, decreasing intracellular levels and consequently decreasing toxicity. Additionally, extracellular biofuels can be recovered more easily, simplifying extraction and downstream processing. Using evolution, mechanisms of toxicity and tolerance can be uncovered. The beauty of an evolutionary approach is that the unexpected or unknown is often brought to light. Using both of these approaches together is an excellent strategy for engineering strains for biofuel production. In the following chapters, we detail how we characterized a transporter, Tpo1, for fatty acid efflux (Chapter 2) and used another transporter, AT-1, to control intracellular acetyl CoA flux (Chapter 6). Unfortunately, attempts to engineer an efflux pump for butanol were unsuccessful (Chapter 3). We also used evolutions to improve medium-chain alcohol tolerance in yeast (Chapter 4), and characterized the resulting mutations in translation initiation factors (Chapter 5).

REFERENCES

1. US Department of Energy. Report on the First Quadrennial Technology Review. 2011.
2. Kopetz H. Renewable resources: Build a biomass energy market. Nature. 2013, 494:29-31.
3. International Energy Agency. World Energy Outlook 2011. 2011.
4. US Department of Energy. Bioenergy Technologies Office Multi-year program plan. 2015.
5. Dunn JB, Mueller S, Kwon H, Wang MQ. Land-use change and greenhouse gas emissions from corn and cellulosic ethanol. Biotechnol Biofuels 2013, 6:51.
6. Gasparatos A, Stromberg P, Takeuchi K. Sustainability impacts of first-generation biofuels. Anim Front. 2013, 3:12-26.
7. Zhang F, Rodrigue S, Keasling JD. Metabolic engineering of microbial pathways for advanced biofuels production. Curr Opin Biotechnol. 2011, 22:775–83.

8. Teixeira MC, Godinho CP, Cabrito TR, Mira NP, Sá-Correia I. Increased expression of the yeast multidrug resistance ABC transporter Pdr18 leads to increased ethanol tolerance and ethanol production in high gravity alcoholic fermentation. Microb Cell Fact. 2012, 11:98.

9. Huffer S, Roche CM, Blanch HW, Clark DS. Escherichia coli for biofuel production: bridging the gap from promise to practice. Trends Biotechnol. 2012, 30(10):538-45.

10. Shen CR, Lan EI, Dekishima Y, Baez A, Cho KM, Liao JC. Driving forces enable high-titer anaerobic 1-butanol synthesis in Escherichia coli. Appl Environ Microbiol. 2011, 77:2905–15.

11. Si T, Luo Y, Xiao H, Zhao H. Utilizing an endogenous pathway for 1-butanol production in Saccharomyces cerevisiae. Metabolic Eng. 2014, 22:60-68.

12. Zhang K, Sawaya MR, Eisenberg DS, Liao JC. Expanding metabolism for biosynthesis of nannatural ammino acids. Proc Natl Acad Sci USA. 2008, 105(52):20653–58.

13. Dekishima Y, Lan EI, Shen CR, Cho KM, Liao JC. Extending Carbon Chain Length of 1-Butanol Pathway for 1-Hexanol Synthesis from Glucose by Engineered Escherichia coli. JACS. 2011, 133:11399-401.

14. Liu X, Sheng J, Curtis III R. Fatty acid production in genetically modified cyanobacteria. Proc Natl Acad Sci USA. 2011, 108:6899–904.

15. Kalscheuer R, Stolting T, Steinbuchel A. Microdiesel: Escherichia coli engeineered for fuel production. Microbiol. 2006, 152(9):2529-36.

16. Renninger NS, Mcphee DJ. (2008) Amyris Biotechnologies, Inc. Fuel compositions comprising farnesane and farnesane derivatives and method of making and using same, 7399323.

17. Davies FK, Work VH, Beliaev AS, Posewitz MC. Engineering limonene and bisabolene production in the wild type and glycogen deficient mutant of Synechococcus sp. PCC 7002. Front Bioeng Biotechnol. 2014, 2:21.

18. Alonso-Gutierrez J. Chan R. Batth TS, Adams PD, Keasling JD. Petzold CJ, Lee TS. Metabolic engineering of Escherichia coli for limonene and perillyl alcohol production. Metab Eng. 2013, 19:33-41.

19. Choi YJ, Lee SY. Microbial production of alkanes. Nature. 2013, 502:571-74.

20. Machado IMP, Atsumi S. Cyanobacterial biofuel production. J Biotechnol. 2012, 162:50-56.

21. Bowles LK, Ellefson WL. Effects of Butanol on *Clostridum acetobutylicum*. App Env. Microbiol. 1985, 50(5):1165-70.

22. Lam F, Ghaderi A, Fink GR, Stephanopoulos G. Engineering alcohol tolerance in yeast. Science. 2014, 346(6205):71-75.

23. Ingram, L. O. 1976. Adaptation of membrane lipids to alcohols. J. Bacteriol. 125:670–78.

24. Cheng C, Kao KC. How to survive being hot and inebriated. Science. 2014, 346(6205):35-36.

25. Madeira A, Leitao L, Soveral G, Dias P, Prista C, Moura T, Loureiro-Dias MC. Effect of ethanol on fluxes of water and protons across the plasma membrane of Saccharomyces cerevisiae. FEMS Yeast Res. 2010, 10(3):252-58.

26. Uribe S, Ramirez J, Peña A. Effects of ß-pinene on yeast membrane functions. J Bacteriol. 1985, 161(3):1195–200.

27. Sikkema J, de Bont JA, Poolman B. Mechanism of membrane toxicity of hydrocarbons. Microbiol Rev. 1995, 59(2):201-22.

28. Miyawaki O, Tatsuno M. Thermodynamic analysis of alcohol effects on thermal stability of proteins. J Biosci Bioeng. 2011, 111(2):198-203.

29. Gaskova D, Plasek J, Zahumensky J, Benesova I, Buriankova L, Sigler K. Alcohols are inhibitors of Saccharomyces cerevisiae multidrug-resistance pumps Pdr5 and Snq2. FEMS Yeast Res. 2013, 13(8):782-95.

30. Moineau S, Levesque C. Control of bacteriophages in industrial fermentations. In Bacteriophages: Biology and Applications (eds: Kutter E, Sulakvelidze A), CRC Press. 2014, 282-93.

31. Park JH, Lee SY. Towards systems metabolic engineering of microorganisms for amino acid production. Curr Opin Biotechnol. 2008, 19:454-60.

32. Pacheco A, Talaia G, Sá-Pessoa J, Bessa D, Gonçalves MJ, Moreira R, Paiva S, Casal M, Queirós O. Lactic acid producction in Saccharomyces cerevisiae is modulated by expresssion of the monocarbocylate transporters Jen1 and Ady2. FEMS Yeast Res. 2012,12(3):375-81.

33. Kim I-K, Roldao A, Siewers V, Nielsen J. A systems-level approach for metabolic engineering of yeast cell factories. FEMS Yeast Res. 2012;(12):228-248.

34. Rose AH. Composition of the envelope layers of *Saccharomyces cerevisiae* in relation to flocculation and ethanol tolerance. J Appl Bacteriol. 1993, 74 Suppl: 100S-118S.

35. Rodriguez S. Kirby J. Denby CM, Keasling JD. Production and quantification of sesquiterpenes in Saccharomyces cerevisiae, including extraction, detection and quantification of terpene products and key related metabolites. Nat Protoc. 2014, 9(8):1980-96.

36. Steen E, Chan R, Prasad N, Myers S, Petzold CJ, Redding A, Ouellet M, Keasling JD. Metabolic engineering of Saccharomyces cerevisiae for the production of n-butanol. Microb Cell Fact. 2008, 7:36.

37. Avalos JL, Fink GR, Stephanopoulos G. Compartmentalization of metabolic pathways in yeast mitochondria improves the production of branched-chain alcohols. Nat. Biotechnol. 2013, 31:335–41.

38. Matsuda F, Furusawa C, Kondo T, Ishii J, Shimizu H, Kondo A. Engineering strategy of yeast metabolism for higher alcohol production. Microbial Cell Fact. 2011, 10:70.

39. Hasunuma T, Kondo A. Development of yeast cell factories for consolidated bioprocessing of lignocellulose to bioethanol through cell surface engineering. Biotechnol Adv. 2012, 30:1207-18.

40. Ma SM, Garcia DE, Redding-Johanson AM, Friedland GD, Chan R, Batth TS, Haliburton JR, Chivian D, Keasling JD, Petzold CJ. Optimization of a heterologous mevalonate pathwya though the use of variant HMG-CoA reductases. Metab Eng. 2011, 13:588-597.

41. Dahl RH, Zhang F, Alonso-Gutierrez, Baidoo E, Batth TS, Redding-Johanson AM, Petzold CJ, Mukhopadhyay A, Lee TS, Adams PD, Keasling J. Engineering dynamic pathway regulatin using stress-response promoters. Nat Biotechnol. 2013, 31:1039-1046.

42. Nicolaou SA, Gaida SM, Papoutsakis ET. A comparative view of metabolite and substrate stress and tolerance in microbial bioprocessing: From biofuels and chemicals, to biocatalysis and bioremediation. Metab Eng. 2010, 12(4): 307-31.

43. Groeneveld P, Stouthamer AH, Westerhoff HV. Super life: how and why 'cell selection' leads to the fastest-growing eukaryote. FEBS J. 2009, 276(1):254–70.

44. Uribe SP, Rangel P, Espínola G, Aguirre G. Effects of Cyclohexane, an Industrial Solvent, on The Yeast Saccharomyces Cerevisiae And on Isolated Yeast Mitochondria. Appl Environ Microbiol. 1990, 56(7):2114-19.

45. Caspeta L, Chen Y, Ghiaci P, Feizi A, Buskov S, Hallstrom BM, Petranovic D, Nielsen J. Altered sterol composition renders yeast thermotolerant. Science 2014, 346(6205):75-78.

46. Huffer S, Clark ME, Ning JC, Blanch HW, Clark DS. Role of Alcohols in Growth, Lipid Composition, and Membrane Fluidity of Yeasts, Bacteria, and Archaea. App Environ Microbiol. 2011, 77(18):6400-08.

47. Park YS, Chang HN, Kim BH. Adaptation of Saccharomyces cerevisiae to solvents used in extractive fermentation. Biotechnol Lett. 1998, 10(4)261-66.

48. Ernst R, Kueppers P, Stindt J, Kuchler K, Schmitt L. Multidrug efflux pumps: Substrate selection in ATP-binding cassette multidrug efflux pumps - first come, first served? FEMS J. 2010, 277(3): 540-49.

49. Krasowska A, Lukaszewics M, Bartosiewics D, Sigler K. Cell ATP level of Saccharomyces cerevisiae sensitively responds to culture growth and drug-

inflicted variations in membrane integrity and PDR pump activity. Biochem Biophys Res Commun. 2010, 395(1):51-55.

50. Sá-Correia I, dos Santos SC, Teixeira MC, Cabrito TR, Mira NP. Drug:H+ antiporters in chemical stress response in yeast. Trends Microbiol. 2009, 17(1): 22-31.

51. Huang YF, Lemieux MJ, Song J, Auer M, Wang DN. Structure and mechanism of the glycerol-3-phosphate transporter from Escherichia coli. Science. 2003, 301(5633):616-20.

52. Yin Y, He X, Szewczyk P, Nguyen T, Chang G. Structure of the multidrug transporter EmrD from Escherichia coli. Science. 2006, 312(5774):741-44.

53. Golin J, Ambudkar SV, Gottesman MM< Habib AD, Sczepanski J, Aiccardi W, May L. Studies with novel Pdr5p substrates demonstrate a strong size dependence for xenobiotic efflux. J Biol Chem. 2003, 278(8):5963-5969.

54. Legras JL, Erny C, Jeune CL, Lollier M, Adolphe Y, Demuyter C, Delobel P, Blondin B, Karst F. Activation of Two Different Resistance Mechanisms in Saccharomyces cerevisiae upon Exposure to Octanoic and Decanoic Acids. Appl Environ Microbiol. 2010, 76(22): 7526–35.

55. Ling H, Chen B, Kang A, Lee J-M, Chang MW. Transcriptome response to alkane biofuels in Saccharomyces cerevisiae: identification of efflux pumps involved in alkane tolerance. Biotechnol Biofuels. 2013, 6(1):95.

56. Teixeira MC, Raposo LR, Mira NP, Lourenco AB, Sá-Correia I. Genome-wide identification of Saccharomyces cerevisiae genes required for maximal tolerance to ethanol. Appl Environ Microbiol. 2009, 75(18):5761-72.

57. Dunlop MJ, Dossani ZY, Szmidt HL, Chu HC, Lee TS, Keasling JD, Hadi M, Mukhopadhyay A. Engineering microbial biofuel tolerance and export using efflux pumps. Mol Syst Biol. 2011, 7:487.

58. Doshi R, Nguyen T, Chang G. Transporter-mediate biofuel secretion. Proc Natl Acad Sci USA. 2013, 110(19):7642-7647.

59. Chen B, Ling H, Chang MW. Transporter engineering for improved tolerance against alkane biofuels in Saccharomyces cerevisiae. Biotechnol Biofuels. 2013, 6(1):21.

60. Fisher MA, Boyarskiy S, Yamada MR, Kong N, Bauer S, Tullman-Ercek D. Enhancing tolerance to short-chain alcohols by engineering the Escherichia coli AcrB efflux pump to secrete the non-native substrate n-butanol. ACS Syn Bio. 2013, 3(1):348-354.

61. Foo JL, Leong SS. Directed evolution of an E. coli inner membrane trasnporter for improved efflux of biofuel molecules. Biotechnol Biofuels. 2013, 6(1):81.

62. Nakayama Y, Yoshimura K, Iida H. A gain-of-function mutation in gating of Corynebacterium glutamicum NCgl1221 causes constitutive glutamate secretion. Appl Environ Microbiol. 2012, 78(15):5432–34.

63. Brooker RJ, Myster SH, Hastings Wilson T. Characterization and Sequencing of the LacY54-41 uncoupled mutant of the lactose permease. J. Biol. Chem. 1989, 264(14):8135–40.

64. Tirosh O, Sigal N, Gelman A, Sahar N, Fluman N, Siemion S, Bibi E. Manipulating the drug/proton antiport stoichiometry of the secondary multidrug transporter MdfA. Proc Natl Acad Sci USA. 2012, 109(31):12473-78.

65. Kell DB, Swainston N, Pir P, Oliver SG. Membrane transporter engineering in industrial biotechnology and whole cell catalysis. Trends Biotechnol. 2015, in press.

66. Ariño J, Ramos J, Sychrová H. Alkali metal cation transport and homeostasis in yeasts. Microbiol Mol Biol Rev. 2010, 74(1):95-120.

67. van Dyk TK. New recombinant yeast cell useful for producing butanol, comprises at least one genetic modification that reduces pleiotropic drug resistant 5 phenotype activity. 2010. Patent WO2010099524-A1.

68. van Dyk TK. Yeast with increased butanol tolerance involving a multidrug efflux pump gene. 2010, Patent US 20100221801 A1.

69. Sonderegger M, Sauer U (2003) Evolutionary engineering of Saccharomyces cerevisiae for anaerobic growth on xylose. Appl Environ Microbiol 69:1990–98.

70. Almario MP, Reyes LH, Kao KC. Evolutionary engineering of Saccharomyces cerevisiae for enhanced tolerance to hydrolysates of lignocellulosic biomass. Biotechnol Bioeng. 2013, 110(10):2616-23.

71. Martín C, Marcet M, Almazán O, Jönsson LJ (2007) Adaptation of a recombinant xylose-utilizing Saccharomyces cerevisiae strain to a sugarcane bagasse hydrolysate with high content of fermenta- tion inhibitors. Bioresour Technol 98:1767–1773.

72. Warnecke TE, Lynch MD, Karimpour-Fard A, Lipscomb ML, Handke P, Mills T, Ramey CJ, Hoant T, Gill RT. Rapid dissection of a complex phenotype through genomic-scale mapping of fitness genes. Metab Eng. 2010, 12(3):241-50.

73. Dettman JR, Rodrigue N, Melnyk AH, Wong A, Bailey SF, Kassen R. Evolutionary insight from whole-genome sequencing of experimentally evolved microbes. Mol Ecol. 2012, 21(9):2058–77.

74. Sauer E. Evolutionary Engineering of Industrially Important Microbial Phenotypes. Advances in Biochemical Engineering/ Biotechnology, 2001,73. Managing Editor: Th. Scheper © Springer-Verlag Berlin Heidelberg.

75. Stanley D, Fraser S, Chambers PJ, Rogers P, Stanley GA. Generation and characterisation of stable ethanol-tolerant mutants of Saccharomyces cerevisiae. J. Ind. Microbiol. Biotechnol. 2010, 37(2):139-49.

76. Reyes LH, Almario MP, Kao KC. Genomic library screens for genes involved in *n*-butanol tolerance in *Escherichia coli*. PLOS1. 2011, 6(3):e17678.

77. Hong ME, Lee KS, Yu BJ, Sung YJ, Park SM, Koo HM, Kweon DH, Park JC, Jin YS. Identification of gene targets eliciting improved alcohol tolerance in Saccharomyces cerevisiae through inverse metabolic engineering. J Biotechnol. 2010;149:52-59.

78. Gonzalez-Ramos D, van den Broek M, van Maris AJA, Pronk JT, Daran JMG. Genome-scale analyses of butanol tolerance in Saccharoymces cerevisiae reveal an essential role of protein degradation. Biotechnol Biofuels. 2013, 6(1): 48.

79. Ma MG, Liu LZ. Quantitative transcription dynamic analysis reveals candidate genes and key regulators for ethanol tolerance in Saccharomyces cerevisiae. BMC Microbiol. 2010, 10:169–189.

80. Stanley D, Chambers PJ, Stanley GA, Borneman A, Fraser S. Transcriptional changes associated with ethanol tolerance in Saccharomyces cerevisiae. Appl Microbiol Biotechnol. 2010, 88(1):231–39.

81. Brown SW, Oliver SG. Isolation of ethanol-tolerant mutants of yeast by continuous selection. Eur. J. Appl. Microbiol. Biotechnol. 1982, 16:119–22.

82. Goodarzi H, Bennett BD, Amini S, Reaves ML, Hottes AK, Rabinowitz JD, Tavazoie S. Regulatory and metabolic rewiring during laboratory evolution of ethanol tolerance in E. coli. Mol Syst Biol. 2010, 6:378.

83. Atsumi S, Wu TY, Machado IM, Huang WC, CHen PY, Pellegrini M, Liao JC. Evolution, genomic analysis, and reconstruction of isobutanol tolerance in Escherichia coli. Mol Syst Biol. 2010, 6:449.

84. Ghiaci P, Norbeck J, Larsson C. Physiological adaptations of Saccharomyces cerevisiae evolved for improved butanol tolerance. Biotechnol. Biofuels. 2013. 6(1):101.

85. Zhao H, Giver L, Shao Z, Affholter JA, Arnold FH. Molecular evolution by staggered extension process (StEP) in vitro recombination. Nat Biotechnol. 1998, 16:258-61.

86. Pinel D, D'Aoust F, del Cardayre SB, Bajwa PK, Lee H, Martin VJJ. Genome shuffling of Saccharomyces cerevisiae through recursive population 2 mating leads to improved tolerance to spent sulfite liquor. Appl Environ Microbiol. 2011, 77(14):4736-43.

Chapter 2
Characterization of transporter of polyamines (Tpo1) of *S. cerevisiae* for activity on medium-chain carboxylic acids

ABSTRACT

Since Maxwell's demon does not exist, cells employ transporters to control small molecules and metabolites across membranes. The yeast drug:H+ antiporter transporter of polyamines (Tpo1) transports polyamines, fatty acids, and drug molecules out of the cell. Tpo1 has been well-characterized with respect to its activity on polyamines, but less work has been done on its carboxylic acid substrate activity. We set out to further characterize Tpo1 with respect to fatty acid substrates. We have identified two substrate binding residues responsible for fatty acid efflux, a serine and a leucine located in the central pore of the transporter. A re-assessment of acidic residues in the pore hints at their involvement in proton relay. Additionally, we found that an N-terminal truncation which removed multiple regulatory sites did not affect Tpo1 activity on fatty acids. Thus the Tpo1 transporter can act on both fatty acid and polyamine substrates with different regulatory requirements. In a larger context, this work highlights the importance of engineering proteins at the amino acid level, in addition to modulating expression level.

INTRODUCTION

Medium chain fatty acids (MCFAs) are promising potential biofuels and biochemical precursors [1,2]. To this end, fatty acid production has been explored in *Escherichia coli* [3] and *Saccharomyces cerevisiae* [4,5,6], as well as algae [7] and cyanobacteria [8]. Yeast are a preferred production organism because they have high tolerance levels and industrial fermentations are well established. Optimizing MCFA production in yeast requires an understanding of toxicity and resistance mechanisms. In yeast, MCFAs are fermentation inhibitors [9], and when fatty acid production enzymes are overexpressed or MCFAs otherwise accumulate in the cell, they are actively secreted into extracellular media [10].

Transporters are important parts of cell physiology and play a crucial role in biochemical production. Notably, by exporting compounds of interest, transporters can improve product titers. For example, overexpressing the yeast transporter Pdr18 enhances ethanol yields [11]. Secreting the biochemical product enables use of the extracellular space as a metabolic sink, in turn reducing intracellular concentrations of toxic, growth-limiting molecules and decreasing product inhibition that can reduce the throughput of the production pathway [12]. Additionally, removing products to the extracellular media simplifies downstream processing by eliminating the need for cell lysis [13]. As *S. cerevisiae* do not require high levels of fatty acids and thus do not accumulate and store them as do oleaginous yeasts [14], exporting MCFAs is an elegant solution to increase titers. Understanding the transporters involved in fatty acid efflux is a key step in utilizing these molecules as biofuels.

In yeast, the transporter of polyamines (Tpo1) is known to export MCFAs with eight and ten carbons [15], though the transporter of longer-chain MCFAs is as-yet unknown.

Tpo1 has a broad substrate range, acting also on drugs such as cycloheximide, quinidine, and ibuprofen [16,17,18,19]. Yet it is best-characterized for its activity on polyamines, for which it was named. Tomitori *et al*. identified the gene and showed that the transporter acts on spermine, spermidine, and putrescine [20]. Polyamine export via Tpo1 is activated during the oxidative stress response [21].

Tpo1 has 12 transmembrane helices (Figure 2.1) and is a part of the major facilitator superfamily (MFS). MFS pumps are antiporters powered by the proton motive force, actively moving substrates out of the cell in acidic environments and taking up molecules in basic environments [17]. In addition to plasma membrane localization, Tpo1 is also found in the vacuole, where it pumps substrates in both directions depending on the pH gradient [18].

Crystal structures of several Tpo1 homologues have been solved, including that of the *Escherichia coli* transporter EmrD, which effluxes amphipathic drugs and detergents [22]. This pump has two loops that extend into the cell membrane and bind substrates, allowing it to remove lipophilic compounds directly from the membrane [22]. Another Tpo-like *E. coli* transporter, GlpT, secretes glycerol-3-phosphate and has the same overall structure and mechanism as EmrD [23]. These transporters have a single substrate-binding site and an alternating “rocker-switch” mechanism [22,23]. Tpo1 is thought to function by the same mechanism.

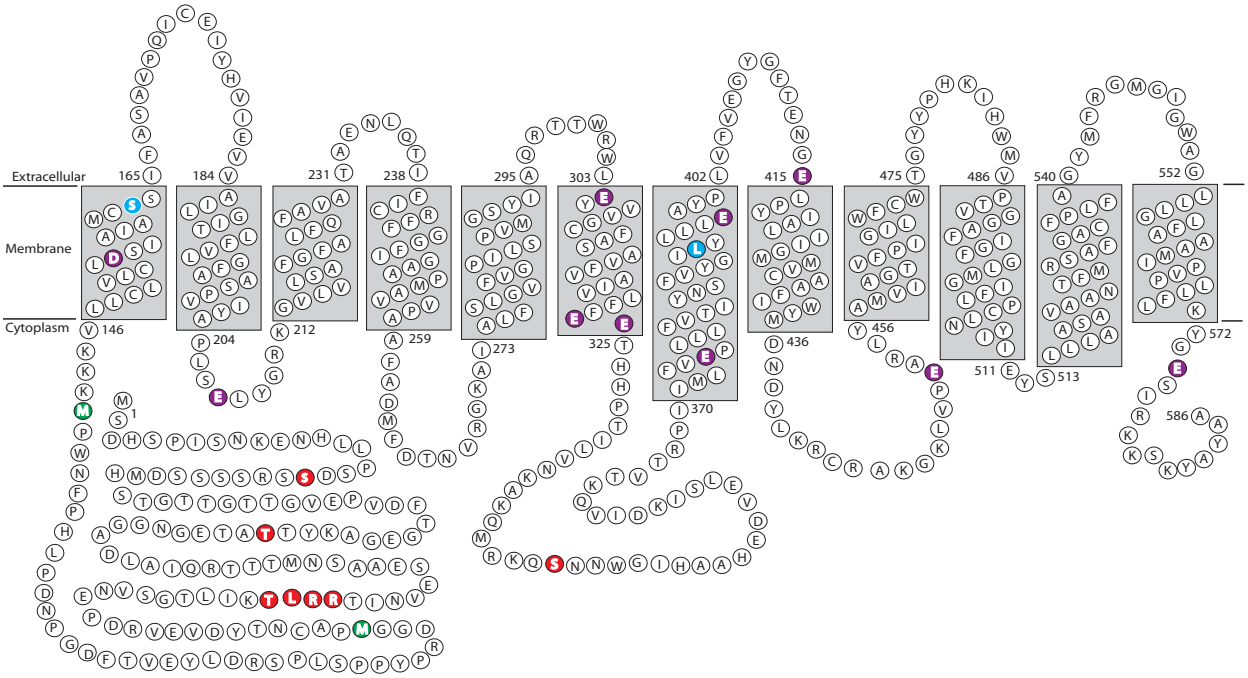

FIGURE 2.1. Tpo1 has twelve transmembrane domains and an N-terminal regulatory domain. Red indicates regulatory phosphorylation sites, blue indicates substrate binding residues, purple indicates acidic residues, and green indicates truncation start sites. Putative transmembrane domains of Tpo1 were predicted using MEMSAT3 [37,38,39,40] and the residues of these domains shown in rectangles.

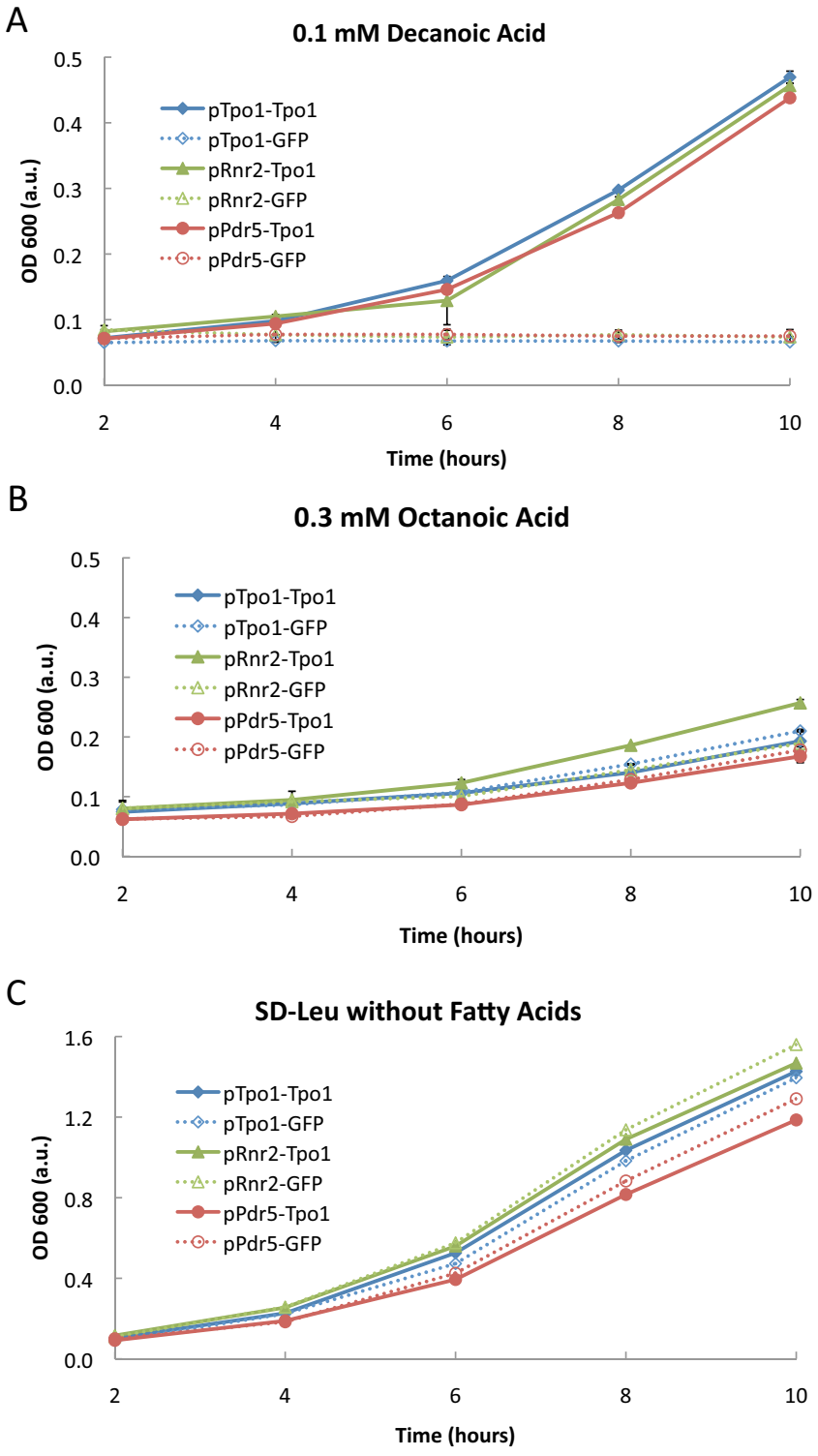

FIGURE 2.2. Tpo1 is the main transporter for decanoic acid efflux but not octanoic acid efflux. Growth curves of strains expressing Tpo1 and GFP under the control of various promoters in the Δ*TPO1*::*KANMX* genetic background. Tpo1-expressing strains are shown in solid lines; control strains expressing GFP are shown in dotted lines. Cultures were grown in SD-Leu media containing either A) 0.10 mM decanoic acid, B) 0.30 mM octanoic acid, or C) no fatty acids.

A detailed knowledge of structure-function relationships is critical for protein engineering and design to make use of Tpo1 and related transporters for biochemical production. Here we identify the residues involved in MCFA substrate binding for Tpo1, and demonstrate that two residues previously indicated in polyamine binding are more likely involved in the proton relay. We also show that the N-terminus, known to regulate Tpo1 function on polyamines, does not impact efflux of MCFAs. We conclude that Tpo1 has at least two sets of substrate specificity residues for multiple substrate classes and that differential regulation enables the cell to employ them as required.

RESULTS

Tpo1 enables growth in inhibitory concentrations of decanoic acid, but not octanoic acid. We monitored the effect of Tpo1 on log-phase growth rates in the presence of decanoic and octanoic acids. A Δ*TPO1* strain (*TPO1*Δ::*KANMX*)[24] was complemented with plasmids encoding *TPO1* or, as a negative control, the green fluorescent protein *GFP*, under three medium-strength promoters. We chose the native *TPO1* promoter (pTpo1, 700 base pairs upstream of the start codon), the native promoter from another multidrug efflux pump, pPdr5, and a constitutive medium strength promoter, pRnr2 [25]. In 0.10 mM decanoic acid, strains containing a plasmid encoding *TPO1* under the control of these medium-strength promoters recovered to about half the growth rate of unstressed cells (Figure 2.2A). Strains lacking a plasmid-borne copy of *TPO1* showed no detectable growth. In contrast, strains bearing *TPO1*-expressing and control plasmids had approximately the same growth profile when exposed to 0.3 mM octanoic acid (Figure 2.2B). Other transporters, particularly Pdr12, can be upregulated enough to compensate for loss of Tpo1 [11]. To isolate the effects of Tpo1 mutations, we used a *TPO1*Δ::*his3 PDR12*Δ::*KANMX* strain for subsequent experiments.

S163 and L393 are fatty acid substrate binding residues. We used the Clustal Omega multiple sequence alignment tool [26] to align Tpo1 with well-characterized MFS transporters including GlpT, EmrD, and PotE (Table 2.1). The substrate binding residues from GlpT, R45 and R269 [23], align with S163 and L393 of Tpo1. We mutated Tpo1 residue S163 to G163, Y163, D163 and V163, and mutated residue L393 to G393, N393, F393 and D393 in order to examine mutations with varied size and polarity. In Δ*TPO1* Δ*PDR12* strains complemented with plasmids encoding *TPO1* variants, we monitored growth rate in the presence of 0.10 mM decanoic acid and 0.20 mM octanoic acid. None of the mutated Tpo1 alleles supported growth comparable to the wild-type *TPO1* expressed from a plasmid (Figure 2.3A). Only the strain expressing the Tpo1^{L393N} mutation was able to grow significantly faster than the negative control, although the full growth rate was not recovered. The Tpo1^{L393N} mutation has the least dramatic difference in amino acid residue size, which may explain why some measure of growth was retained.

Table 2.1: Tpo1 Alignment with Homologous Transporters

```
TPO1            LAIQRTTTMNSAAESEVNITRRLTKILTGSVNEPDRVEVDYTNCAPMGGDRPYPPSLPSR 120
GlpT            ---------------------------------------------MLSIFKPAPHKARLPAA 17
EmrD            ------------------------------------------------------------
PotE            ---------------------------------------------SQAKSNKMGVVQL 13

TPO1            DLYEVTFDGPNDPLHPFNWPMKKKVLLCLVLCLDSIAIAMCSSIFASAVPQICEIYHVIE 180
GlpT            EIDPTYR--------------RLRWQIFLGIFFGYAAYYLVRKNFALAMPYLVEQG-FSR 62
EmrD            ----MKR--------------QRNVNLLLMLVLLVAVGQMAQTIYIPAIADMARDLNVRE 42
PotE            TILTMVN-------------MMGSGIIMLPTKLAEVGTISIISWLVTAVGSMALAWAFAK 60

TPO1            VVAILGITLFVLGFAASPVIYAP--LSELYGRKGVLVLS----AFGFALFQFAVATAENL 234
GlpT            GDLGFALSGISIAYGFSKFIMGS--VSDRSNPRVFLPAGLILAAAVMLFMGFVPWATSSI 120
EmrD            GAVQSVMGAYLLTYGVSQLFYGP--ISDRVGRRPVILVG----MSIFMLATLVAVTTSSL 96
PotE            CGMFSRKSGGMGGYAEYAFGKSGNFMANYTYGVSLLIANVAIAISAVGYGTELLGASLSP 120

TPO1            QTIFICRFFGGFIGAAPMAVVPAAFADMFDTNVRGKAIALFSLGVFVGPILSPVMGSYIA 294
GlpT            AVMFVLLFLCGWFQGMGWPPCGRTMVHWWSQKERGGIVSVWNCAHNVGGGIPPLLFLLGM 180
EmrD            TVLIAASAMQGMGTGVGGVMARTLPRDLYERTQLRHANSLLNMGILVSPLLAPLIGGLLD 156
PotE            VQIGLATIGVLWICTVANFGGARITGQISSITVWGVIIPVVGLCIIGWFWFSPTLY---V 177

TPO1            QRTTWRWLEYVVGCFASAVFVAIVLFFEETHHPTILVNKAKQMRKQSNNWGIHAAHEDVE 354
GlpT            AWFNDWHAALYMPAFCAILVALFAFAMMRDTPQSCGLPPIEEYKN-------DYPDDYNE 233
EmrD            TMWNWRACYLFLLVLCAG----VTFSMARWMPETR---PVDAPRT-------RLLTSY-- 200
PotE            DSWNPHHAPFFSAVGSSIAMTLWAFLGLESACANTDVVENPERNVP-----IAVLGGTLG 232

TPO1            LSIKDIVQKTVTRPIIMLFVEPLLLFVTIYNSFVYGILYLLLEAYPLVFVEGYGFTENGE 414
GlpT            KAEQELTAKQIFMQYVLPNKL--LWYIAIANVFVYLLRYGILDWSPTYLKEVKHFALDKS 291
EmrD            ---KTLFGNSGFNCYLL------MLIGGLAGIAAFEACSGVLMG----------AVLGLS 241
PotE            AAVIYIVSTNVIAGIVPN-----MELANSTAPFGLAFAQMFTPEVGKVIMALMVMSCCGS 287

TPO1            LPYIALIIGMMVCAAFIWYMDNDYLKRCRAKGKLVPEARLYAMVIAGTVFPIGILWFCWT 474
GlpT            SWAYFLYEYAGIPGTLLCGWMSDKVFRG----------NRGATGVFFMTLVTIATIVYWM 341
EmrD            SMTVSILFILPIPAAFFGAWFAG----------RPNKRFSTLMWQSVICCLLAGLLMWI 290
PotE            LLGWQFTIAQVFKSSSDEGYFPKIFSRV---------TKVDAPVQGMLTIVIIQSGLALM 338

TPO1            GYYPHKIHWMVPTVGGAFIGFGLMGIFLPCLNYIIESYLLLAASAVAANTFMRSAFGACF 534
GlpT            NPAGNPTVDMICMIVIGFLIYGPVMLIGLHALELAP--KKAAGTAAGFTGLFG-YLGGSV 398
EmrD            PDWFGVMNVWTLLVPAALFFFGAGMLFPLATSGAMEPFPFLAGTAGALVGGLQ-NIGSGV 349
PotE            TISPSLNSQFNVLVNLAVVTNIIPYILSMAALVIIQKVANVPPSKAKVANFVA--FVGAM 396

TPO1            PLFAGYMFRGMGIGWAGLLLGLFAAAMIPVPLLFLKYGESIRKKSKYAYAA--- 585
GlpT            AASAIVGYTVDFFGWDGGFMVMIGGSILAVILLIVVMIGEKRRHEQLLQERNGG 452
EmrD            LASLSAMLPQTGQGSLGLLMTLMG---LLIVLCWLPLATRMSHQGQPV------ 394
PotE            YSFYALYSSGEEAMLYGSIVTFLGWTLYGLVSPRFELKNKHG---------- 438
```

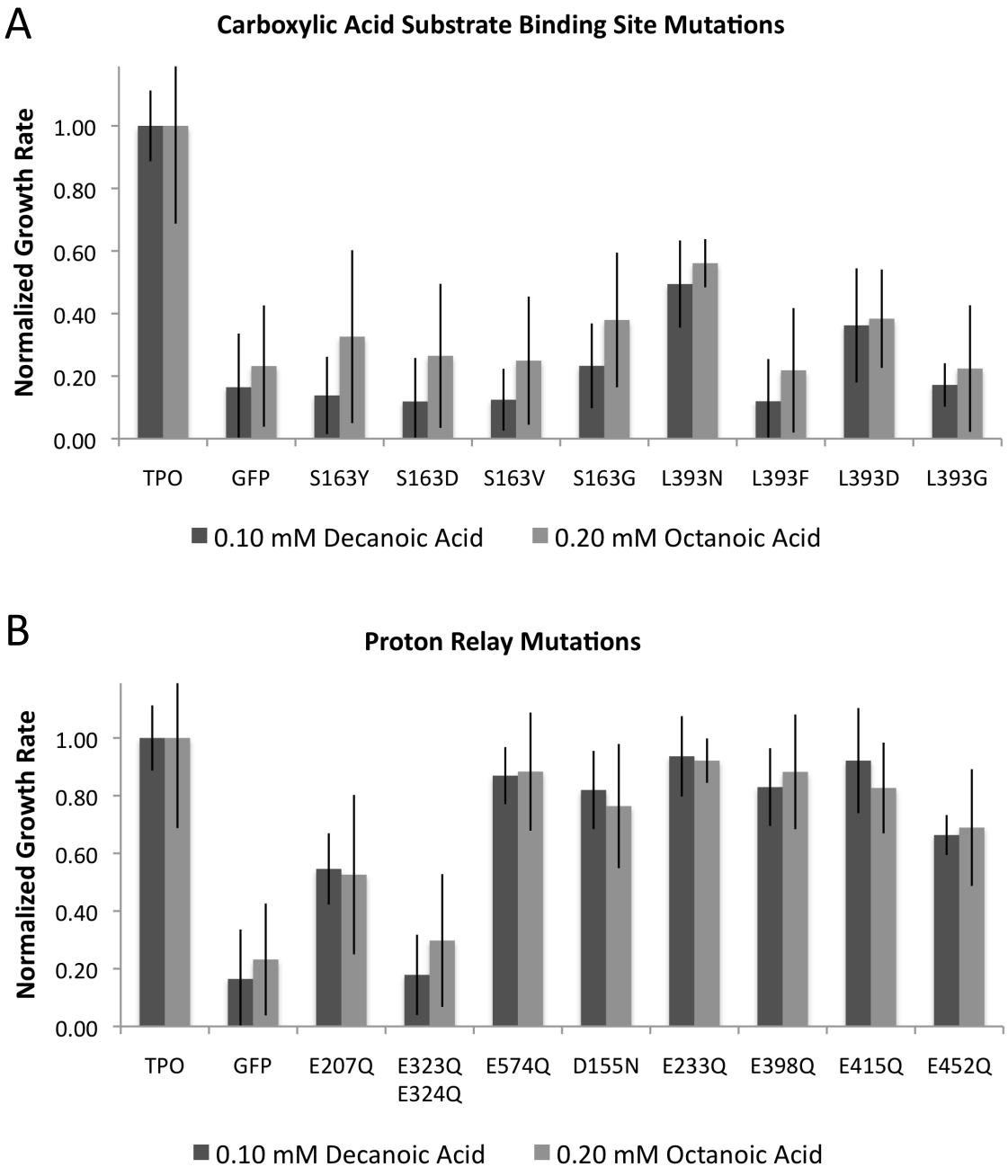

FIGURE 2.3. The fatty acid substrate binding and proton relay residues of Tpo1. Growth rates were calculated for Tpo1 point mutations in the presence of 0.10 mM decanoic or 0.20 mM octanoic acids. Tpo1 alleles and GFP were expressed from plasmids in the *ΔTPO1 ΔPDR12* strain. Error bars signify standard deviation of n=8 replicates. A) Mutations to the carboxylic substrate binding residues of Tpo1. B) Mutations of various Asp residues to Asn and Glu residues to Gln.

Three glutamines in the transmembrane helices may be part of the proton relay. As an H+:drug antiporter, Tpo1 is powered by the proton motive force, though it is not known which residues are a part of the proton relay. In order to assess the effect of acidic residues in the transmembrane domains, we mutated the residues to their polar but uncharged counterparts. We individually mutated six glutamic acids and one glutamic acid pair to glutamines, and one aspartic acid to asparagine. We then assessed growth rates in the presence of 0.10 mM decanoic and 0.20 mM octanoic acids (Figure 2.3B). While most mutations only slightly decreased fitness under acid stress, the Tpo1^{E207Q} and Tpo1$^{E323Q/E324Q}$ mutations significantly decreased growth rates. These findings indicate that E207 and E323/E324 glutamates may be important in the proton relay of Tpo1.

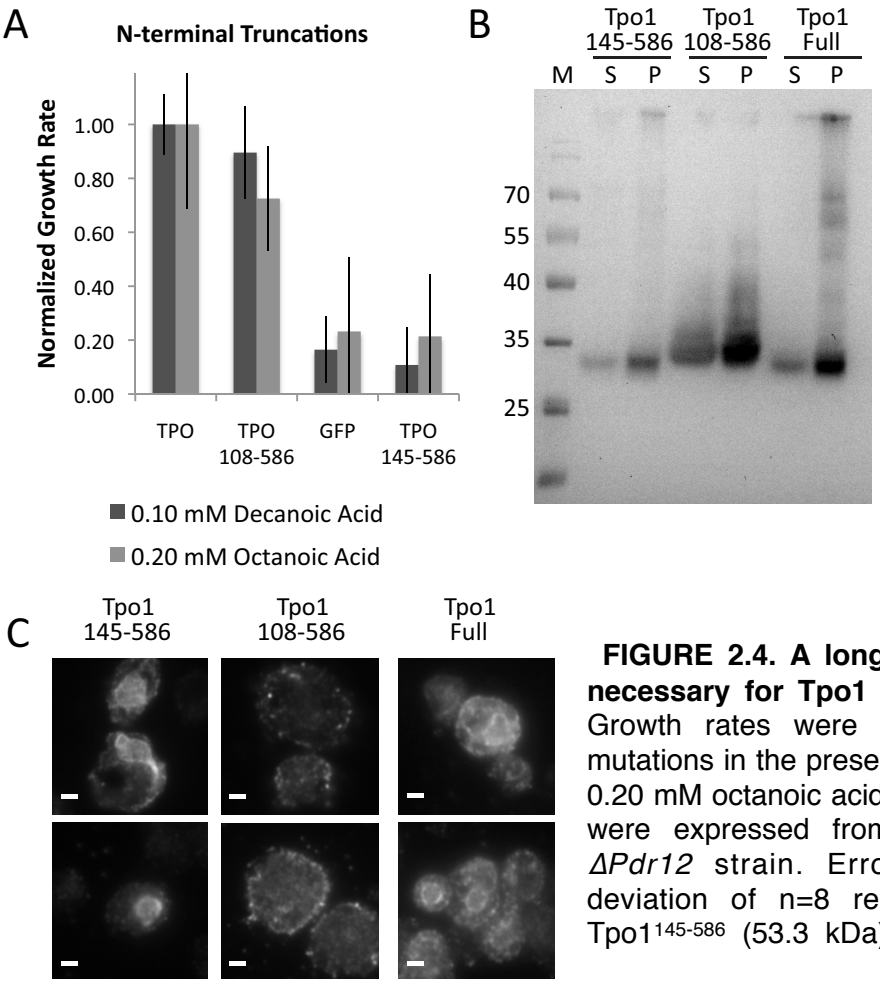

FIGURE 2.4. A long N-terminal region is not necessary for Tpo1 activity on fatty acids. A) Growth rates were calculated for Tpo1 point mutations in the presence of 0.10 mM decanoic or 0.20 mM octanoic acids. Tpo1 mutations and GFP were expressed from plasmids in the *ΔTpo1 ΔPdr12* strain. Error bars signify standard deviation of n=8 replicates. B) FLAG-tagged Tpo1$^{145-586}$ (53.3 kDa), Tpo1$^{108-586}$ (57.1 kDa), from plasmids. Whole cell lysates were separated via 15% SDS PAGE and transferred to a PVDF membrane. Membrane was probed with mouse anti-FLAG primary and HRP-conjugated anti-mouse secondary antibodies, then imaged with chemiluminescent substrate. M: Marker; S: Supernatant; P: Pellet. C) Cells expressing FLAG-tagged Tpo1 and truncations from plasmids were grown to exponential phase and fixed with formaldehyde and adhered to cover slips. Coverslips were incubated with mouse anti-FLAG primary and FITC-conjugated anti-mouse secondary antibodies. Slides were imaged as described in materials and methods.

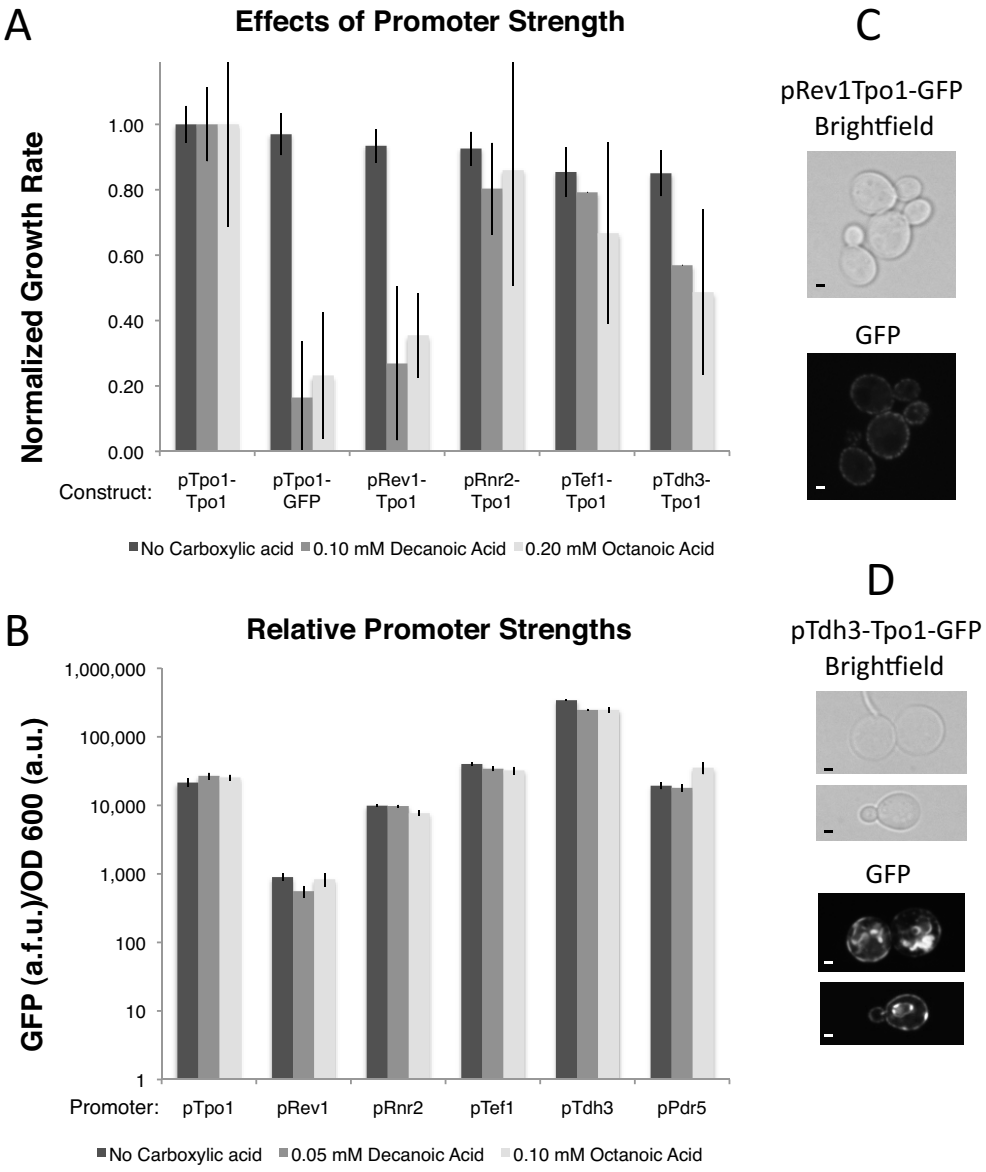

FIGURE 2.5. Tpo1 expression is a balance between pump toxicity and the acids it acts upon. A) Growth rates were calculated for Tpo1 under control of a small promoter library in the presence of 0.10 mM decanoic or 0.20 mM octanoic acids. Tpo1 mutations and GFP were expressed from plasmids in the Δ*TPO1* Δ*PD12* strain. Error bars signify standard deviation of n=8 replicates. B) Fluorescence was measured from stationary phase cultures of the Δ*TPO1* Δ*PDR12* strain expressing GFP under the control of various promoters. Error bars signify standard deviation of n=3 replicates. C-D) Tpo-GFP fusions were expressed from plasmids under the pRev1 and pTdh3 promoters in the Δ*TPO1* Δ*PDR12* strain. Exposure times were 10 sec for pRev1 promoter and 2 msec for the pTdh3 promoter.

The N-terminal region of Tpo1 is not required for function on decanoic acid. We examined two methods of regulation for Tpo1: promoter strength and removal of the N-terminal regulatory domain. C-terminally FLAG-tagged Tpo1 migrates more quickly in a denaturing polyacrylamide gel than expected for a 68.4 kDa peptide, as judged by Western blots (Figure 2.4B). This led us to suspect possible truncation of the protein. We generated two constructs with genetically encoded N-terminal truncations and C-terminal FLAG tags, in order to confirm that the band corresponding to the smaller fragment was not an artifact of our method or due to the unpredictable behavior of membrane proteins run in SDS-PAGE [27]. Surprisingly, the full Tpo1-FLAG construct migrates similarly in a gel to the Tpo1$^{145\text{-}586}$-FLAG construct, which is a full 15 kDa smaller at 53.3 kDa. This truncation removed the entire N-terminal region up to the transmembrane domains, but all of the subsequent domains are likely intact. Western blotting also indicates that the truncation is expressed at lower levels than the wild-type Tpo1 (Figure 2.4B). We tested the activity of the Tpo1 truncations by measuring growth rates in the presence of the fatty acids. Overexpression of Tpo1$^{145\text{-}586}$ was unable to rescue yeast from fatty acid toxicity, while overexpression of Tpo1$^{108\text{-}586}$ resulted in nearly wild-type growth against decanoic acid (Figure 2.4A). The large error in the octanoic acid growth rates precluded analysis. Immunofluorescence shows that wild-type Tpo1 is localized in the plasma membranes and the vacuole. Tpo1$^{145\text{-}586}$ has a similar localization pattern, though the fluorescence intensity appears lower. Tpo1$^{108\text{-}586}$, however, only localizes to the plasma membrane (Figure 2.4C).

The native Tpo1 promoter outperforms several constituitive promoters to optimize Tpo1 expression levels in stressed conditions. Overexpression of a transporter is a simple way to increase efflux of toxic compounds. Optimizing Tpo1 expression for toxic levels of MCFAs will be required for most efficient production in yeasts. We therefore tested the ability of a range of promoter strengths [25] to optimally express Tpo1 in the Δ*TPO1* Δ*PDR12* strain (Figure 2.5A). There is a slight downward trend in growth rates in the absence of fatty acids correlating with increasing promoter strength, as seen in the unstressed growth rates of Figure 2.5A. The promoters are not affected by decanoic or octanoic acid, as seen in Figure 2.5B. Microscopic analysis of Tpo1-GFP fusion localization shows that high expression of *TPO1* under the pTdh3 promoter leads to a buildup in vacuoles and saturation of the plasma membrane (Figure 2.5D). In the presence of fatty acids, the native *TPO1* promoter is likely dynamically regulated and optimizes expression to confer maximal growth rates, balancing toxicity of transporter overexpression with necessity of expressing enough transporters to remove the fatty acids. The Rnr2 promoter best mimics the native Tpo1 promoter level (Figure 2.5A).

DISCUSSION

Octanoic and decanoic acids have overlapping yet different responses in the cell, as previously explored by Legras [15]. That study showed that Pdr12 is also responsible for octanoic acid response while Tpo1 is the main exporter of decanoic acid [15]. Our experiments confirm this, as expressing Tpo1 in a Δ*TPO1* strain confers a significant increase in growth rates as compared to the negative control expressing GFP, which is unable to grow in the presence of toxic concentrations of decanoic acid. In contrast, strains expressing Tpo1 and the negative control had similar growth profiles when

grown in 0.30 mM octanoic acid. Even so, there is significant variance in growth in octanoic acid, which may be attributable to the utilization of other tolerance mechanisms.

We identified the likely key residues for fatty acid substrate specificity of Tpo1 transporter based on homology to the *E. coli* transporter GlpT (Table 2.2). We expected polar and hydrophobic residues to bind to the carboxylic group and hydrophobic tail of the fatty acids, respectively. The GlpT substrate binding sites R45 and R269 align with S163 and L393 of Tpo1 (Table 2.2). Mutating these residues conferred a greatly reduced growth rate in the presence of both octanoic and decanoic acids, but Tpo1^{L393N} conferred an intermediate growth rate as compared to the wild-type and the negative control, so the transporter likely retains some activity upon mutation. Leucine and asparagine residues are of comparable size, so it is possible that in this part of the pore, substrate selection is driven more by steric interactions than polarity, or that this residue is not as exclusive as S163. Both S163 and L393 are undeniably important for fatty acid efflux by Tpo1.

Tomitori *et al.* proposed that three glutamate residues are involved in substrate binding of polyamine substrates [28]. These residues were identified based on homology to the PotE polyamine binding sites [28,29]. Interestingly, we mutated these residues and several other acidic residues in Tpo1 and found that mutation of two of the glutamates identified by Tomitori also reduces tolerance toward MCFAs, as shown in Figure 3B. This suggests that these residues also have a role in MCFA transport. Negatively charged glutamates are more likely to bind positively charged substrates such as polyamines than negatively charged carboxylic acids, so it may be that these residues are involved in proton relay rather than substrate specificity. Additionally, it was shown by Kashiwagi *et al.* that tyrosine, tryptophan, and cysteine residues have the greatest involvement in putrescine transport, rather than acidic residues [29]. We hypothesize that acidic glutamates at positions 207, 323, and 324 of Tpo1 are in fact part of the proton relay rather than involved in substrate specificity. Other glutamate residues and an aspartate residue, when mutated to glutamine or asparagine, did not decrease growth rate as dramatically, so are unlikely to be involved in proton relay.

The N-terminal portion of Tpo1 includes a long segment that is not part of the transmembrane domains. It contain many potential regulatory sites, including an S19 and T52 that increase polyamine transport activity when phosphorylated, and an RRTL motif that is involved in vacuolar sorting [30] (See Figure 2.2). A 108 residue N-terminal truncation (Tpo1$^{108\text{-}586}$) that removes these regulatory sites supports growth at nearly the wild-type level (Figure 2.4A), though localization is limited to the plasma membrane (Figure 2.4C). A more dramatic 145-residue truncation (Tpo1$^{145\text{-}586}$) does not appear to be active (Figure 2.4A), though the localization and size as judged by Western blot is more similar to the wild type (Figure 2.4B). Tpo1$^{145\text{-}586}$ seems to have a much lower expression level than the wild-type or Tpo1$^{108\text{-}586}$, which may account for lower activity and inability to support growth in the presence of toxic levels of fatty acids. Future investigations could explore the effects of expressing the truncated Tpo1$^{145\text{-}586}$ under a stronger promoter, to determine whether it is merely an expression deficit.

We hypothesize that different regulatory mechanisms exist for Tpo1 depending on whether the critical substrate is a polyamine or a fatty acid. In the case of the fatty acids, efflux to the extracellular space immediately removes a toxic compound that is not

otherwise useful for the cell [14]. This is how Tpo1$^{108\text{-}586}$, which is only detected in the plasma membrane, is able to support growth in media with fatty acids. On the other hand, polyamines are essential in low amounts for translation, so sequestration in the vacuole is a way to store the compounds until they are needed. The balance between beneficial and toxic levels of cytoplasmic polyamines is a delicate one, which necessitates careful regulation by phosphorylation.

In addition to post-translational regulation, regulation of Tpo1 expression level is critical. As with many membrane proteins, overexpression of Tpo1 is toxic to the cell. We tested a range of promoter strengths and found that medium-strength promoters are best for mimicking the native Tpo1 promoter and expressing appropriate levels of Tpo1 (Figure 5A). There is a small decrease in the growth rate under normal media conditions as the promoter strength increases. We expect that the transporter has saturated the already-crowded plasma membrane and is depleting the proton gradient, as well as posing a metabolic burden through excess protein production. High expression levels of Tpo1-GFP fusions show a high density in the vacuoles and plasma membrane (Figure 2.5D), which is likely impairing function of these membranes by packing them with multiple copies of Tpo1. Even in the presence of toxic levels of octanoic and decanoic acids, high expression of Tpo1 is deleterious to the cell, as evidenced by the drop in growth rate with increasing promoter strength in Figure 5A. Previous work by Marks *et al.* has shown that many commercial strains have "amplification" of Tpo1, and it is upregulated as fermentation progresses [31]. However, in our lab strain, improving fatty acid efflux must be balanced carefully against the stress of overexpression. The native regulation must balance the multiple roles of Tpo1: high expression level for Tpo1 is necessary in the presence of toxic MCFAs, which are produced during normal growth; however, excess Tpo1 works to deplete essential polyamine concentrations, thus hindering translation and concomitantly lowering growth rates. More study on the differential regulation of Tpo1 for its multiple substrate classes is needed to clearly link its regulation mechanisms and various intracellular effects**.**

MATERIALS AND METHODS

Strains and media

S. cerevisiae strains *ΔTPO1* and *ΔPDR12* were obtained from the Yeast Deletion Project BY4741 library (*MAT*a *his3Δ1 leu2Δ0 met15Δ0 ura3Δ0*) [24]. A *ΔTPO1ΔPDR12* strain was generated by replacing the *TPO1* gene with a *his3* cassette in the *ΔPDR12* strain and confirming by PCR of the junctions. Strains were transformed with plasmids containing the *LEU2* auxotrophic marker and selected and grown on synthetic dropout media without leucine (SD-Leu: 0.67% Yeast Nitrogen Base (BD Chemical), 2% α-Dextrose (Amresco), 0.2% amino acid mix without leucine from US Biological).

Genetic Methods

The *TPO1* gene was amplified from the BY4741 genome using primers 5'-TAAATCGATACTGCATTTCTAGGCATATCCAGCGAGATCTatgtcggatcattctcccat-3' and 5'-AAATCATAAATCATAAGAAATTCGCCTCGAGttaGGATCCttaagcggcgtaagcatact-3' and homologously recombined [24] into plasmid pSD279 [25]. *TPO1* mutations were generated using two-step PCR and homologous recombination. The promoter library

was a gift from Dueber lab [25]. *GFP* fusions and FLAG-tagged *TPO1* were generated by PCR amplifying the *GFP* or 4X FLAG sequence (gattataaagatgacgatgacaag) and using homologous recombination to append it 3' of the *TPO1* gene with a linker sequence (ggtgacggtgctggttta). The *TPO1* promoter (pTpo1) was generated by cloning 706 base pairs upstream of the *TPO1* start codon into the pSD279 vector. The *PDR5* promoter (pPdr5) was generated by cloning 698 base pairs upstream of the *PDR5* start codon into the pSD279 vector.

Growth Curves
Single colonies were inoculated into 5 mL SD-Leu in culture tubes. Cultures were grown 36 hours at 30°C with 280 rpm shaking. Stationary phase cultures were diluted to an optical density at 600 nm (OD_{600}) of .30-.33 a.u. as measured with a Nanodrop 2000c spectrophotometer, and 5 mL dilute culture was aliquoted into screw-cap tubes. 5 mL SD-Leu with 0 or 0.2 mM decanoic acid (Sigma), or 0.6 mM octanoic acid (Sigma) was added. Each sample was run in triplicate. Screw-cap tubes were grown at 30°C with 280 rpm shaking and measurements were taken *in situ* every 2 hours using a Genesys-20 spectrophotometer.

Growth Rate Calculations
Single colonies were used to inoculate 3 mL SD-Leu in a 24-well culture block. Cultures were grown 36 hours at 30°C with 280 rpm shaking. Stationary phase cultures were sub-cultured 1:50 into 3 mL SD-Leu, SD-Leu + 0.1 mM decanoic acid, and SD-Leu + 0.2 mM octanoic acid, and grown 4 hours at 30°C with 280 rpm shaking. At 4 and 10 hours, OD_{600} was measured for 100 µL of culture using a Molecular Devices SpectraMax M2 plate reader. The growth rate was calculated as $\ln(10\text{hour } OD_{600}/4\text{hour } OD_{600})/6\text{hr}$. Reported growth rates are averages of two samples per day on three different days.

Fluorescent protein measurements
Strains containing plasmids expressing Tpo1 or GFP were grown 24 hours at 30°C with 280 rpm shaking in SD-Leu + 0.0 or 0.05 mM decanoic acid or 0.1 mM octanoic acid. Cell density (OD_{600}) and fluorescence (a.f.u.) were measured using a Biotek Synergy HTX plate reader. Fluorescence measurements were divided by the corresponding OD_{600} for each sample, and background fluorescence, measured as the fluorescence from strains expressing only Tpo1, was subtracted.

Microscopy
Images were captured using an Andor Clara-Lite digital camera and a Nikon Ni-U upright microscope with a 100x, 1.45 n.a. plan apochromat oil immersion objective. Images were acquired at room temperature. Immunofluorescence images were taken in 90% glycerol, live cell images were taken in SD-Leu media. Fluorescence images were collected using a C-FL Endow GFP HYQ band pass filter. Images were captured using the Nikon NIS Elements software.

Immunofluorescence
S. cerevisiae BY4741 *ΔTPO1 PDR12* containing plasmids expressing Tpo1 and truncations with C-terminal 4X FLAG tags were grown to stationary phase in SD-Leu.

The cells were then subcultured 1:100 and grown 4 hours. Cells were fixed in 3.7% formaldehyde (Sigma), washed with 100 mM potassium phosphate, pH 6.5. The cell wall was digested with zymolyase (Zymo) and cells were adhered to coverslips with polylysine (Sigma). Coverslips were incubated in 4°C methanol for 6 min and 4°C acetone for 30 s. PBS-BSA (PBS {1.37 M NaCl (Sigma), 27 mM KCl (Spectrum), 100 mM Na_2HPO_4 (Fisher) 18 mM KH_2PO_4 (Fisher) pH 7.4}+ 5 mg/ml BSA (Sigma)) was used to block. Coverslips were incubated in a 1:500 dilution of mouse anti-FLAG (Sigma) overnight. After three washes with PBS-BSA, a 1:100 dilution of a goat anti-mouse FITC conjugated antibody (Sigma) was added and incubated two hours at room temperature. Coverslips were washed three times with PBS-BSA, then three times with PBS and dried. Coverslips were placed on 90% glycerol on slides and sealed with nail polish. Images were taken as described above.

Westerns

Whole cell lysates were prepared by resuspending 2 mL of stationary phase cells in 200 uL Homogenization Buffer (50 mM Tris (Sigma), pH 7.5, 1 mM EDTA, 1 mM ß-mercaptoethanol (Amresco), 10% glycerol (Fisher), 17.4 ug/ml PMSF (Sigma)). Cells were lysed by vortexing 2 minutes with glass beads. Lysed cells were pelleted by spinning at 10,000 xg for 2 minutes. Supernatants were separated and pellets resuspended in 200 uL Homogenization Buffer. 4X SDS running buffer (200 mM Tris, 4% ß-mercaptoethanol, 8% SDS (Fisher), 0.04% bromophenol blue (Acros Organics), 40% glycerol, pH 6.8) was added and samples were boiled 95°C for 5 minutes. 10 uL of sample were run through a 15% SDS-PAGE gel. Proteins were transferred to polyvinylidine fluoride (PVDF) membrane (Millipore) using a semi-dry blotting protocol. Membranes were blocked in 5% milk in TBST (50 mM Tris, 150 mM NaCl, 0.05% Tween-20 (Fisher), pH 7.5) for 30 minutes at room temperature. Membrane was incubated in a 1:7,000 dilution of mouse anti-FLAG antibody (Sigma) in TBST + 1% milk overnight, washed 3X 5 minutes with 10 mL TBST, then incubated 2 hours at room temperature in a 1:1000 dilution of HRP-conjugated goat anti-mouse antibody in TBST. Membranes were imaged using the SuperSignal West Pico Chemiluminescent substrate (Pierce) and Chemidoc Imager.

TABLE 2.2. Plasmids used in this study.

Plasmid	Promoter	Insert
pSD350	pTpo1	Tpo1
pSD359	pTpo1	GFP
pSD303	pRev1	Tpo1-link-GFP
pSD301	pTdh3	Tpo1-link-GFP
pSD417	pTpo1	145-586 Tpo1
pSD418	pTpo1	108-586 Tpo1
pSD409	pTpo1	Tpo1 S163Y
pSD410	pTpo1	Tpo1 S163V
pSD411	pTpo1	Tpo1 S163D
pSD415	pTpo1	Tpo1 S163G
pSD412	pTpo1	Tpo1 L393N
pSD413	pTpo1	Tpo1 L393F
pSD414	pTpo1	Tpo1 L393D
pSD416	pTpo1	Tpo1 L393G
pSD629	pTpo1	Tpo1 E207Q
pSD630	pTpo1	Tpo1 E323Q/E324Q
pSD631	pTpo1	Tpo1 E574Q
pSD646	pTpo1	Tpo1 D155N
pSD647	pTpo1	Tpo1 E233Q
pSD648	pTpo1	Tpo1 E398Q
pSD649	pTpo1	Tpo1 E415Q
pSD650	pTpo1	Tpo1 E452Q
pSD266	pRev1	Tpo1
pSD270	pRev1	GFP
pSD322	pTef1	Tpo1
pSD323	pTef1	GFP
pSD328	pRnr2	Tpo1
pSD329	pRnr2	GFP
pSD280	pTdh3	Tpo1
pSD270	pTdh3	GFP
pSD401	pPdr5	Tpo1
pSD406	pPdr5	GFP
pSD575	pTpo1	$Tpo1^{145-586}$-FLAG
pSD576	pTpo1	$Tpo1^{108-586}$-FLAG
pSD657	pTpo1	Tpo1-FLAG

REFERENCES

1. Pinel D, D'Aoust F, del Cardayre SB, Bajwa PK, Lee H, Martin VJJ. Genome shuffling of Saccharomyces cerevisiae through recursive population 2 mating leads to improved tolerance to spent sulfite liquor. Appl Environ Microbiol. 2011, 77(14):4736-43.

2. Chen L, Zhang J, Chen WN. Engineering the Saccharomyces cerevisiae β-oxidation pathway to increase medium chain fatty acid production as potential biofuel. PLoS One. 2014, 9(1):e84853.

3. Zhou YJ, Buijs NA, Siewers V, Nielsen J. Fatty Acid-Derived Biofuels and Chemicals Production in Saccharomyces cerevisiae. Front Bioeng Biotechnol. 2014, 2:32.

4. Steen E, Chan R, Prasad N, Myers S, Petzold CJ, Redding A, Ouellet M, Keasling JD. Metabolic engineering of Saccharomyces cerevisiae for the production of n-butanol. Microb Cell Fact. 2008, 7:36.

5. Michinaka Y, Shimauchi T, Aki T, Nakajima T, Kawamoto S, Shigeta S, Suzuki O, Ono K. Extracellular secretion of free fatty acids by disruption of a fatty acyl-CoA synthetase gene in Saccharomyces cerevisiae. J Biosci Bioeng. 2003, 95(5): 435–40.

6. Tang X, Feng H, Chen WN. Metabolic engineering for enhanced fatty acids synthesis in Saccharomyces cerevisiae. Metabol Eng. 2013, 16:95-102.

7. Runguphan W, Keasling JD. Metabolic engineering of Saccharomyces cerevisiae for production of fatty acid-derived biofuels and chemicals. Metabol Eng 2014, 21:103-10.

8. Chisti, Y. Biodiesel from microalgae. Biotechnol Adv. 2007, 25:294–306.

9. Liu X, Sheng J, Curtiss R. Fatty acid production in genetically modified cyanobacteria. Proc Natl Acad Sci USA 2011, 108(17):6899-904.

10. Viegas CA, Rosa MF, Sá-Correia I, Novais JM. Inhibition of Yeast Growth by Octanoic and Decanoic Acids Produced during Ethanolic Fermentation. Appl Environ Microbiol. 1989, ;55(1):21-28.

11. Scharnewski M, Pongdontri P, Mora G, Hoppert M, Fulda M. Mutants of Saccharomyces cerevisiae deficient in acyl-CoA synthetases secrete fatty acids due to interrupted fatty acid recycling. FEBS J. 2008, ;275(11):2765-78.

12. Teixeira MC, Godinho CP, Cabrito TR, Mira NP, Sá-Correia I. Increased expression of the yeast multidrug resistance ABC transporter Pdr18 leads to increased ethanol tolerance and ethanol production in high gravity alcoholic fermentation. Microb Cell Fact. 2012, 11:98.

13. Lian J, Zhao H. Recent advances in biosynthesis of fatty acids derived products in Saccharomyces cerevisiae via enhanced supply of precursor metabolites. J Ind Microbiol Biotechnol. 2015, 42(3):437-51.

14. Metcalf KJ, Finnergy C, Azam A, Valdivia E, Tullman-Ercek D. Using transcriptional control to increase titers of secreted heterologous proteins using the type III secretion system. Appl Environ Microbiol. 2014, 80(19):5927-34.

15. Lian J, Zhao H. Recent advances in biosynthesis of fatty acids derived products in Saccharomyces cerevisiae via enhanced supply of precursor metabolites. J Ind Microbiol Biotechnol. 2014, 42(3):437-51.

16. Legras JL, Erny C, Le Jeune C, Lollier M, Adolphe Y, Demuyter C, Delobel P, Blondin B, Karst F. Activation of Two Different Resistance Mechanisms in Saccharomyces cerevisiae upon Exposure to Octanoic and Decanoic Acids. Appl Environ Microbiol. 2010, 76(22):7526-7535.

17. Tomitori H, Kashiwagi K, Sakata K, Kakinuma Y, Igarashi K. Identification of a gene for a polyamine transport protein in yeast. J Biol Chem. 1999, 274(6): 3265-67.

18. Krüger A, Vowinckel J, Mülleder M, Grote P, Capuano F, Bluemlein K, Markus Ralser. Tpo1-mediated spermine and spermidine export controls cell cycle delay and times antioxidant protein expression during the oxidative stress response. EMBO Rep. 2013, 14(12): 1113-19.

19. Sá-Correia I, dos Santos SC, Teixeira MC, Cabrito TR, Mira NP. Drug:H+ antiporters in chemical stress response in yeast. Trends Microbiol. 2009, 17(1): 22-31.

20. do Valle Matta MA, Jonniaux JL, Balzi E, Goffeau A, van den Hazel B. Novel target genes of the yeast regulator Pdr1p: a contribution of the TPO1 gene in resistance to quinidine and other drugs. Gene. 2001, 272(1-2):111-19.

21. Tucker CL, Fields S. Quantitative genome-wide analysis of yeast deletion strains sensitivities to oxidative and chemical stress. Comp Funct Genomics. 2004, 5:216-24.

22. Mima S, Ushijima H, Hwang HJ, Tsutsumi S, Makise M, Yamaguchi Y, Tsuchiya T, Mizushima H, Mizushima T. Identification of the Tpo1 gene in yeast, and its human orthologue TETRAN, which cause resistance to NSAIDs. FEBS Lett. 2007, 581:1457-63.

23. Yin Y, He X, Szewczyk P, Nguyen T, Chang G. Structure of the multidrug transporter EmrD from Escherichia coli. Science. 2006, 312(5774):741-44.

24. Huang Y, Lemieux MJ, Song J, Auer M, Wang DN. Structure and mechanism of the glycerol-3-phosphate transporter from Escherichia coli. Science. 2003, 301(5633):616-20.

25. Giaever G, Chu AM, Ni L, Connelly C, Riles L, Véronneau S, Dow S, Lucau-Danila A, Anderson K, André B, Arkin AP, et al. Functional Profiling of the Saccharomyces cerevisiae Genome. Nature. 2002, 418(6896):387-91.

26. Lee ME, Aswani A, Han AS, Tomlin CJ, Dueber JE. Expression-level optimization

of a multi-enzyme pathway in the absence of a high-throughput assay. Nucleic Acids Res. 2013, 41(22):10668-78.

27. Sievers F, Wilm A, Dineen D, Gibson TJ, Karplus K, Li W, Lopez R, McWilliam H, Remmert M, Soding J, Thompson JD, Higgins DG. Fast, scalable generation of high-quality protein multiple sequence alignments using Clustal Omega. Mol.Syst Biol. 2011, 7:539.

28. McLane MW, Yuan J, McCan U, Ricaurte G. Heat induces aggregation and decreases detection of serotonin transporter protein on western. Synapse 2007, 61(10):875-76.

29. Tomitori H, Kashiwagi K, Asakawa T, Kakinuma Y, Michael AJ, Igarashi K. Multiple Polyamine transport systems on the vacuolar membrane in yeast. Biochem J. 2001, 353(3):681-8.

30. Kashiwagi K, Kuraishi A, Tomitori H, Igarashi A, Nishimura K, Shirahata A, Igarashi K. Identification of the Putrescine Recognition Site on Polyamine Transport Protein PotE. J Biol Chem. 2000, 275(46):36007-12.

31. Uemura T, Tachihara K, Tomitori H, Kashiwagi K, Igarashi K. Characteristics of the Polyamine Transporter TPO1 and Regulation of Its Activity and Cellular Localization by Phosphorylation. J Biol Chem. 2005, 280(10):9646-52.

32. Marks VD, Ho Sui SJ, Erasmus D, van der Merwe GK, Brumm J, Wasserman WW, Bryan J, van Vuuren HJ. Dynamics of the yeast transcriptome during wine fermentation reveals a novel fermentation stress response. FEMS Yeast Res. 2008, 8(1):35–52.

33. Giger L, Caner S, Obexer R, Kast P, Baker D, Ban N, Hilvert D. Evolution of a designed retro-aldolase leads to complete active site remodeling. Nat Chem Biol. 2013, 9(8):494-8.

34. Romero PA, Arnold FH. Exploring protein fitness landscapes by directed evolution. Nat Rev Mol Cell Biol. 2009, 10(12):886-76.

35. Graf L, Craik CS, Patthy A, Roczniak S, Fletterick RJ, Rutter WJ. Selective alteration of substrate specificity by replacement of aspartic acid-189 with lysine in the binding pocket of trypsin. Biochemistry.1987, 26:2616–23.

36. Rana S, Pozzi N, Pelc LA, Di Cera E. Redesigning allosteric activation in an enzyme. Proc Natl Acad Sci USA. 2011, 108(13):5221-25.

37. Rajagopalan S, Wang C, Yu K, Kuzin AP, Richter F, Lew S, Miklos AE, Matthews ML, Seetharaman J, Su M, Hunt JF, Cravatt BF, Baker D. Design of activated serine-containing catalytic triads with atomic level accuracy. Nat Chem Biol. 2014, 10(5):386-91.

38. Buchan DWA, Minneci F, Nugent TCO, Bryson K, Jones DT. Scalable web services for the PSIPRED Protein Analysis Workbench. Nucleic Acids Res. 2013, 41(Web Server issue):W340-W348.

39. Nugent T, Jones DT. Transmembrane protein topology prediction using support vector machines. BMC Bioinformatics. 2009, 10:159.

40. Jones DT. Improving the accuracy of transmembrane protein topology prediction using evolutionary information. Bioinformatics. 2007, 23(5):538-44.

41. Jones DT, Taylor WR, Thornton JM. A Model Recognition Approach to the Prediction of All-Helical Membrane Protein Structure and Topology. Biochemistry. 1994, 33(10):3038-49.

Chapter 3
Engineering Tpo1 for the Efflux of Medium-Chain Alcohols

INTRODUCTION

Worldwide, people are looking toward greener, more sustainable energy sources. Biofuels are one attractive energy source. However, most desirable fuel molecules are toxic to the production organisms, which limits biofuel titers. A promising strategy for combating this toxicity is to use transporters to actively remove biofuels from the cell. Removing biofuels has the dual advantage of decreasing toxicity within the cell and increasing extracellular concentrations, which can simplify recovery processing. The efflux process also permits the use of the extracellular space as a metabolic sink, reducing intracellular product such that the pathway is pulled forward and inhibition is minimized.

In general, there are few native pumps known to act on biofuel-relevant molecules. Solvents such as toluene can be effluxed by the Ttg and Mex transporter families in *Pseudomonas putida* [1]. Transporters for molecules such as geraniol [2] and zeaxanthin, a biofuel-like molecule [3] were identified and can be heterologously expressed in *E. coli*. Medium-chain alcohol substrates are particularly underrepresented, either by lack of necessity on the part of organisms or because such pumps are yet to be discovered. Nonetheless, there are some examples; for instance, the srpABC pump from *P. putida* can efflux octanol [1]. Recently, it was shown that over-expression of the yeast ABC pump Pdr18 increases tolerance to ethanol [4]. The RND pump AcrB has been successfully engineered to remove *n*-butanol from *E. coli* [5]. To our knowledge, there are not any native *S. cerevisiae* pumps that act upon the biofuel molecules *n*-butanol or *n*-hexanol, nor have any been engineered to efflux these substrates. We chose to re-engineer an *S. cerevisiae* pump for biofuel specificity.

The pump we chose as a basis for engineering, Tpo1, has been studied in the context of tolerance toward polyamines, drugs, and medium-chain fatty acids [6,7]. Recently, it was shown that overexpression of Tpo1 and related antiporters Tpo2, Tpo3, and Tpo4, did not improve *S. cerevisiae* tolerance to ethanol [5]. Medium-chain alcohols such as *n*-butanol and *n*-hexanol are more structurally similar to native substrates than ethanol. Both polyamines and fatty acids have medium length hydrocarbon tails with polar “handles,” very much like medium chain alcohols. Thus, the Tpo1 transporter is a good basis for engineering medium-chain alcohol specificity.

For this work, we went beyond simply over-expressing or creating knock-outs of Tpo1. We attempted to modulate substrate specificity of the Tpo1 transporter, in order to increase activity upon *n*-butanol and *n*-hexanol. Unfortunately, we were unable to achieve this goal.

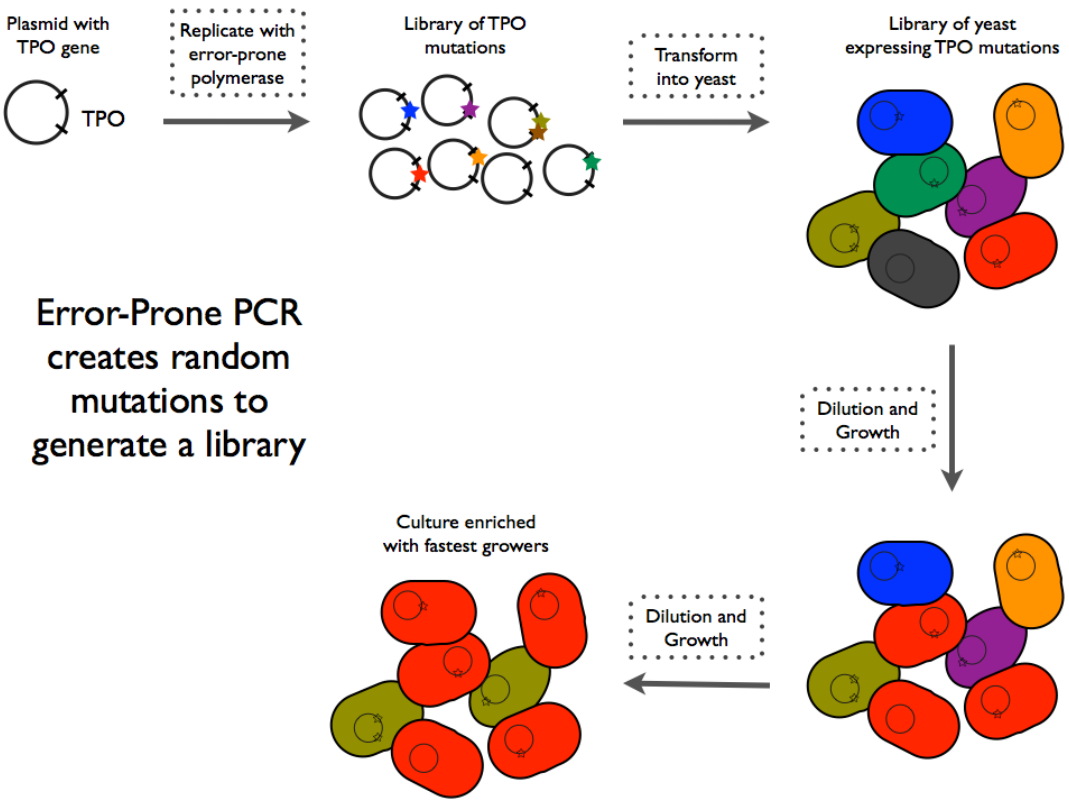

Figure 3.1. Strains can be improved via competitions of libraries generated by error-prone PCR. A library of Tpo1 mutations is generated with error-prone PCR. The library is transformed into wild-type *S. cerevisiae.* This library is competed under selective conditions, such as in 1.0% *n*-butanol or 0.12% *n*-hexanol. The competition is sub-cultured daily into fresh media with alcohols until the most fit strains take over the culture by virtue of their higher growth rates. The competition enriched in fast-growing strains is plated, and single colonies are selected and characterized.

RESULTS

A model competition establishes how fast tolerant strains overtake competition cultures. Our strategy for engineering a transporter for butanol was to generate libraries of mutated transporters using error-prone PCR, then compete strains expressing these transporters in media containing alcohols, as shown in Figure 3.1.To determine how fast tolerant strains would overtake cultures, we set up a model competition, using strains with varying levels of hexanol tolerance. The development of these strains is detailed in Chapter 4. We started with a wild-type transformed with an Emerald plasmid, and added in varied-tolerance strains containing mKate at 10^4, 10^5, and 10^6 dilutions. We used strains with growth rates of 0.12 (wild-type), 0.17 (sSD009) and 0.27 (sSD002) in 0.12% *n*-hexanol, to show the effects of different tolerance levels. The results of this competition are shown in Figure 3.2

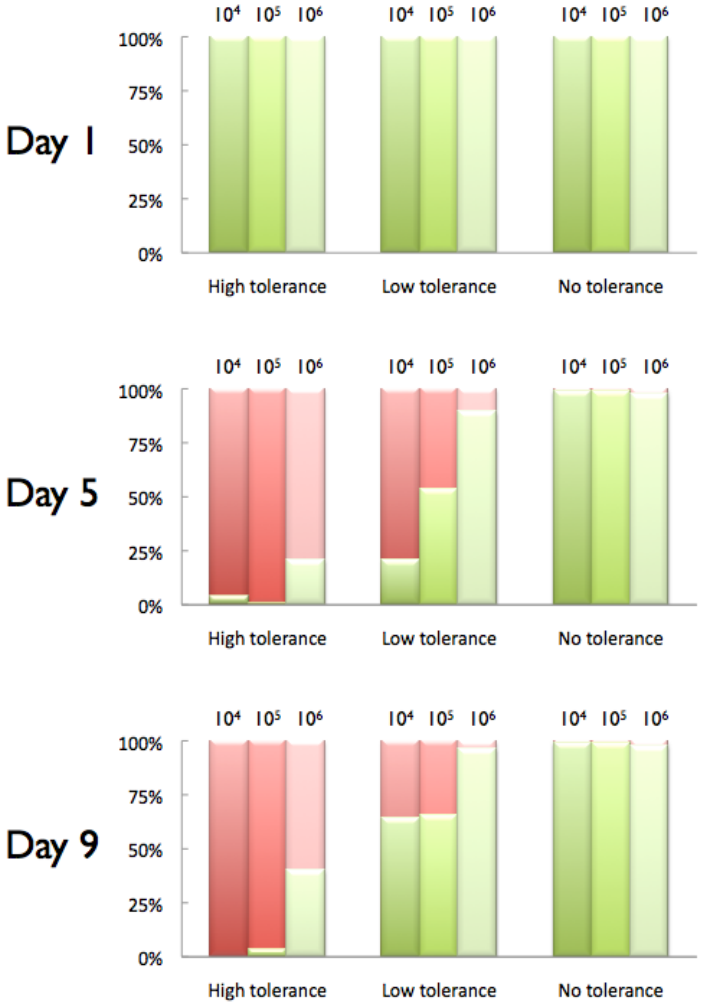

Figure 3.2. Model competition shows that tolerant strains can quickly take over a culture. *S. cerevisiae* strains with high and low tolerance (described in Chapter 4) were transformed with RFP expressing plasmids and diluted 1:10^4, 1:10^5, or 1:10^6 in wild-type *S. cerevisiae* transformed with an Emerald-expressing plasmid. Cells were grown in 0.12% *n*-hexanol with daily subculturing to 1:100. After 5 and 9 days, competitions were plated to single colonies, and counts of RFP and Emerald expressing colonies were recorded.

By day 5, the highly tolerant strain easily overtakes the culture at all dilution levels (Figure 3.2, middle panel). The low tolerance strain comprises approximately 75% of the culture of the 10^4 dilution, approximately 50% of the 10^5 dilution, and is now detectable in the 10^6 dilution. On day 9, the results vary significantly from the expected trend. It seems that the wild-type strains expressing Emerald have begun to re-take the cultures at the expense of the tolerant strains expressing mKate. This is likely due to beneficial genomic mutations arising in the Emerald-expressing strains.

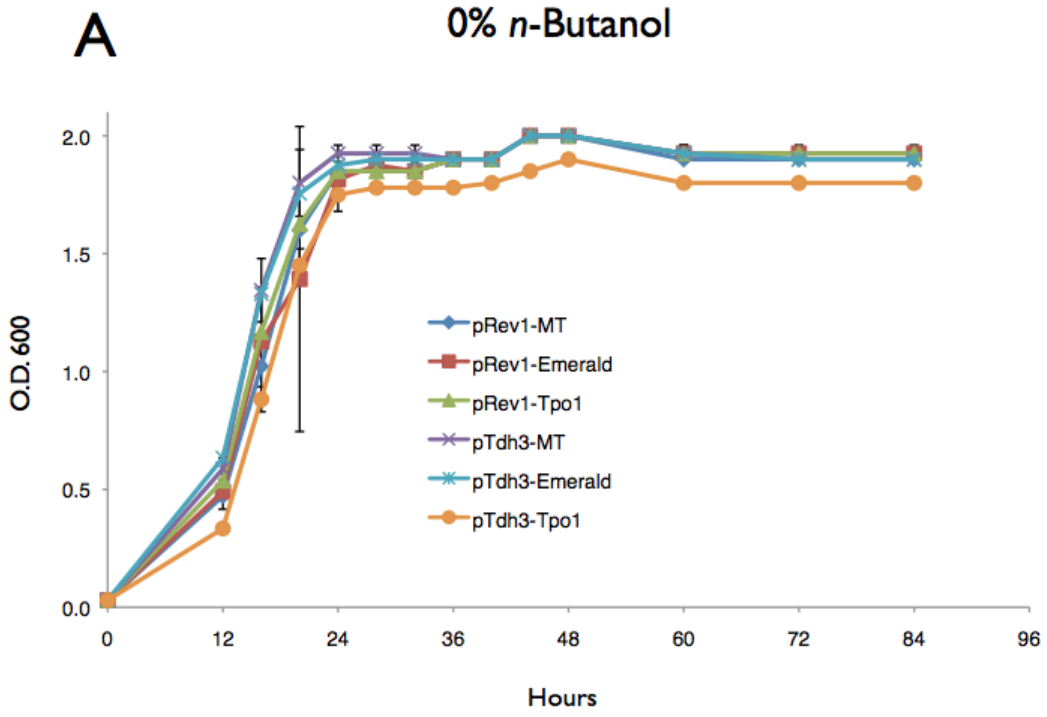
A
0% n-Butanol
O.D. 600
Hours
pRev1-MT
pRev1-Emerald
pRev1-Tpo1
pTdh3-MT
pTdh3-Emerald
pTdh3-Tpo1

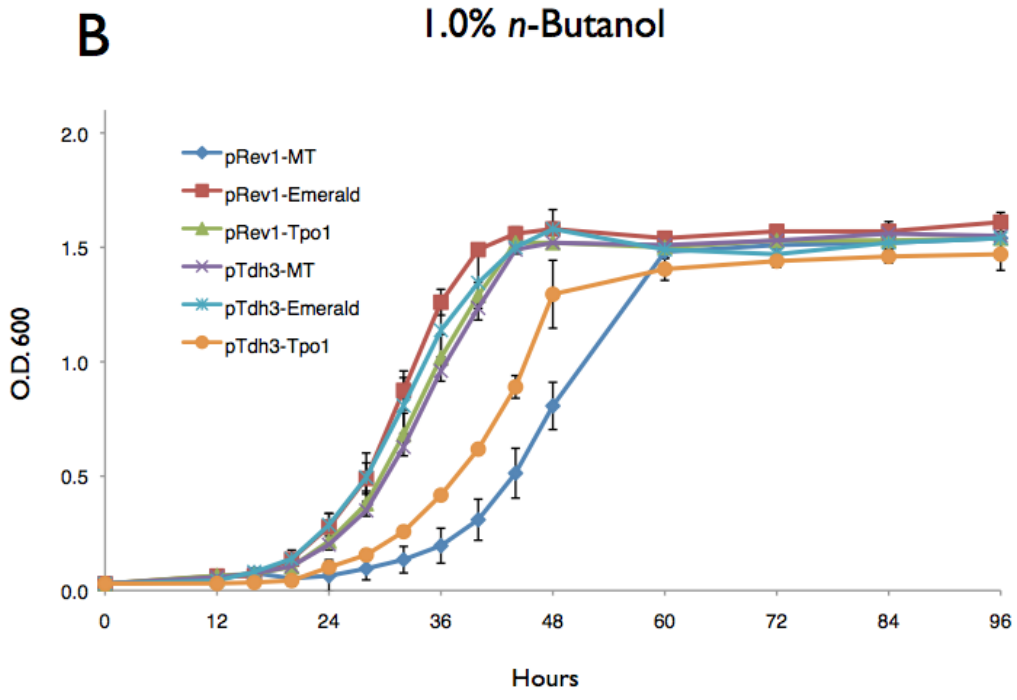
B
1.0% n-Butanol
O.D. 600
Hours
pRev1-MT
pRev1-Emerald
pRev1-Tpo1
pTdh3-MT
pTdh3-Emerald
pTdh3-Tpo1

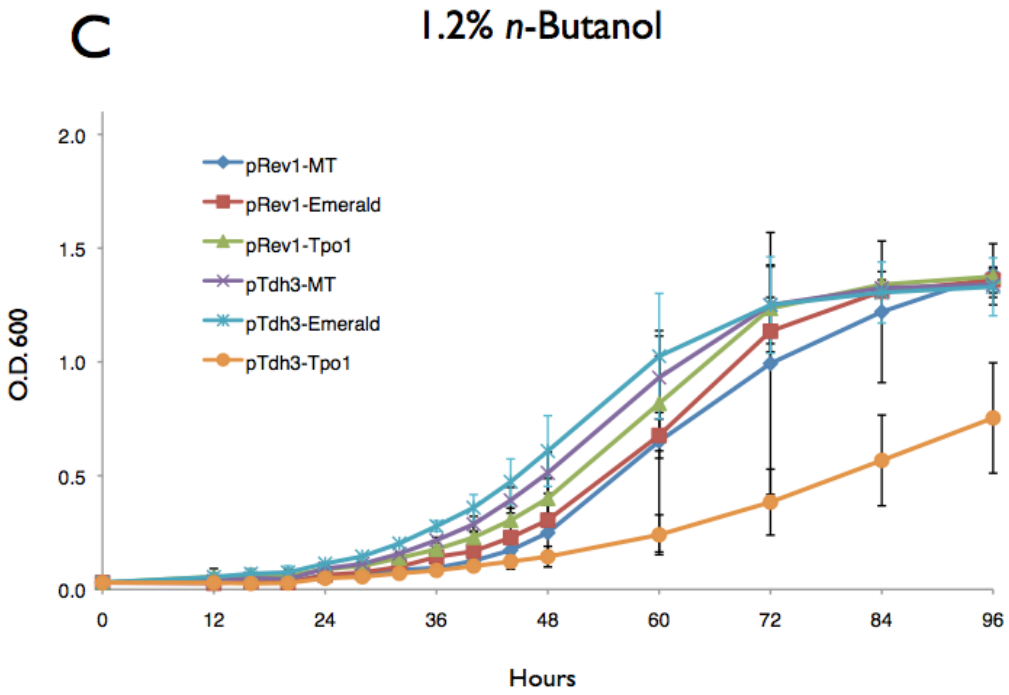

Figure 3.3. Tpo1 does not improve tolerance toward *n*-butanol. *S. cerevisiae* transformed with plasmids containing the Rev1 or Tdh3 promoter and empty vector (MT), Emerald, or Tpo1 were grown in A) SD-Leu media B) SD-Leu + 1.0% *n*-butanol or C) SD-Leu + 1.2% *n*-butanol.

Tpo1 does not improve tolerance toward n*-butanol.* We tested whether the overexpression of Tpo1 under the low-strength Rev1 promoter or the high-strength Tdh3 promoter could improve growth rates in the presence of *n*-butanol. Wild-type *S. cerevisiae* strains expressing Tpo1, Emerald (a yeast-optimized GFP version), or empty vector had approximately the same growth rates in SD-Leu media, as seen in Figure 3.3A. The exception is the strain harboring Tpo1 under the Tdh3 promoter, which had a lower growth rate. We hypothesize that this is due to toxic effects of the transporter at these high expression levels, and is not surprising given the characterization work we did on Tpo1 overexpression in Chapter 2. In 1.0% and 1.2% *n*-butanol (Figure 3.3B and 3.3C), the the strains expressing Tpo1 failed to improve growth rates above the Emerald and empty vector controls. Overexpression of Tpo1 did not confer improved growth rates in the presence of *n*-butanol, though this does not preclude an engineered version from improving butanol tolerance.

Strains expressing *a library of variants of Tpo1 did not improve tolerance toward* n-*butanol.* We generated three libraries of approximately 10^4 colonies using the non-optimal dNTP method, with varying mutation rates. Using Mutazyme, we generated two small libraries of about 500 colonies each, at low and high mutation rates. After 14 days of competition in 0.1% *n*-hexanol and 1.0% *n*-butanol, we plated competitions to single colonies and screened colonies for alcohol tolerance. Figure 3.3 shows an experimental outline. Unfortunately, none of the colonies had consistently better growth rates in the presence of alcohols. In Figure 3.4, we show that one hexanol competition winner is reproducibly more tolerant, though the improvement is extremely slight. None of the butanol competition winners were significantly more tolerant.

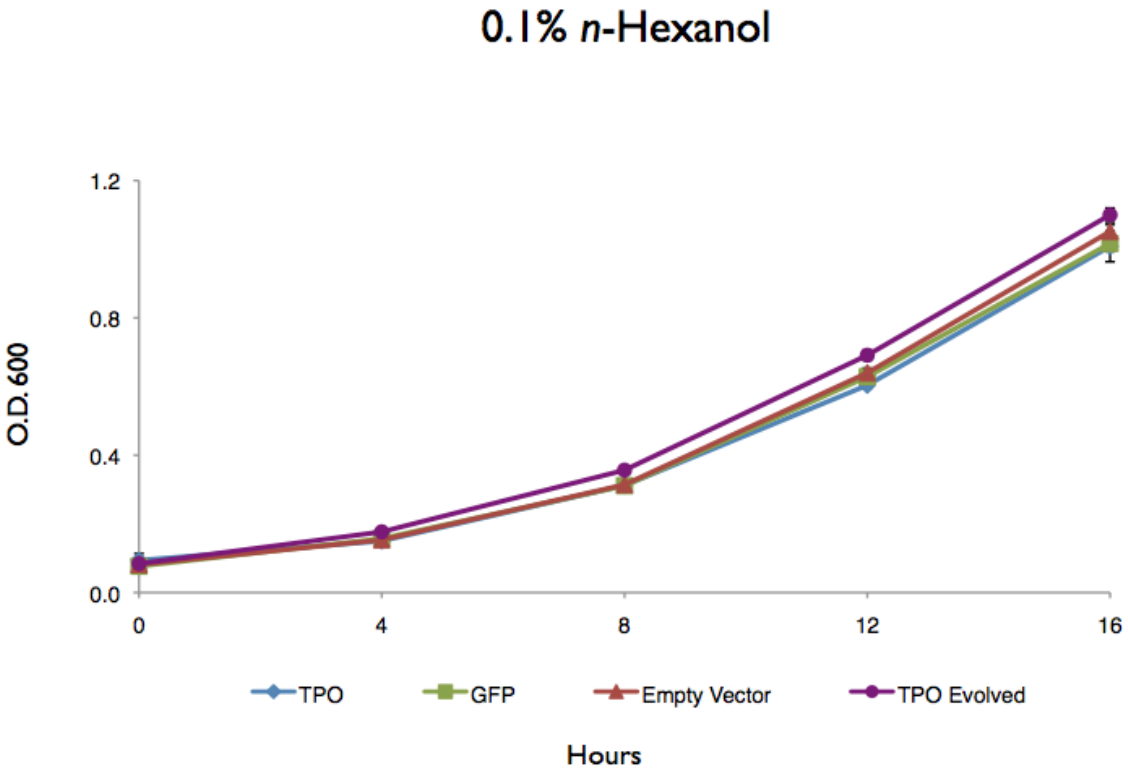

Figure 3.4. Hexanol competition winner has slightly improved growth in 0.1% *n*-hexanol. *S. cerevisiae* transformed with a mutated Tpo1 plasmid from the competition was grown in SD-Leu media + 0.1% *n*-hexanol alongside control strains expressing empty vector, Emerald, and unmutated Tpo1.

Competitions selected for strain improvements rather than Tpo1 improvements. We back-transformed plasmids from hexanol competition winners into wild-type yeast and found that any tolerance improvement was lost. We show in Figure 3.5 that 9 different strains carrying back-transformed plasmids have approximately the same growth rates as strains carrying an unmutated Tpo1-expressing plasmid or control plasmids expressing Emerald or empty vector. Next, we compared a larger sample of competition winners to back-transformed plasmids, as shown in Figure 3.6. We screened 93 colonies from both butanol and hexanol competitions at both 7 and 14 days against back-transformed plasmids. After the butanol competition, back-transformed plasmids are less tolerant than original library or unmutated Tpo1 after 7 days, but the large error bars on the samples makes interpretation tenuous. The data from the hexanol competition is similarly plagued with large error bars. The trends, however, are toward back-transformed plasmids having lower tolerance than the strains that went through the competition.

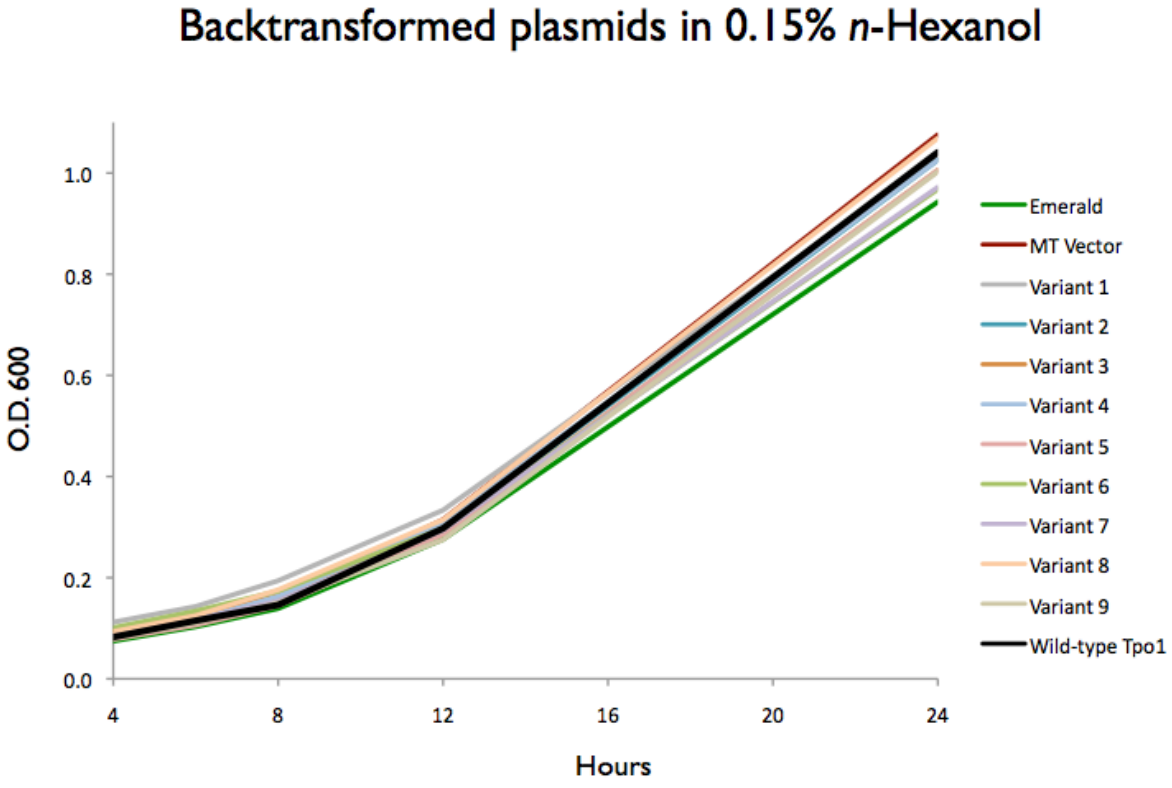

Figure 3.5. Backtransformed plasmids do not help growth in 0.1% *n*-hexanol. *S. cerevisiae* were transformed with mutated Tpo1 plasmids miniprepped from competition winners. Strains were grown in SD-Leu media + 0.1% *n*-hexanol alongside controls expressing empty vector, Emerald, and unmutated Tpo1.

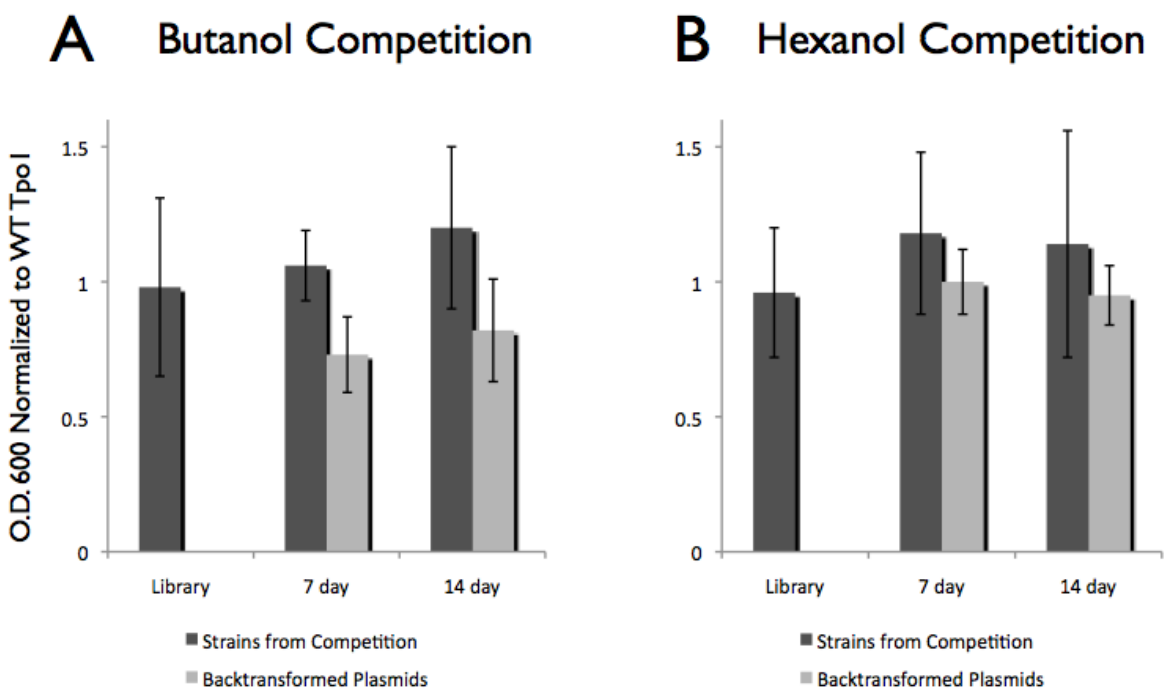

Figure 3.6. Tpo1 plasmids are not responsible for tolerance of competition winners. *S. cerevisiae* transformed with a mutated Tpo1 plasmid library. 93 colonies were picked and grown in 1% *n*-butanol or 0.12% n-hexanol. 93 colonies plated after 7 days of competition were picked and grown in 1.2% *n*-butanol or 0.12% *n*-hexanol. Plasmids were transformed into wild-type yeast and 93 colonies were picked and grown in 1.2% *n*-butanol or 0.12% *n*-hexanol. 3 colonies of wild-type Tpo1 were grown as controls.

DISUCSSION

Tpo1 overexpression did not increase growth rate in the presence of *n*-butanol. Moreover, at high overexpression levels the transporter itself was detrimental to growth even in the presence of toxic concentrations of butanol. This follows what we learned in Chapter 2: namely that Tpo1 overexpression is detrimental and the native promoter has established an optimal expression level. González-Ramos *et al.* recently screened a yeast deletion library for *n*-butanol activity. They did not report any significant Tpo1 involvement in butanol tolerance [10]. Additionally, Tpo1 does not affect ethanol tolerance [5]. Taken together, we conclude that wild-type Tpo1 is not active on short-chain alcohols.

With such a varied group of substrates, we expect Tpo1 to have flexible and accommodating substrate binding sites, so that we could easily introduce mutations without reducing activity. As we learned by engineering AcrB for *n*-butanol specificity,

whole-genome mutagenesis is effective [4]. We used both error-prone PCR with non-optimal dNTPs and a polymerase engineered to make mutations, Mutazyme II, to generate several small libraries of the gene encoding Tpo1. It is likely that our small library sizes was too limiting, as we did not find any Tpo1 variants that improved tolerance to alcohols.

Interestingly, we did see a trend of increased tolerance to *n*-hexanol, though back-transformation showed that it was not due to the mutated Tpo1 plasmid. When we further examined the tolerance levels of strains that had been through the competition versus those harboring the back-transformed plasmids, we found that the strains apart from the Tpo1 plasmids had some improved tolerance. We reasoned that genomic mutations were likely obscuring any improvements due to the Tpo1 library, resulting in our competition strategy being biased toward the more effective genomic mutations. The rapid response of the yeasts to *n*-hexanol was intriguing, prompting us to explore the phenomenon further. We will discuss these results in Chapter 4.

We set up model competition experiments in order to look more closely at tolerance evolution, so we could design more effective competition protocols. We competed Emerald-expressing wild-type *S. cerevisiae* against mKate-expressing strains with three tolerance levels. mKate strains were diluted into a population of Emerald strains at $1{:}10^4$, $1{:}10^5$, or $1{:}10^6$ ratios, to mimic a variety of library sizes. These cultures were grown in 0.12% *n*-hexanol and diluted 1:100 daily, as would be done for a library competition. At days 5 and 9, we plated samples of each culture, then counted the red vs. green populations. We saw that the highly tolerant strains easily overtook the cultures at all dilution levels by day 5. Any Tpo1 mutations that increased solvent tolerance to this extent would easily be uncovered from a library after such a competition. The low tolerance strains were successful in taking over the cultures as well, though the percentages varied depending on the starting dilutions. It is interesting to note that while the day 5 trends correlate with the starting dilution, the actual values do not match what would be predicted mathematically: ie, the 10^5 dilution is not 1/10th that of the 10^4 dilution. By day 9, the experimental results were noticeably different than would be expected. In the 10^6 dilution of high-tolerance strains, the wild-type strain increased in prevalence, which suggests that some of the originally wild-type yeasts had acquired mutation(s) that conferred a high level of tolerance as well. In competitions with the low-tolerance strain, the wild-type strains are also gaining back lost ground. For competitions of plasmid-based libraries in highly-evolvable solvents such as *n*-hexanol, it is necessary to back-transform plasmids every 5 days, in order to prevent genomic mutations from skewing results. Another option is to execute the competitions in a strain that has been evolved for solvent tolerance. The Tpo1 library competitions were done over a 14 day period, so it is likely that any tolerance improvements from Tpo1 mutations were obscured by genomic mutations that improved tolerance. This may explain why they were unsuccessful.

To our knowledge, medium-chain alcohol tolerance, apart from butanol, has not been explored in *S. cerevisiae*. The wild-type strains were extremely amenable to tolerance-improving mutations. We took this unexpected opportunity to develop strains of *S. cerevisiae* that are tolerant to medium-chain alcohols, which will be discussed fully in Chapters 4 and 5. Though evolutions of Tpo1 for medium-chain alcohol efflux were unsuccessful, we learned a great deal about competition design. The importance of

back-transforming competition libraries was clear, especially under evolution-friendly conditions. Future directed evolutions will include back-transformation steps.

MATERIALS AND METHODS

Strains and Media

Saccharomyces cerevisiae strain BY4741 (*MAT*a *his3Δ1 leu2Δ0 met15Δ0 ura3Δ0*), derived from strain S288C was used for all experiments. Yeasts were transformed with plasmids containing the *Leu2* auxotrophic marker and selected and grown on synthetic dropout media without leucine (SD-Leu: 0.67% Yeast Nitrogen Base, 2% alpha-Dextrose, 0.2% amino acid mix without leucine from US Biological).

Genetic Methods

The Tpo1 gene was cloned out of the genome using primers SDa27
5'-TAAATCGATACTGCATTTCTAGGCATATCCAGCGAGATCTatgtcggatcattctcccat-3'
and SDa28
5'-AAATCATAAATCATAAGAAATTCGCCTCGAGttaGGATCCttaagcggcgtaagcatact-3'
and homologously recombined into plasmid pSD279, a gift from the Dueber lab.

Error-prone PCR: Non-optimal dNTP

Each reaction contained 2.5 uL each forward and reverse primers at 10 mM, 10 µL 5X GoTaq buffer, 2 µL dNTP mix (5 mM dATP, 5 mM dGTP, 25 mM dCTP, 25 mM dTTP), 11 µL 25 mM $MgCl_2$, 1 µL GoTaq, 1 µL template at 100 ng/µL, and 20 µL H_2O. The PCR cycle was: 95°C 2', 32X[95°C 30", 53°C 30", 72°C 2'], 72°C 10'. PCRs were run in a Bio-Rad C1000 and S1000 thermocyclers. For the Tpo1 library, primers were SDa27 and SDa28, and the template was pSD266.

Error-prone PCR: Mutazyme

Each reaction contained 1 uL each forward and reverse primers, 5 µL 10X Mutazyme buffer, 1 µL 10 mM dNTP mix, 1 µL Mutazyme II, 1 µL template, and 40 µL H_2O. Templates were at 10, or 100 ng/µL to give varying mutagenesis levels. PCR cycle was: 95°C 2', 32X[95°C 30", 52°C 30", 72°C 2'], 72°C 10'. PCRs were run in a Bio-Rad C1000 and S1000 thermocyclers. For the Tpo1 library, primers were a27 and a28, and the template was pSD266. For the Tpo1 library, primers were SDa27 and SDa28, and the template was pSD266.

Library generation

PCR products were cleaned up using the DNA Clean & Concentrator-5 kit from Zymo Research. Vector pSD266 was digested with BglII and BamHI, vector band was excised from a 1% agarose gel (1% agarose, 40 mM Tris, 20 mM acetate, 1 mM EDTA, pH 8.0) and extracted using the DNA Clean & Concentrator-5 kit from Zymo Research. 1000 ng PCR product and 500 ng vector were transformed into wild-type yeast using the LiOAC method [8]. Ten transformations were done simultaneously and plated on SD-Leu plates. Plates were resuspended in SD-Leu and aliquots were saved as glycerol stocks.

Competition

Libraries were grown overnight in SD-Leu media. Cultures were subcultured daily by 1:10 dilution into SD-Leu media containing 1% or 1.2% n-butanol, or 0.10% or 0.12% n-hexanol for a total of 14 days. Cultures were grown in a 30°C water-bath shaker at 200 rpm. At the end of the evolution, glycerol stocks were made and culture was streaked to single colonies on plates.

Model competition
Strains BY4741 (wild-type), sSD002, and sSD009 were transformed with plasmids pSD270 or pSD268, and plated on SD-Leu agar plates. Single colonies were picked and grown 2 days in 5 mL SD-Leu media in culture tubes. Saturated cultures were diluted to an OD_{600} of 0.300 using the nanodrop. 5 mL of sSD001-pSD270 was aliquoted into a screw-cap tube. Strains sSD001, sSD002, and sSD009 containing pSD268 were added at a 10^4, 10^5, or 10^6 ratio. 5 mL SD-Leu + 0.24% *n*-hexanol was added to each tube and cultures were grown in a 30°C water-bath shaker at 200 rpm. Cultures were subcultured daily 1:10 into fresh SD-Leu media + 0.12% *n*-hexanol. At days 5 and 9, 1 uL of culture was plated on SD-Leu plates. Red vs. green colonies per plate were counted and charted.

Growth Curves
Single colonies were picked into 5 mL SD-Leu media in culture tubes. Cultures were grown overnight to saturation at 30°C with 280 rpm shaking. Stationary phase cultures were diluted to an OD_{600} of .300-.330 as measured with a Nanodrop 2000c, 5 mL dilute culture was aliquoted into screw-cap tubes. 5 mL SD-Leu plus appropriate amount of alcohols was added. Each sample was run in triplicate. Screw-cap tubes were grown at 30°C with 280 rpm shaking and measurements were taken every 2 hours with Genesys-20 spectrophotometer.

Table 3.1 Strains and Plasmids used in this study

Plasmid	Promoter	Insert	Marker	Reference
pSD266	pRev1	Tpo1	Leu2	This Study
pSD279	pRev1	Emerald	Leu2	Lee et al. [9]
pSD306	pRev1	MT	Leu2	This Study
pSD270	pTdh3	Emerald	Leu2	Lee et al. [9]
pSD268	pTdh3	mKate	Leu2	Lee et al. [9]
pSD280	pTdh3	Tpo1	Leu2	This Study
pSD307	pTdh3	MT	Leu2	This Study

Strain	Parent	Genotype	Reference
BY4741		*MATa his3Δ1 leu2Δ0 met15Δ0 ura3Δ0*	
sSD002	BY4741	*BY4741 GCD1-E85 CIT2-C338*	Chapter 4
sSD009	BY4741	*BY4741 evolved*	Chapter 4

REFERENCES

1) Kieboom J, Dennis JJ, de Bont JAM, Zylstra GJ. Identification and molecular characterization of an efflux pump involved in Pseudomonas putida S12 solvent tolerance. J. Biol. Chem. 1998, 273:85-91.

2) Dunlop MJ, Dossani ZY, Szmidt HL, Chu HC, Lee TS, Keasling JD, Hadi M, Mukhopadhyay A. Engineering microbial biofuel tolerance and export using efflux pumps. Mol. Syst. Biol. 2011, 7:487.

3) Doshi R, Nguyen T, Chang G. Transporter-mediate biofuel secretion. PNAS 2013, 110(19):7642-7647.

4) Teixeira MC, Fernandes AR, Mira NP, Becker JD, Sá-Correi I. Early transcriptional response of Saccharomyces cerevisiae to stress imposed by the herbicide 2,4-dichlorophenoxyacetic acid. FEMS Yeast Res. 2006, 6(2):230-48.

5) Fisher MA, Boyarskiy S, Yamada MR, Kong N, Bauer S, Tullman-Ercek D. Enhancing tolerance to short-chain alcohols by engineering the Escherichia coli AcrB efflux pump to secrete the non-native substrate n-butanol. ACS Syn Bio 2013, 3(1): 348-354.

6) Teixeira MC, Godinho CP, Cabrito TR, Mira NP, Sá-Correia I. Increased expression of the yeast multidrug resistance ABC transporter Pdr18 leads to increased ethanol tolerance and ethanol production in high gravity alcoholic fermentation. Microb Cell Fact. 2012,11:98.

7) Legras JL, Erny C, Jeune CL, Lollier M, Adolphe Y, Demuyter C, Delobel P, Blondin B, Karst F. Activation of Two Different Resistance Mechanisms in Saccharomyces cerevisiae upon Exposure to Octanoic and Decanoic Acids. Appl Environ Microbiol. 2010, 76(22):7526–7535.

8) Sá-Correia I, dos Santos SC, Teixeira MC, Cabrito TR, Mira NP. Drug:H+ antiporters in chemical stress response in yeast. Trends Microbiol. 2008, 17(1): 22-31.

9) Geitz D, St Jean A, Woods RA, Schiestl RH. Improved method for high efficiency transformation of intact yeast cells. Nucleic Acids Res. 1992, 20(6):1425.

10) Lee ME, Aswani A, Han AS, Tomlin CJ, Dueber JE. Expression level optimization of a multi-enzyme pathway in the absence of a high-throughput assay. Nucleic Acids Res. 2013, 41(22):10668-10678.

11) Gonzalez-Ramos D, van den Broek M, van Maris AJA, Pronk JT, Daran JMG. Genome-scale analyses of butanol tolerance in Saccharoymces cerevisiae reveal an essential role of protein degradation. Biotechnol Biofuels. 2013,

Chapter 4
Evolving Strains for Medium-chain Alcohol Tolerance

ABSTRACT

For microbially-produced biofuels to be cost-effective, high production titers need to be achieved. One cause of low titers is the biofuels themselves, which are toxic and decrease growth rates and cell viability. Improving production organism tolerance can help improve titers by allowing cells to continue growth and production in higher biofuel concentrations. Toward the goal of highly tolerant production hosts, we have evolved a laboratory strain of *S. cerevisiae* to be more tolerant toward the medium-chain alcohol *n*-hexanol. These evolved strains display log-phase growth rates more than double that of the wild-type strain in the presence of toxic levels of *n*-hexanol. The hexanol evolution yielded strains with log-phase growth rates of 0.27 /hr in YPD media with 0.1% *n*-hexanol, whereas for wild-type strain K = 0.12 /hr under the same conditions. A second round of evolution starting with these more tolerant strains further improved tolerance. In 0.18% hexanol, K = 0.1 /hr for round two strains, K = 0.06 /hr for round one strains, and the wild type does not have significant growth. The phenotype is stable in the absence of solvent pressure, and is dominant: when mated with a non-tolerant yeast, the diploids have tolerance levels matching those of the tolerant haploid strains. The tolerance extends to other medium-length alcohols such as *n*-pentanol and *n*-heptanol. We have sequenced the genomes and found that the responsible mutations are $Gcd1^{D85E}$ and $Sui2^{D77Y}$. Re-creating these mutations in a wild-type strain confirmed that they confer tolerance to the *S. cerevisiae*. These results will be useful for engineering effective biofuel production hosts.

INTRODUCTION

Biofuels are a promising alternative to traditional fuel sources that are fraught with negative environmental impacts and rising costs. Medium-chain alcohols such as *n*-butanol and *n*-hexanol have higher energy densities and less corrosivity than ethanol, making them promising biofuel molecules [1]. However, these solvents are toxic and are thus produced at low levels [2]. Lamsen and Atsumi explain that toxicity of solvents prevents strains from reaching industrial production titers [3]. One way to combat low titers is to improve tolerance toward industrially relevant solvent concentrations, thus allowing the cell to survive higher solvent levels and thus produce more biofuels.

S. cerevisiae is an attractive biofuel production host because it is genetically tractable and resistant to phage infection, and industrial fermentations are well established. Since humans first started using the yeast *S. cerevisiae* for ethanol production, strains have naturally evolved for growth in fermentative conditions and high ethanol tolerance. Modern advances permitted lab-scale investigations to determine several specific mutations that improve tolerance to ethanol. Recently, Stanley et al showed that strains evolved for ethanol tolerance using spontaneous mutation outperformed strains from evolutions employing chemical mutation (though they did not report which mutations were responsible for tolerance improvements) [4]. These lab-

scale evolutions have continued to improve upon thousands of years of evolution, and at the same time as reveal valuable insights into genetic and regulatory mechanisms of ethanol tolerance.

Laboratory evolutions have also been designed to improve butanol tolerance. Gonzalez-Ramos and co-workers investigated the impact of libraries of overexpressed and knocked-out genes in order to assess butanol stress responses and pinpoint target proteins for tolerance optimization [5]. In that study, protein degradation pathways were found to be key in minimizing butanol toxicity. Several proteins involved in butanol tolerance have been uncovered through evolution experiments. For example, mitochondrial proteins are upregulated under isobutanol stress [6]. Gonzalez-Ramos *et al.* identified mutations in RPN4, a proteasome transcription factor, and RTG1, another transcription factor involved in intraorganelle communication [5]. A mutated version of glycerol-3-phosphatase (Gpp2) also confers higher isobutanol tolerance [6]. Although these evolutionary experiments led to enhanced understanding of the proteins involved in tolerance, the evolved strains had only marginally improved *n*-butanol tolerance levels.

We carried out evolutions of *S. cerevisiae* in *n*-butanol and *n*-hexanol. To our knowledge, strain evolution had not previously been used to improve tolerance toward alcohols with more than four carbons. Even though *n*-hexanol production in yeast has only been demonstrated, we elected to preemptively improve strain tolerances. Additionally, we expected that tolerance to longer chain lengths might require different mutations than those beneficial in butanol evolutions, thereby uncovering new tolerance mechanisms. The *n*-hexanol tolerance evolutions were successful, improving growth rates in alcohols from five to eight carbons. The tolerant phenotype is stable and dominant and is caused by mutations Gcd1^{D85E} and Sui2^{D77Y}.

Chemostats for Microaerobic Evolutions

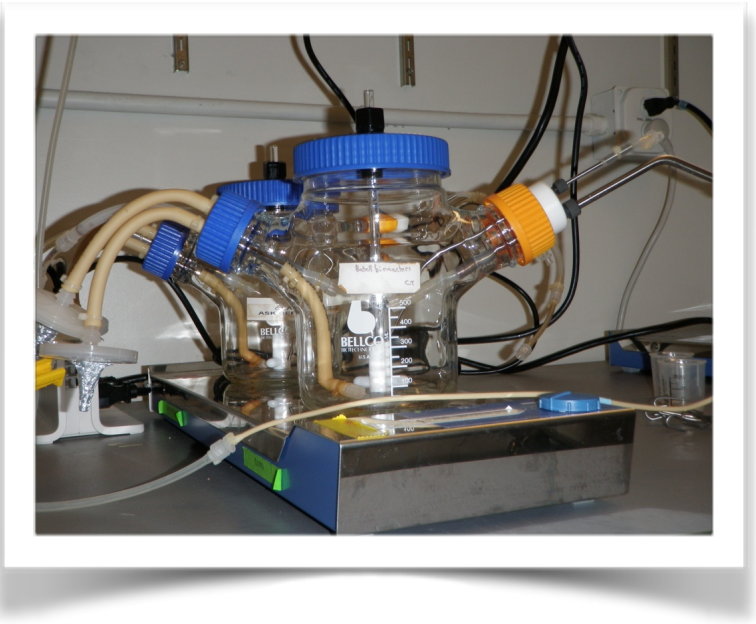

Figure 4.1. Chemostats simplify anaerobic evolutions. Fresh media enters a port on the left and spent media and cells are removed via the right port, maintaining log phase culture.

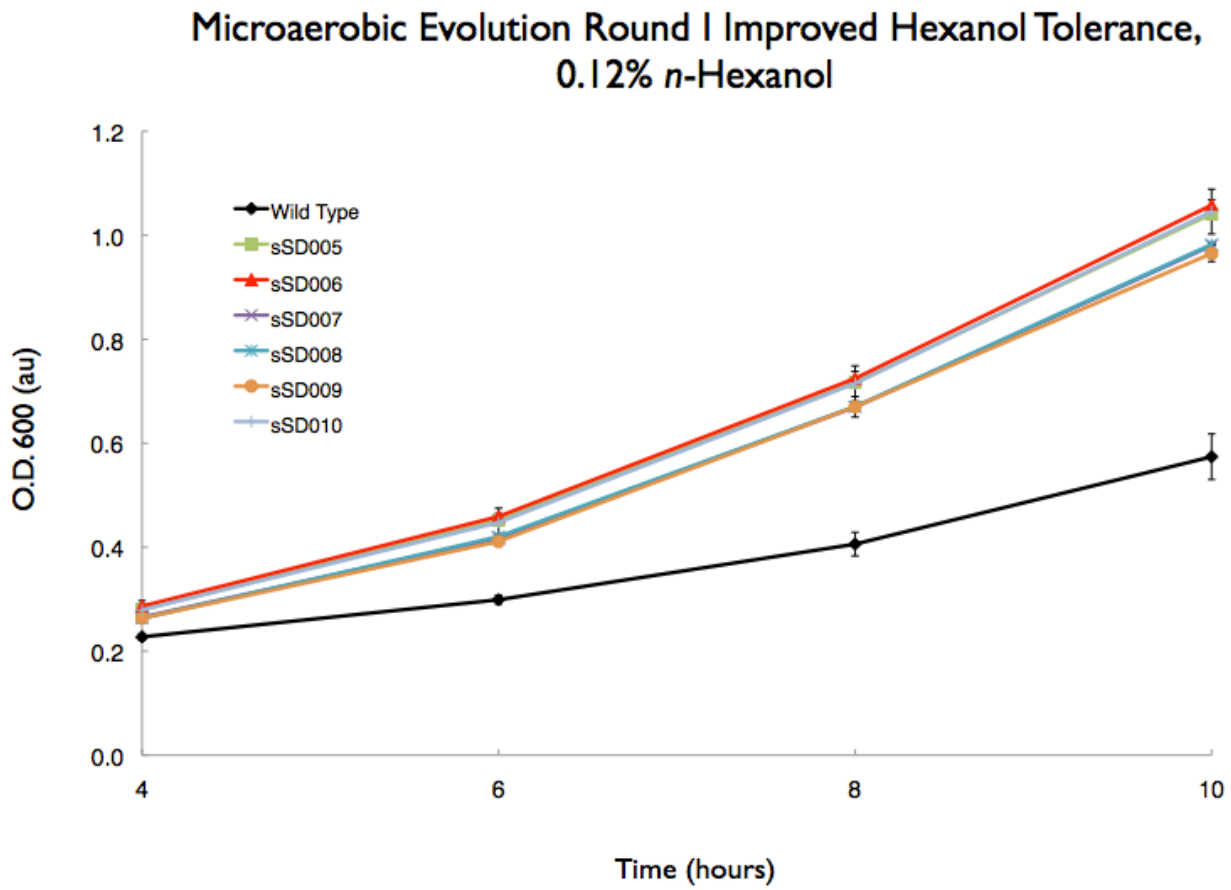

Figure 4.2. Microaerobically evolved strains have improved growth rates in 0.12% *n*-hexanol when compared to the wild type. Growth was monitored by measuring OD_{600} of cultures grown aerobically in YPD + 0.15% *n*-hexanol v/v. Wild type is shown in a solid black line. Strains from round I evolution are shown in colored lines. Samples are run in triplicate and error bars represent standard deviations.

RESULTS

Evolutions. We ran one set of evolutions in chemostats, using increasing concentrations of *n*-butanol and *n*-hexanol. The chemostats (Figure 4.1) did not have air inlets/outlets, so the culture was microaerobic, mimicking conditions that would be found in large-scale fermentation tanks. Chemostats were difficult to maintain in sterile condition, resulting in a bacteria, *Staphylococcus warneri*, overtaking the cultures at various intervals. *S. warneri* was the only significant contaminant: *E. coli* and a long rod-shaped bacteria that was likely *Lactobacillus* were also present, but these bacteria were unable to outcompete the yeast at the high alcohol concentrations. The *n*-butanol evolution failed to produce strains that had an improved growth rate in the presence of *n*-butanol. The *n*-hexanol evolution produced one strain, sSD006, which had significantly improved growth rate in the presence of *n*-hexanol (Figure 4.2).

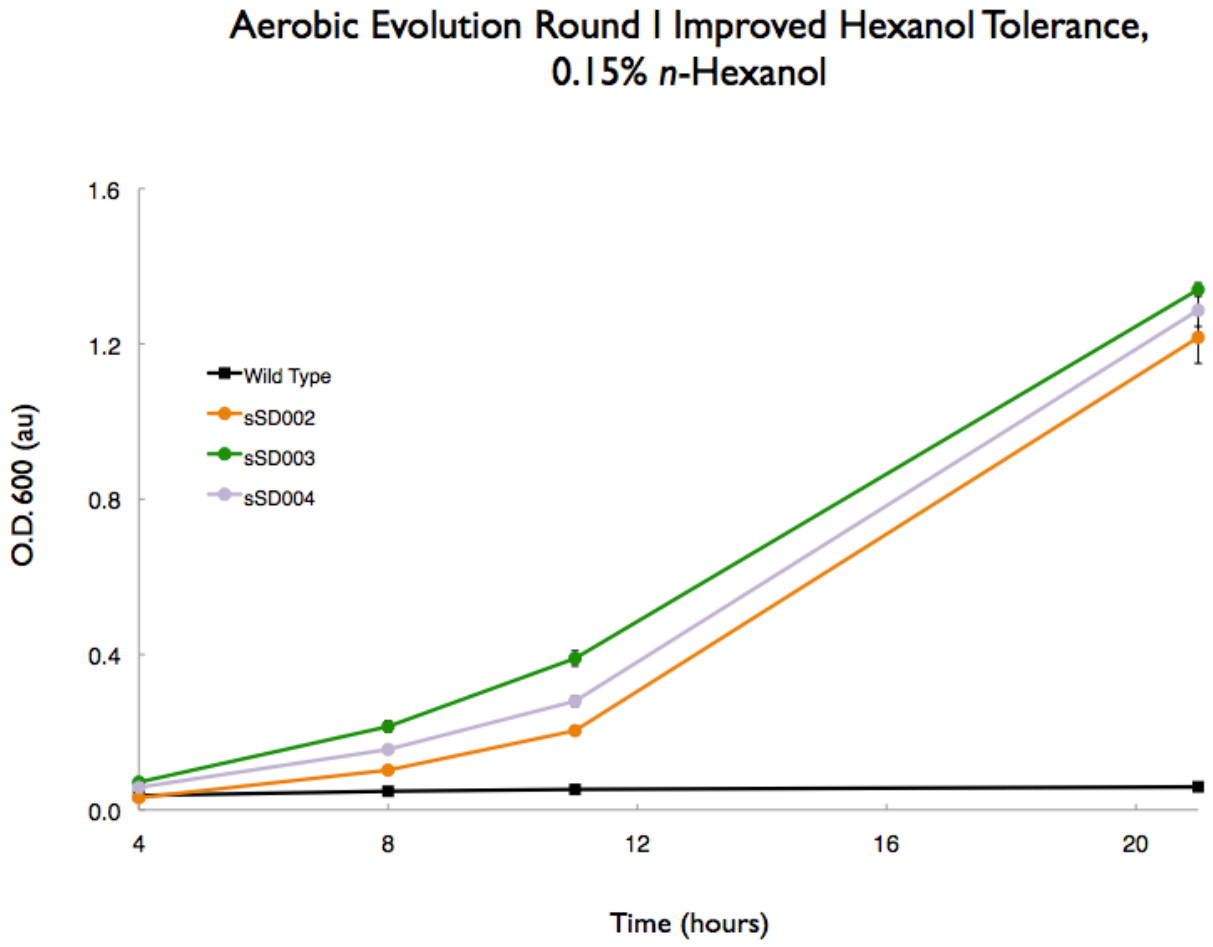

Figure 4.3. Aerobically evolved strains show greatly improved growth rates in 0.15% *n*-hexanol when compared to the wild type. Growth was monitored by measuring OD_{600} of cultures grown aerobically in YPD + 0.15% *n*-hexanol v/v. Wild type is shown in a solid black line. Strains from round I evolution are shown in colored lines. Samples are run in triplicate and error bars represent standard deviations.

We ran another set of evolutions aerobically, via daily dilution in screw-cap tubes. Again, the butanol evolutions failed to produce strains that had an improved growth rate in the presence of *n*-butanol. The hexanol evolutions produced several strains with improved growth rates, of which sSD002, sSD003, and sSD004 were the most successful (Figure 4.3). In round II, we tried aerobic evolutions in YPD and SC media. The YPD media produced strains with improved growth rates, while the SC media evolutions did not. The best strains from round II were sSD019, derived from sSD003, and sSD021, derived from sSD006 (Figure 4.4).

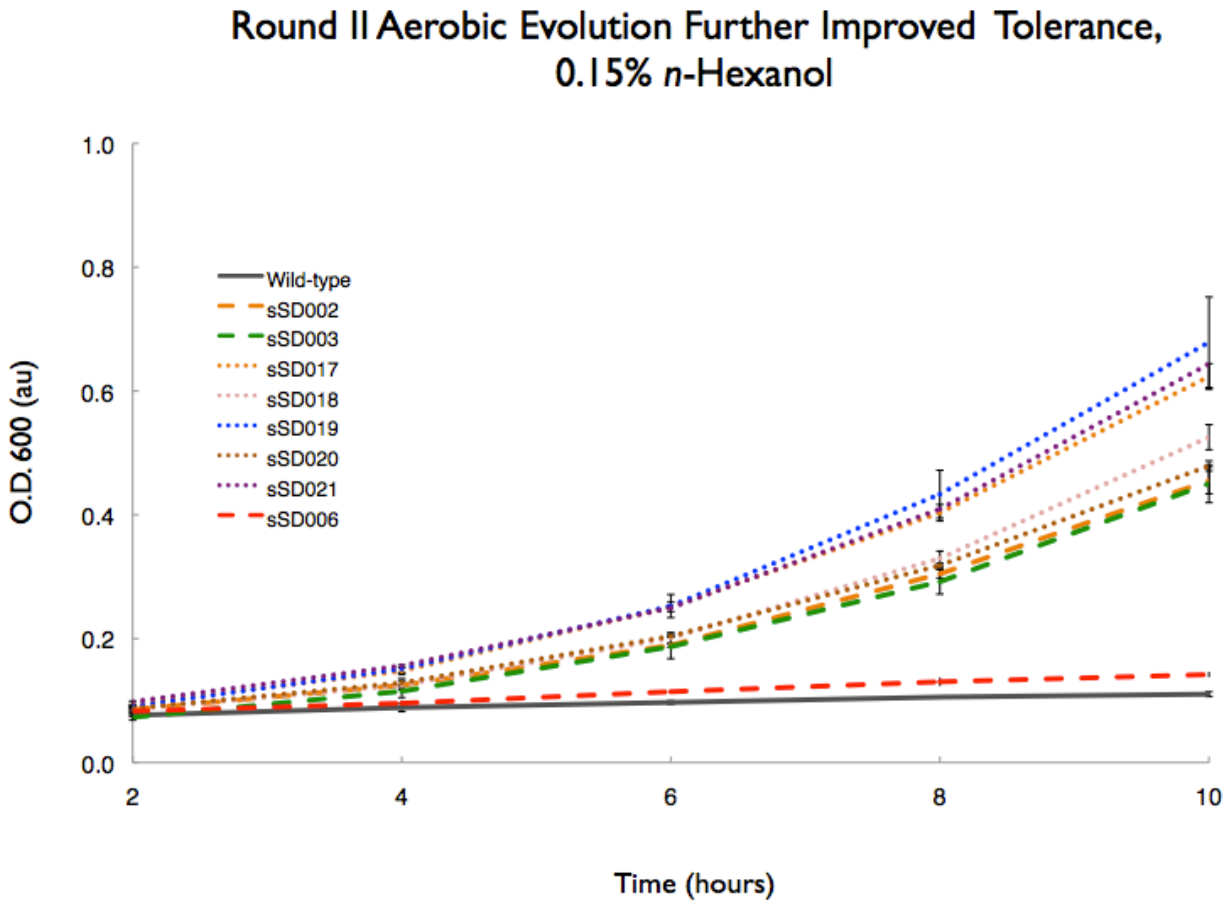

Figure 4.4. A second round of aerobic evolution further enhanced growth rates in 0.15% *n*-hexanol. Growth was monitored by measuring OD_{600} of cultures grown aerobically in YPD + 0.15% *n*-hexanol v/v. Wild type is shown in a solid black line. Strains from round I evolution are shown in dashed lines. Strains from round II evolution are shown in dotted lines. Samples are run in triplicate and error bars represent standard deviations.

Characterization. We characterized several evolved strains for tolerance to a variety of alcohols. Figure 4.4 shows growth rates of evolved strains in YPD + 0.15% *n*-hexanol. The wild-type yeast (black line) is viable but not noticeably growing under these conditions. sSD006 (red dashed line), which came from the microaerobic evolution, has a slight growth rate improvement. Strains sSD002 and sSD003 (green and blue dashed lines) have significant growth rate improvements in *n*-hexanol. Round II evolutions further improved growth rates. There was a large jump in tolerance as strain sSD006 gained extra mutations in strain sSD021 (red dotted line). sSD003 evolved further to sSD019 (blue dotted line), though the improvement was not as dramatic as for sSD021.

Strain	Evolution Round	Mutations	BuOH	PtOH	HxOH	HpOH	OcOH
Wild Type	-	-	0	0	0	0	0
sSD003	I	*GCD1* D85E	+	++	+++	++	++
sSD019	II	*GCD1* D85E	+	+++	++++	++++	+++
sSD006	I	*GCD7* R56C	0	0	+	+	0
sSD021	II	*SUI2; GCD7* D77Y; R56C	0	+++	++++	++++	+++

Table 4.1. Evolved strains show improved tolerance toward medium-chain alcohols, particularly *n*-hexanol and *n*-heptanol. A) Qualitative assessment of evolved strain tolerances based on growth rate improvements in the presence of toxic levels of alcohols. Growth rates (h^{-1}); 0 = 0.0 - 0.03; + = 0.04 - 0.10; ++ = 0.11 - 0.17; +++ = 0.18 - 0.24; ++++ ≥ 0.25. Growth rates were based on three experimental days with n=3 each day. Butanol tolerance is based on final OD_{600} after 48 hrs, rather than growth rate. BuOH: *n*-butanol, 1.2%. PtOH: *n*-pentanol, 0.5%. HxOH: *n*-hexanol, 0.15%. HpOH: *n*-heptanol, 0.05%. OcOH: *3*-octanol, 0.05%.

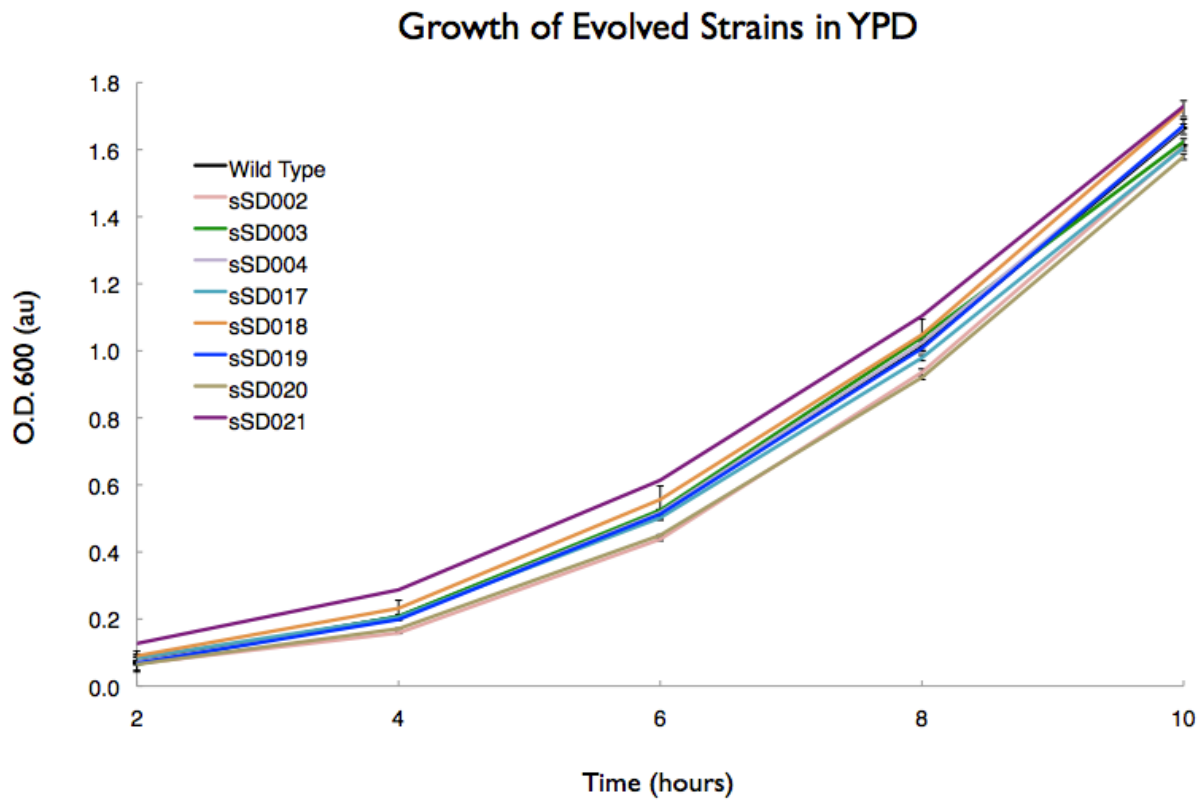

Figure 4.5. Evolved strains have the same growth phenotype in unstressed media. Growth was monitored by measuring OD_{600} of cultures grown aerobically in YPD. Wild type is shown in a solid black line. Evolved strains are shown in colored lines. Samples are run in triplicate and error bars represent standard deviations.

We characterized strains sSD003, sSD019, sSD006, and sSD021 for tolerance to other alcohols, as detailed in Table 4.1. The wild-type level of tolerance was considered to be 0, as these strains had a negligible growth rate. Growth rates of 0.0-0.03 were marked as 0 tolerance. Growth rates of 0.04-0.10 were listed as +, 0.11-0.17 were listed as ++, 0.18-0.24 were listed as +++, and growth rates of 0.25 and over were listed as ++++. sSD006 had minimal tolerance improvements, and only for *n*-hexanol and *n*-heptanol. sSD003 had improved tolerance to *n*-hexanol, but tolerance levels dropped off for shorter or longer carbon chains. Strains sSD019 and sSD021 from the second round of evolution had the highest tolerance levels to all alcohols. Unfortunately, *n*-butanol tolerance was only seen for strains sSD003 and sSD019, and the tolerance improvement is minimal. In YPD without alcohols, the wild-type and evolved strains have indistinguishable growth (Figure 4.5).

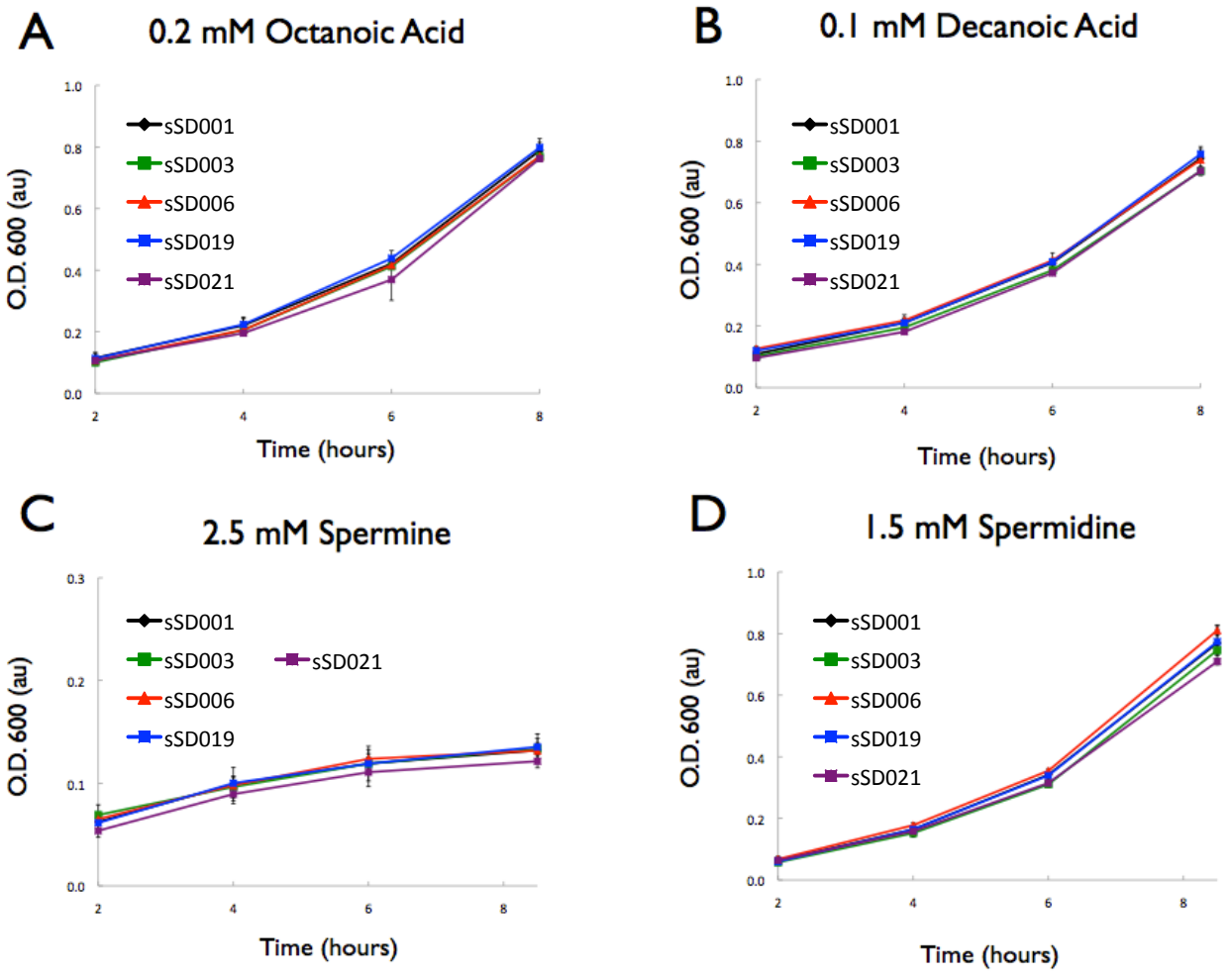

Figure 4.6. Evolved strains show greatly improved growth rates in 0.15% n-hexanol when compared to the wild type. Growth was monitored by measuring OD_{600} of cultures grown aerobically in YPD + A) 0.2 mM Octanoic acid, B) 0.10 mM decanoic acid, C) 2.5 mM Spermine or D) 1.5 mM Spermidine. Wild type is shown in a solid black line. Evolved strains are shown in colored lines. Samples are run in triplicate and error bars represent standard deviations.

The evolved strains have tolerance that is specific for medium-chain alcohols. We also examined their tolerance toward 0.4 and 0.6 mM octanoic acids (Figure 4.6A) and 0.2 and 0.4 mM decanoic acids (Figure 4.6B), but did not see improved growth rates with the exogenous addition of these fatty acids. We next tested growth in the presence of the polyamines, spermine (Figure 4.6C) and spermidine (Figure 4.6D), but no tolerance improvement was seen at multiple concentrations of each polyamine

Evolved strains are also hexanol tolerant in anaerobic conditions. We examined the strains with 0.15% n-hexanol, and observed that the aerobically evolved strains all grew much better than the wild-type strain even when grown under the anaerobic conditions of a sealed, oxygen-free test tube(Figure 4.7A). As expected, the microaerobically evolved strains retained tolerance in anaerobic conditions (Figure 4.7B), though they did not perform better than aerobically evolved strains sSD002, sSD003, or sSD004.

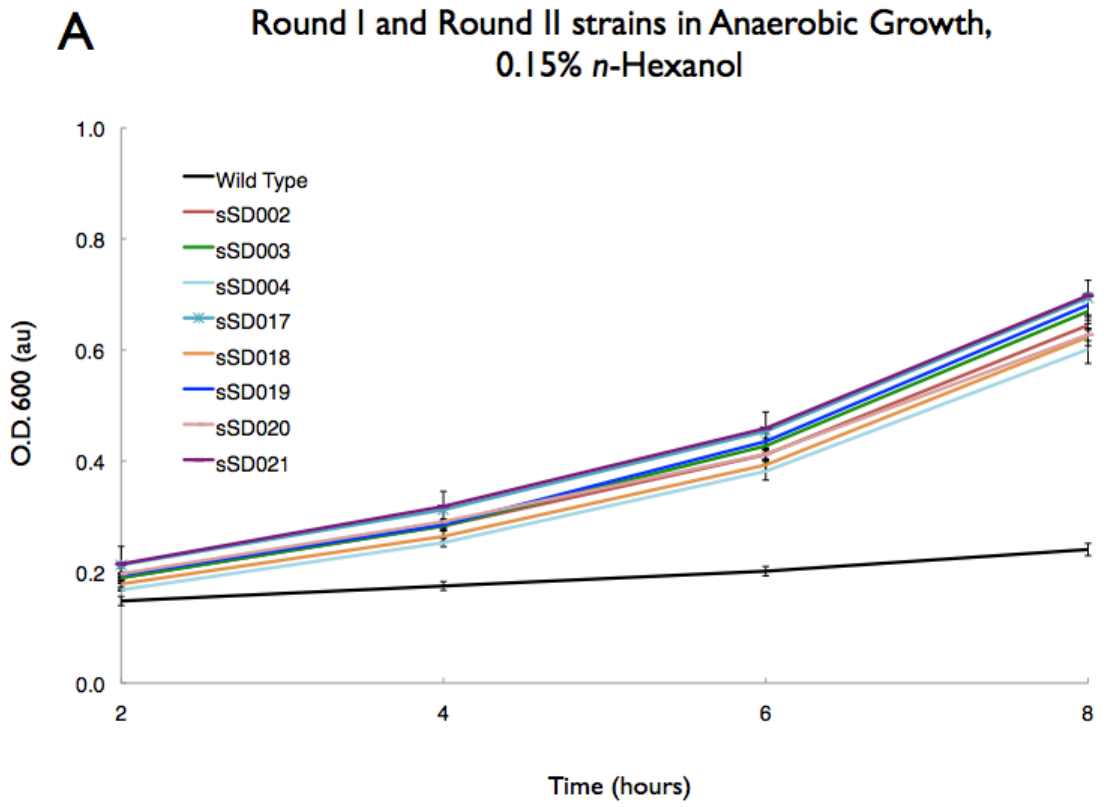

Figure 4.7. Evolved strains maintain improved growth rates in 0.15% *n*-hexanol under anaerobic conditions. Cultures in YPD + 0.15% *n*-hexanol were flushed with argon prior to growth. Anaerobic growth was monitored by measuring OD_{600}. Samples are run in triplicate and error bars represent standard deviations. A) Wild type is shown in a solid black line. Aerobically evolved strains are shown in colored lines. B) Wild type is shown in a solid black line. Aerobically evolved strains are shown in colored lines.

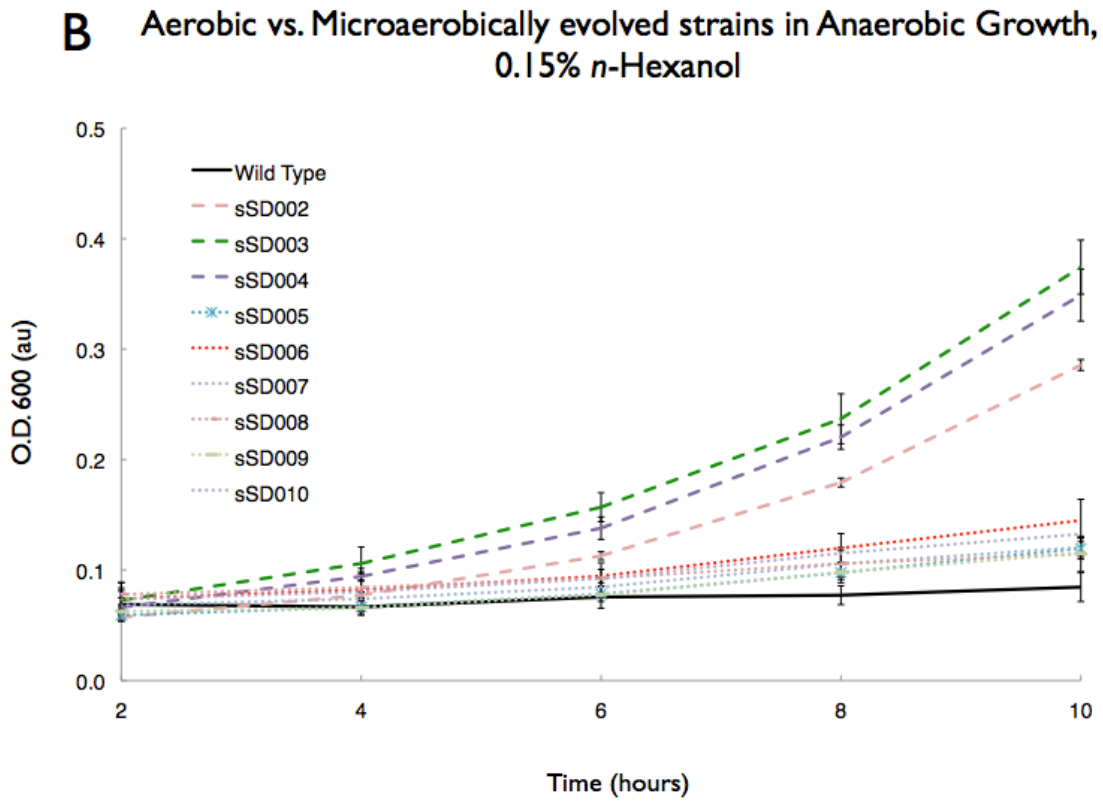

Growth in medium-chain alcohols causes yeasts to flocculate. We grew wild type yeast and strains sSD003 and sSD019 in YPD and YPD + 0.15% *n*-hexanol. We took images to compare flocculation phenotypes, and found that the strains evolved for tolerance appear to be flocculating at the same level as the wild-type strain, as seen in Figure 4.8D-E. When grown without hexanol (Figure 4.8A-C), the strains had the same non-flocculating morphology.

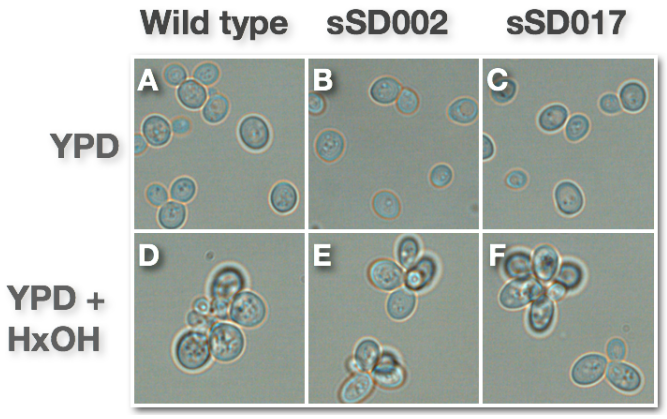

Figure 4.8. Growth in 0.15% *n*-hexanol causes yeasts to flocculate. The evolved strains had a similar morphology to the wild-type when grown in 0.15% *n*-hexanol. Images were taken using brightfield microscopy. A-C) YPD media D-F) YPD + 0.15% *n*-Hexanol v/v. A,D) Wild-type. B,E) sSD002. C,F) sSD017.

We determined that the tolerant phenotype is stable, and is likely a genetic mutation rather than a transient adaptation. We streaked evolved strains on YPD plates weekly for 8 weeks, in order to allow for growth without selective pressure. Growth in 0.15% *n*-hexanol was then monitored. In Figure 4.9A, strains sSD002, sSD003, and sSD004 grew relatively well in hexanol, while the wild type was not noticeably growing. Figure 4.9B shows growth of the round II evolved strains after 8 weeks without selective pressure. They are again growing more quickly than the wild-type, and have not lost their evolved tolerance. This suggest that genomic mutations are responsible for the tolerance.

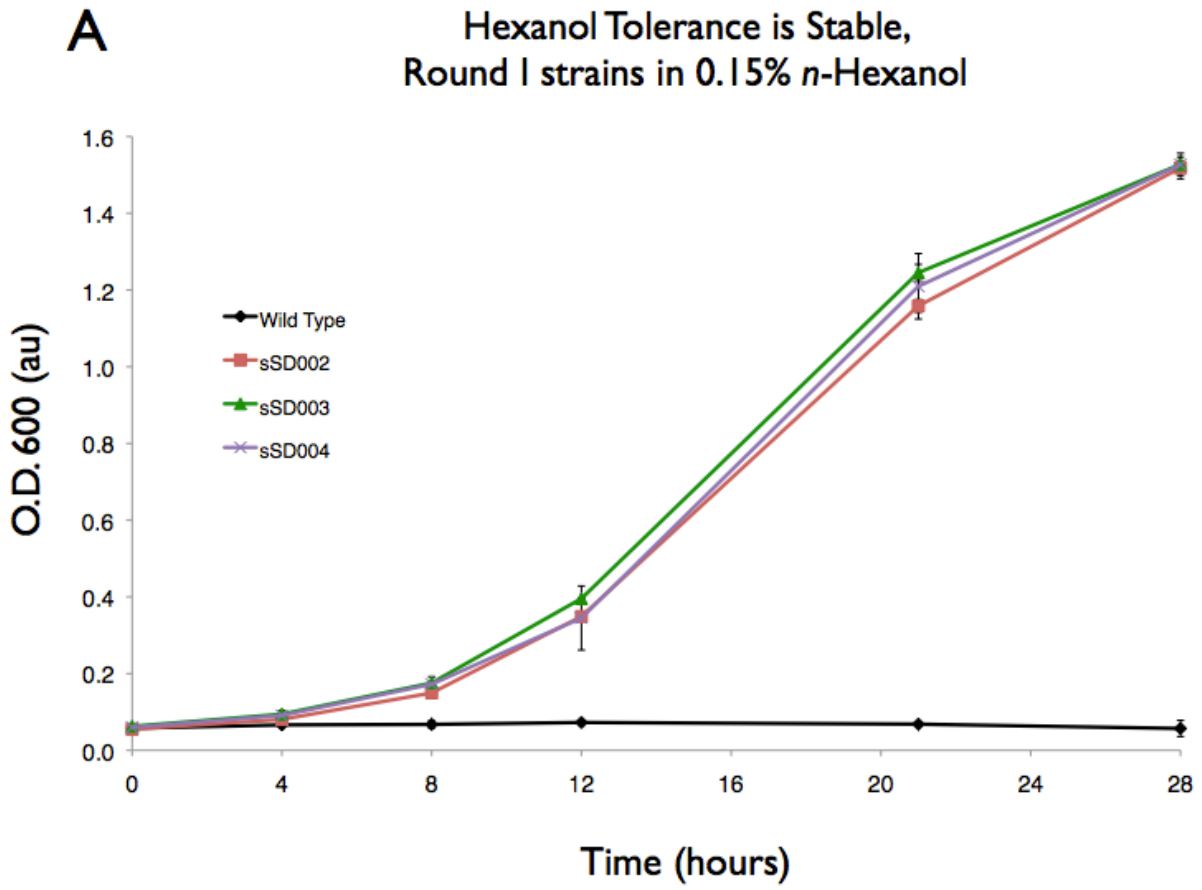

Figure 4.9. Evolved hexanol tolerance is maintained after 8 weeks without selective pressure. Strains were grown on YPD plates for 8 weeks, with strains streaked to single colonies weekly. Growth of these colonies was monitored by measuring OD_{600} of cultures grown aerobically in YPD + 0.15% *n*-hexanol. Cultures were flushed with argon prior to growth. Wild type is shown in a solid black line. Evolved strains are shown in colored lines. Samples are run in triplicate and error bars represent standard deviations. A) Aerobically evolved strains from round I compared to wild type. B) Aerobically evolved strains from round II, compared to wild type and strain sSD002 from round I.

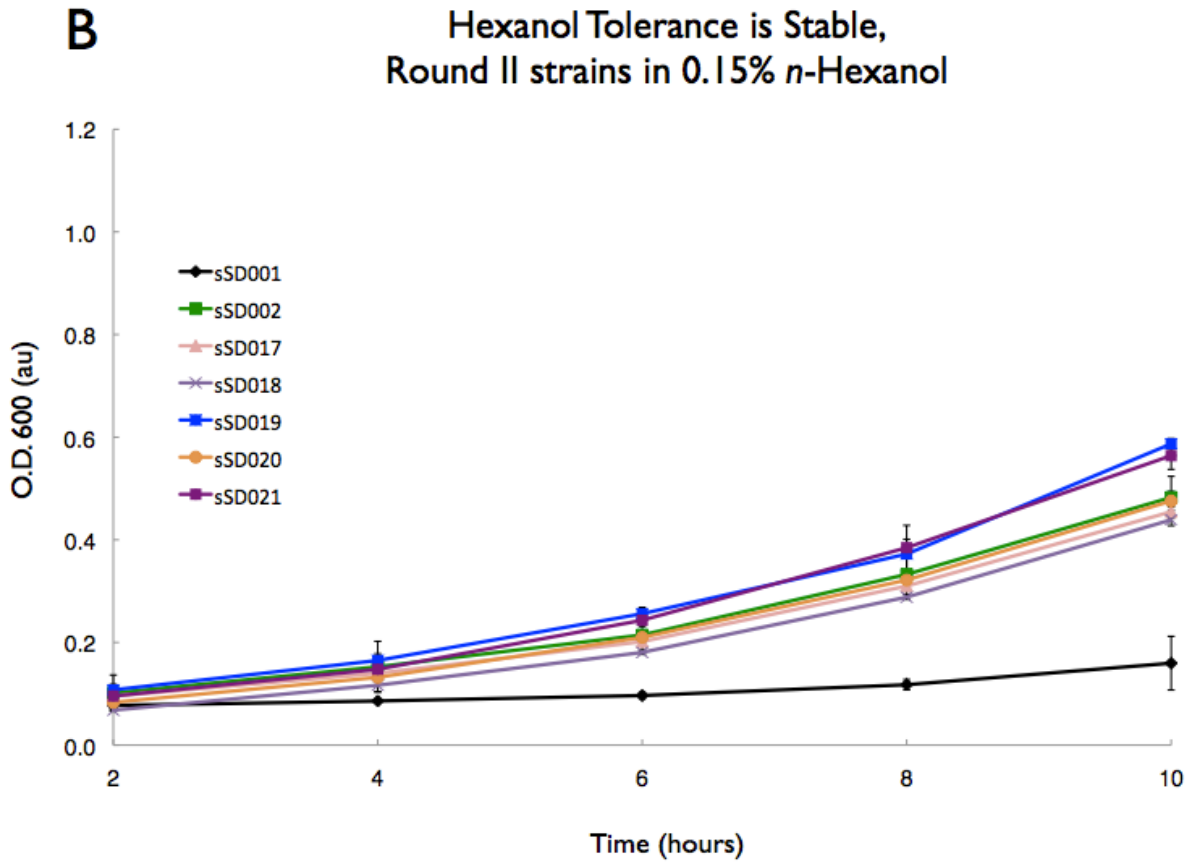

	Tolerant : non-tolerant					Tetrads
Parent Strain	4:0	3:1	2:2	1:3	0:4	Counted
sSD002	40%	60%	40%	0%	0%	14
sSD003	6%	28%	66%	0%	0%	32
sSD017	0%	14%	79%	7%	0%	29
sSD018	0%	4%	86%	11%	0%	28
sSD019	0%	7%	9%	7%	0%	29
sSD020	8%	56%	36%	0%	0%	25
sSD021	0%	29%	43%	29%	0%	28
sSD022	8%	52%	67%	0%	0%	25
Total	5%	27%	61%	7%	0%	210

Table 4.2. Tetrad Tolerance Assessment shows one gene is responsible for tolerance. Tolerance was scored based on final OD_{600} after 24 hour growth in 0.15% *n*-hexanol in 96-well blocks.

Genomic Characterization Working under the assumption of a genetic basis for alcohol tolerance, we used tetrad analysis to determine that one mutation per strain was responsible for tolerance. The evolved strains were derived from BY4741, which has mating type MATa. We mated the tolerant strains with wild type BY4742, which has mating type MAα. The resulting diploids were sporulated, and full tetrads selected and sorted. The four daughter cells were grown in YPD + 0.15% *n*-hexanol and tolerance was assessed by growth after 24 hours. Table 4.2 tabulates the ratios of tolerant to non-tolerant daughter cells from each tetrad. Tetrads from strain sSD002 seem to have more tolerant daughter cells than from the other parent strains. This may be due to an imperfect scoring system or errors during tetrad selection. Overall, a 2:2 tolerant:non-tolerant ratio was predominant, indicative of one gene being responsible for alcohol tolerance. The spread of the data can be explained by the numerous auxotrophic markers in the BY4741 and BY4742 strains: shuffling of these will give variation in the unstressed growth rates. Such differences will be enhanced by depression of growth rates in hexanol. Despite these variations, there is a 2:2 tolerant:non-tolerant ratio trend.

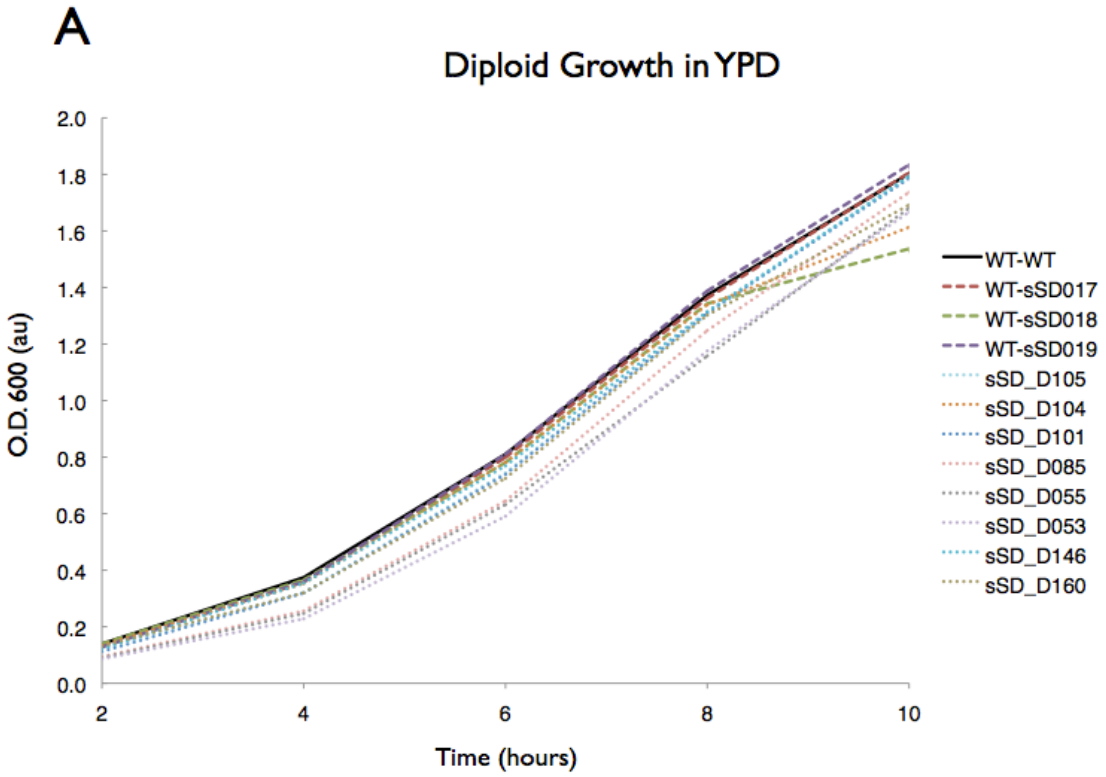

Figure 4.10. Tolerant phenotype is dominant in mixed diploids. Growth of diploid yeast was monitored by measuring OD_{600} of cultures grown aerobically. Diploids generated from two wild-type strains are shown with a black solid line. Diploids generated from a wild type strain and sSD017, sSD018, and sSD019 are shown in dashed lines. Diploids generated from randomly mated haploids after sporulation of tolerant diploids are shown in dotted lines. A) Growth in YPD. Single samples run. B) YPD + 0.15% *n*-hexanol. Samples are run in duplicate and error bars represent standard deviation.

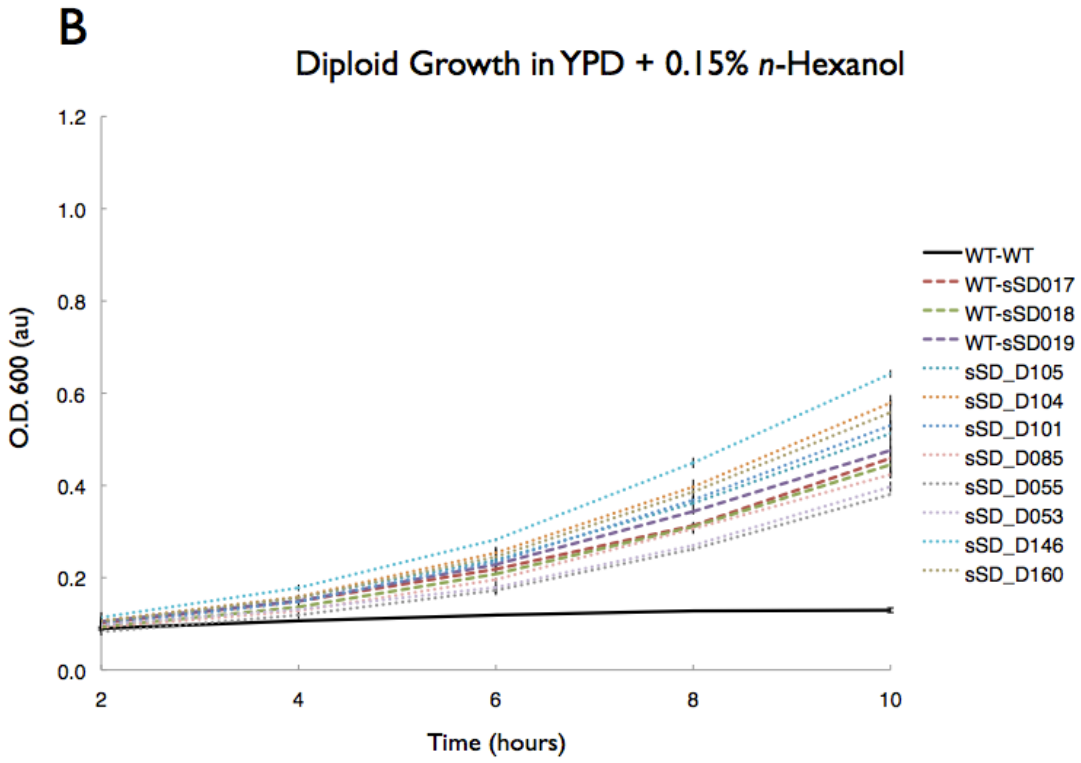

We tried to improve upon the evolved strains by generating diploids with multiple tolerance-conferring mutations. We pooled the tolerant daughter cells, which have random mating types, and mated them to create diploids with genes from two different tolerant strains. We selected several of these diploids and grew them alongside diploids from known parents. All diploids have similar growth in YPD (Figure 4.10A), while there is a range of growth rates among the diploids grown in 0.15% *n*-hexanol (Figure 4.10B). A few strains, particularly sSD004 and sSD146, had better growth than diploids derived from sSD017, sSD018, and sSD019. This suggests that a combination of evolved mutations can even further enhance tolerance levels. We did not further characterize or work with these tolerant diploids.

Genomic Sequencing We used genomic sequencing to determine which genomic mutations were responsible for medium-chain alcohol tolerance. The evolved strains and the mutations are shown in Table 4.3. Strains evolved for one 30-day round (sSD003 and sSD006) accumulated fewer mutations than strains that underwent two 30-day rounds (sSD019 and sSD021).

Evolved Strain Mutations			
sSD003	**sSD019**	**sSD006**	**sSD021**
Gcd1 D85E	Gcd1 D85E	GCD7 R56C	GCD7 R56C
Cit2 G338C	Cit2 G338C		SUI2 D77Y
	Pdr5 Q446*		PDR5 G925A
	Ubp13 G135V		SEY1 A529E
	LSB6 S234C		
	NST1 A662G		
	COX1 silent		

Table 4.3. Evolved Strain Mutations and Gene Descriptions.

- **GCD1** - γ subunit of eIF2B (GEF)
- CIT2 - Citrate Synthase
- PDR5 - ABC drug efflux pump
- UBP13 - Ubiquitin protease
- LSB6 - Type II phosphotidylinositol 4-kinase
- NST1 - unknown, salt sensitivity
- COX1 - Cyotchrome C oxidase
- **GCD7** - ß subunit of eIF2B (GEF)
- **SUI2** - α subunit of eIF2
- SEY1 - role in ER fusion and morphology

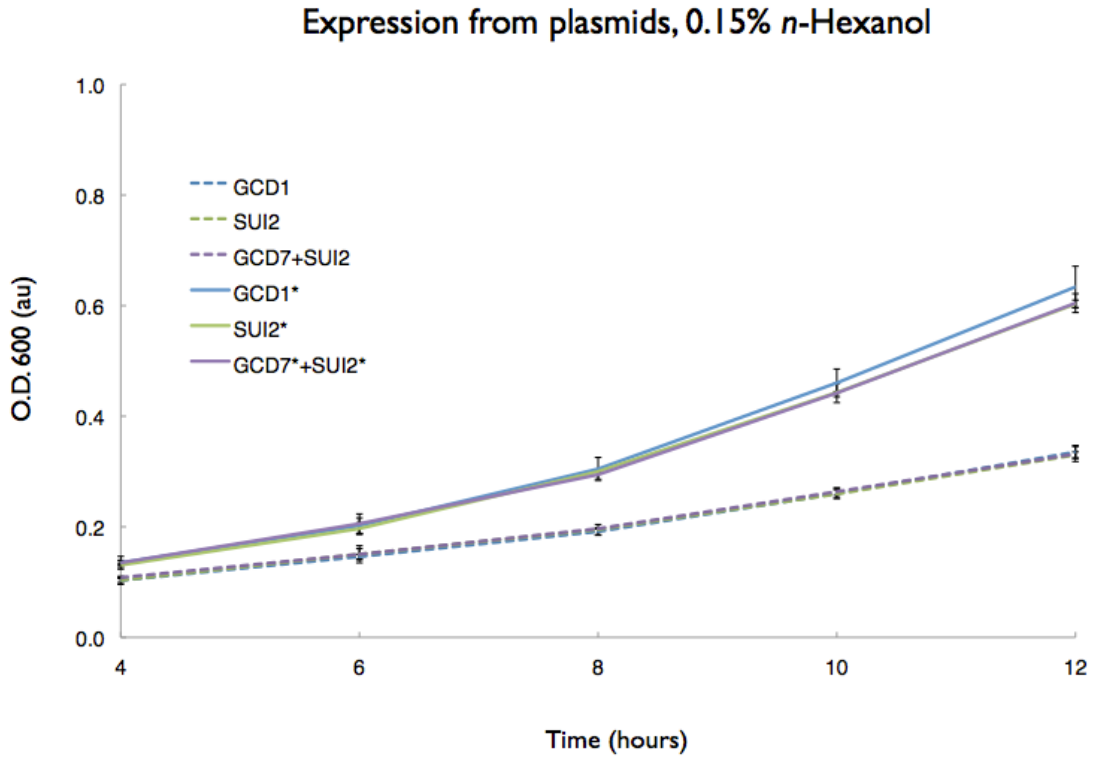

Figure 4.11. The Gcd1 and Sui2 mutations can be expressed from plasmids. Mutated (solid lines) and un-mutated (dashed lines) versions of the GCD1, SUI2, and GCD7 genes were expressed from plasmids in the wild-type strain. These strains were grown in SD-Leu-Ura plus 0.12% *n*-hexanol and OD_{600} was measured every 2 hours. Samples are run in triplicate and error bars represent standard deviation.

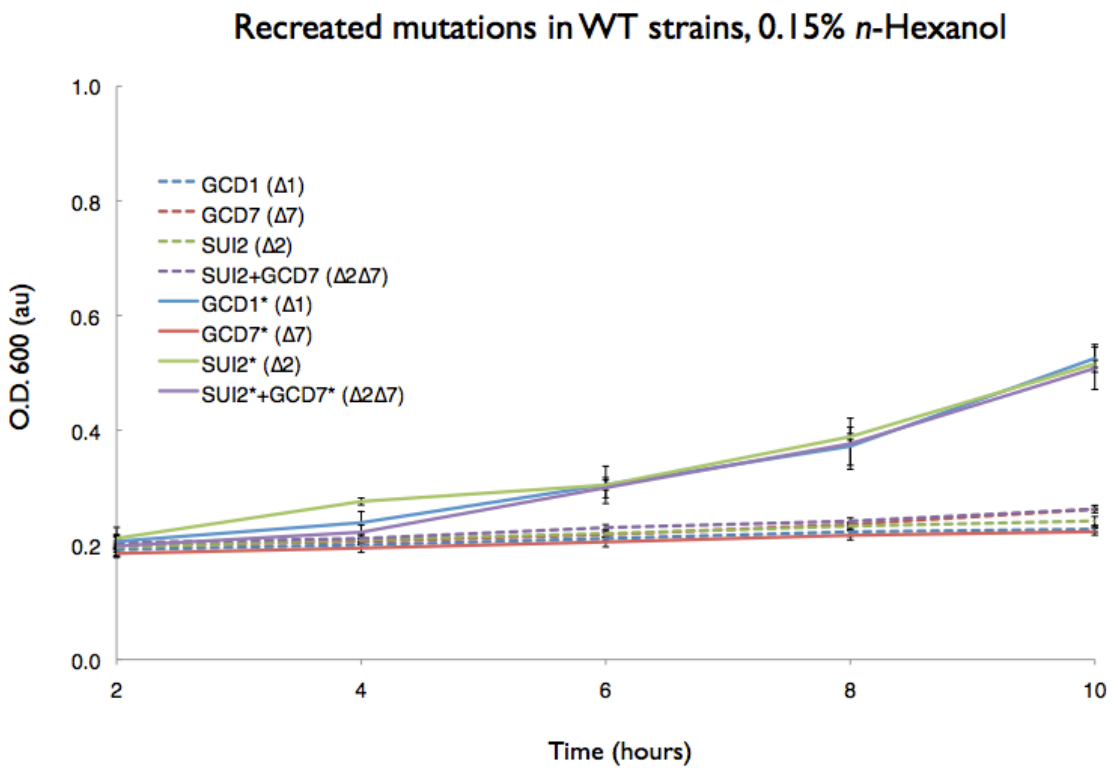

Figure 4.12. Translation initiation mutations Gcd1 D85E and Sui2 D77Y are responsible for alcohol tolerance. Mutated (solid lines) and un-mutated (dashed lines) versions of the GCD1, SUI2, and GCD7 genes were expressed in strains with the respective gene knocked out. These strains were grown in YPD plus 0.15% *n*-hexanol and OD_{600} was measured every 2 hours. Samples are run in triplicate and error bars represent standard deviation.

Each strain had relatively few mutations, enabling us to reconstruct each individual mutation and identify those that confer tolerance. We began by introducing the mutations that appeared in the translation initiation machinery proteins, Gcd1, Gcd7, and Sui2, because at least one of these proteins was mutated in each of the evolved tolerant strains. As the tolerance phenotype is dominant, we were able to express copies of the mutated genes from plasmids and assess growth in the presence of toxic concentrations of the alcohols (Figure 4.11). $Gcd7^{R56C}$ does not confer significant tolerance, as growth rates of strains carrying the mutation are indistinguishable from wild-type strains (Figures 4.11, 4.12). The $Sui2^{D77Y}$ mutation confers hexanol tolerance. It arose in a strain with the Gcd7 mutation, so we tested both mutations together, as well. The Gcd7 mutation did not improve upon the tolerance conferred by $Sui2^{D77Y}$. $Gcd1^{D85E}$ is sufficient for hexanol tolerance. We also knocked out genomic copies of these genes, so that the plasmid copy was the only copy (Figure 4.12). We saw the same tolerance levels in strains with the $Gcd1^{D85E}$ and $Sui2^{D77Y}$ mutations. The $Gcd7^{R56C}$ mutation seemed to reduce tolerance as compared to wild type Gcd7.

In addition to translation initiation factor mutations, strains sSD019 and sSD021 had mutations in Pdr5, a multidrug efflux pump. In sSD019, Pdr5 was truncated after residue 445. In sSD021, Pdr5 had a G925A mutation. It is unknown what effect this mutation has upon Pdr5 activity, though we expect that it is reducing or eliminating activity. Pdr5 has a high basal energy use, so ΔPdr5 mutations improve overall strain fitness and growth rates. We tested growth rates of a ΔPdr5 strain in 0.15% *n*-hexanol (Figure 4.13) but did not see a significant growth rate increase in the ΔPdr5 strain.

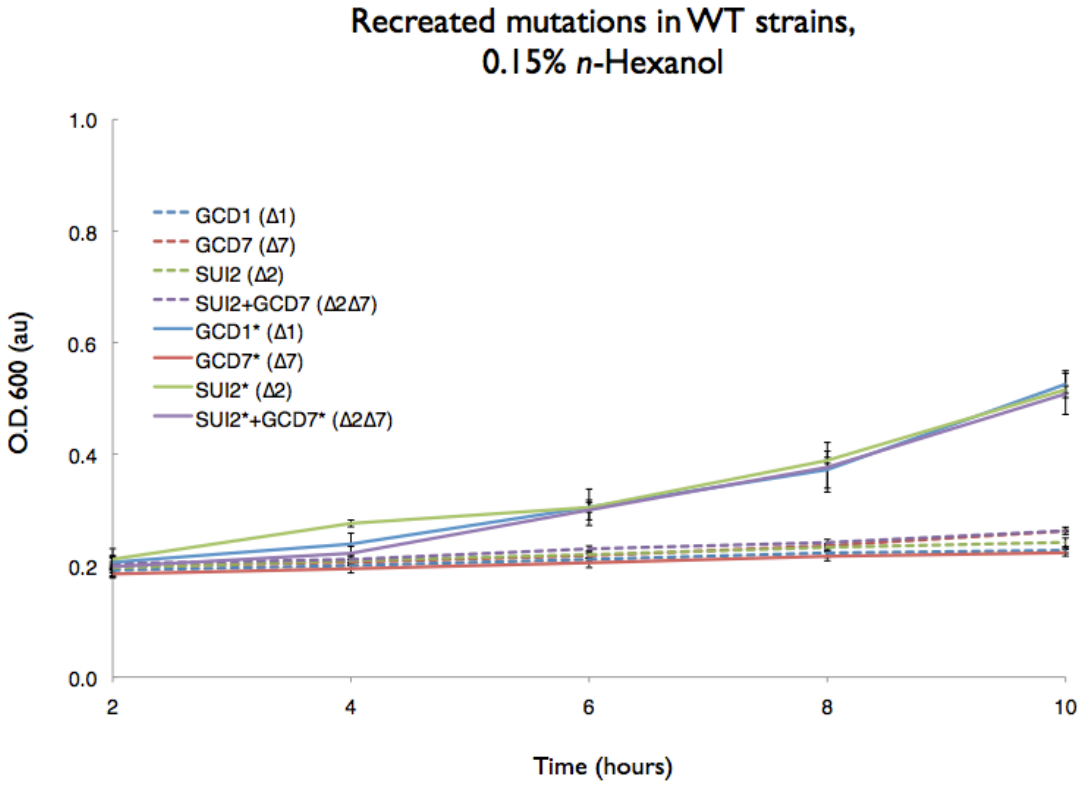

Figure 4.13. ΔPdr5 does not improve tolerance toward *n*-hexanol. Mutated (solid lines) and un-mutated (dashed lines) versions of the GCD1 and GCD7 genes were expressed in strains with the respective gene knocked out. A wild type strain (orange dashed line) and ΔPdr5 strain (solid orange line) were also grown. These strains were grown in YPD plus 0.15% *n*-hexanol and OD_{600} was measured every 2 hours. Single samples run, no error reported.

DISCUSSION

We evolved yeast strains for improved medium-chain alcohol tolerance using several methods. The simplest and most efficient method was daily subculturing in YPD media in the presence of exogenously added alcohols. Performing the evolutions in rich YPD media gave rise to more tolerant strains than in defined SC media. We suspect that this was the case because strains generally grow faster in YPD media than SC media, thus allowing more generations in the same time period. The more limiting conditions of SC media reduced number of generations and accumulation of mutations during the evolution time. We hypothesize that increasing the evolution period for SC media may help, but given the promising results from the YPD evolutions, we did not pursue this direction. Additionally, the particular mutations that arose (e.g. Sui2 and Gcd1) may have required a nutrient-rich environment, to evade regulatory mechanisms that may suppress mutations. Sui2 and Gcd1 are tightly regulated translation initiation factors, and translation initiation is slowed or turned off during starvation condition. It is plausible that the alcohol tolerance conferring mutations are detrimental in nutrient-limiting conditions, and may have been selected against in media such as SC media. We have not yet characterized the Sui2 and Gcd1 mutations under amino-acid- or sugar- limited conditions.

The microaerobic chemostat evolutions were difficult to maintain, and bacterial contamination was a frequent problem. Even after the full 30 days, the most tolerant strains from the hexanol evolution were much less tolerant than the strains from the aerobic evolutions, even in anaerobic conditions (Figure 4.7B). It is surprising that the larger chemostat cultures did not also produce the same point mutations as did the aerobic evolutions. It is possible that microaerobic conditions were limiting, in a similar way as SC media, which hindered evolution or specifically suppressed the translation initiation mutations. Using the microaerobically evolved strains as parent strains for another round of aerobic evolution was successful, since the chemostat strains did not reach the tolerance levels of the aerobically evolved strains. The Gcd7^{R56C} mutation itself did not confer much tolerance, but after the second round of evolution, this strain developed the Sui2^{D77Y} mutation, which greatly improved tolerance. We are unsure whether the Gcd7^{D85E} mutation was required for the Sui2^{D77Y} mutation to arise under the conditions of our evolution, as the two mutations do not seem to be working in concert (Figures 4.11, 4.12).

Although none of the butanol evolutions produced more tolerant strains, we were able to evolve a strain with somewhat improved butanol tolerance. Strains sSD003 and sSD019, with the Gcd1^{D85E} mutation, have a small improvement in butanol tolerance, with a growth rate of about 0.03/hour in 1.2% *n*-butanol. This improvement is on par with other butanol tolerance evolutions [1,2]. It is puzzling that multiple groups have been unable to evolve yeast strains with improved butanol tolerance. Yeast has been highly evolved for ethanol tolerance, so it is possible that this alcohol tolerance extends to butanol as well. Yeasts can grow in much higher levels of butanol than *E. coli*: 2.0% for *S. cerevisiae* [8] vs. 0.8% for *E. coli* [9]. Despite lower tolerance to butanol, *E. coli* can produce significantly more *n*-butanol, at 5 g/L [10], while *S. cerevisiae* can only produce 0.2 g/L [11]. This suggests that despite relatively high growth rates in extracellular butanol, butanol is still highly disrupting metabolism. Another possible explanation for the difficulties evolving yeast for butanol is that butanol has particularly

toxic properties, such that tolerance may require substantial structural or regulatory changes or combinations of changes. For example, butanol disrupts internal pH by increasing membrane permeability, which in turn inhibits ATPases and glucose uptake [12]. It has also been shown to inhibit Pdr5 in yeasts [13]. Perhaps there are as-yet unknown additional butanol toxicity mechanisms which prevent evolutions from being successful.

The strains evolved for hexanol tolerance are also tolerant toward a range of medium-chain alcohols. *n*-Hexanol and *n*-heptanol tolerance were the most improved, though *n*-pentanol and *3*-octanol tolerance are also increased (Table 4.1). Tolerance was not improved for alcohols of four or fewer carbons. We did not test chains longer than eight carbons. It is known that straight-chain alcohols with ten or more carbons have reduced solubility, thus decreasing toxicity of the alcohol. These longer chain alcohols tend to "layer" on top of the culture, rather than enter the cells. The strains do not have tolerance to two other classes of molecules, polyamines and carboxylic acids (Figure 4.6). We expect that the tolerance is alcohol specific, rather than a general fitness improvement. When grown without any stress, evolved strains have growth that is indistinguishable from the wild type strain (Figure 4.5).

Before determining the causative mutations, we fully characterized the evolved hexanol tolerant strains. In anaerobic conditions, the tolerant phenotype is maintained (Figure 4.7). Wild-type yeasts flocculate in alcohols. The evolve strains also flocculated in 0.15% *n*-hexanol despite their improved growth rates, so the tolerance did not effect this phenotype (Figure 4.8). We determined that the tolerance is a stable, genetic mutation, since the phenotype was not lost after eight weeks without selective pressure (Figure 9). Since it was a genetic modification, we did not look at upregulation or down regulation of gene expression, or do any sort of proteomics analysis. These studies have been done before for butanol evolutions [1,2], though not for hexanol evolutions, to our knowledge. This would be an interesting future direction for research. We also established that the phenotype is dominant. Diploids with one tolerant parent have the same tolerance level as the tolerant parents (Figure 4.10B). Tolerance can be conferred by expressing causative mutations on plasmids in wild type cells (Figure 4.11). Finally, tetrad analyses showed that one gene was responsible for tolerance (Table 4.2).

Genomic sequencing was a key experiment in determining the cause of hexanol tolerance. Table 3 lists the mutations found in each evolved strain, as well as a short explanation of each gene. The most striking result was that each strain had a mutation in a translation initiation factor. We expressed these mutated genes from plasmids in strains with the respective strain knocked out (Figure 4.12) and saw that the Gcd1^{D85E} and Sui2^{D77Y} mutations were responsible for hexanol tolerance. The Gcd7^{R56C} mutation, which arose in strain sSD006, did not confer much tolerance. Since the Gcd1 and Sui2 mutations had such significant effects on tolerance, we focused on these mutations for further studies. It is also of note that round II evolved strains both had a Pdr5 mutation (Table 4.3). Strain sSD019 has a stop codon after residue 446, and in strain sSD021, there is a G925A mutation, which we expect is reducing or eliminating Pdr5 activity. Pdr5 is a highly expressed multi-drug efflux pump [14]. It is an ABC transporter and can use a significant amount of cellular energy [15]. Strains with Pdr5 knocked out are known to have better growth rates in the presence of isobutanol, likely because the strain is more fit [16]. We expect that these mutations were responsible for an overall

cell fitness increase, rather than an alcohol tolerance increase. A Pdr5 knockout did not show any improvement in growth rate in 0.15% *n*-hexanol (Figure 4.13).

MATERIALS AND METHODS

Strains and Media

We used wild-type *Saccharomyces cerevisiae* strains BY4741 (*MAT*a *his3Δ1 leu2Δ0 met15Δ0 ura3Δ0*) and BY4742 (*MAT*α *his3Δ1 leu2Δ0 lys2Δ0 ura3Δ0*). Yeast without plasmids were grown in YPD (1% yeast extract (Amresco), 2% peptone (BD Chemical), 2% α-dextrose (Amresco)). Yeast with plasmids were grown in appropriate synthetic dropout media, eg SD-Leu (0.67% Yeast Nitrogen Base (BD Chemical), 2% α-Dextrose(Amresco), 0.2% amino acid mix without leucine from US Biological).

Microaerobic evolutions.

We began the chemostat with 0.5 L YPD media and 5 mL of a saturated culture BY4741. The initial alcohol concentrations were 0.8% *n*-butanol and 0.1% *n*-hexanol. The flux rate was 0.25-0.5 mL/minute, due to the alcohols dramatically suppressing growth rate. Chemostats were maintained in a 30°C room with a medium-speed stir bar. The OD_{600} of the chemostats were maintained at 0.5 - 2.0. As the ODs increased, the alcohol concentrations were steadily increased to final concentrations of 1.2% *n*-butanol and 0.3% n-hexanol. Every 7 days, a glycerol stock of the culture was made. Samples from the chemostat were taken daily and checked for bacterial contamination using bright field microscopy. When contamination was found, the chemostats were re-started using the latest glycerol stock from that chemostat. At the end of the evolution, glycerol stocks were made and culture was streaked to single colonies on plates.

Aerobic Evolutions.

Aerobic evolutions were started with a 1:1000 dilution of a saturated overnight culture of strain BY4741. The initial cultures were 10 mL of YPD media with alcohols added. Cultures were grown in a 30°C water-bath shaker at 200 rpm. The *n*-butanol concentration was increased from 1.1% to a final 1.3% and daily dilutions were decreased from 1.0 mL into 10 mL fresh media to 0.5 mL into 10 mL fresh media. The *n*-hexanol concentration was maintained at 0.12% and daily dilutions were decreased from 1.0 mL into 10 mL fresh media to 0.7 mL into 10 mL fresh media. Every 7 days, a glycerol stock of the culture was made. At the end of the evolution, glycerol stocks were made and culture was streaked to single colonies on plates.

Evolutions Round II.

Strains sSD002. sSD003, and sSD004 from the aerobic evolution I and strains sSD006 and sSD010 from the microaerobic evolution were grown overnight to saturation. Overnights were subcultured into YPD media + 0.12% n-hexanol or SD media + 0.12% n-hexanol. 0.5 mL of cultures were diluted into 10 mL fresh media daily, and n-hexanol concentrations were increased from 0.12% to 0.21%. Samples were checked daily for bacterial contamination using bright field microscopy. For days 14-30, 100 ug/mL chloramphenicol was added to YPD cultures to prevent bacterial growth. Every 7 days, a glycerol stock of the culture was made. At the end of the evolution, glycerol stocks were made and culture was streaked to single colonies on plates.

Microscopy
Images were taken using an Andor Clara-Lite digital camera and a Nikon Ni-U upright microscope with a 100x, 1.45 n.a. plan apochromat objective.

Growth Curves
Single colonies were picked from the post-evolution plates into 5 mL YPD media in culture tubes. Cultures were grown overnight to saturation at 30°C with 280 rpm shaking. Stationary phase cultures were diluted to an OD_{600} of .30-.33 a.u. as measured with a Nanodrop 2000c, 5 mL dilute culture was aliquoted into screw-cap tubes. 5 mL YPD with 0 or 0.24% or 0.30% *n*-hexanol was added. Each sample was run in triplicate. Screw-cap tubes were grown at 30°C with 280 rpm shaking and measurements were taken every 2 hours with Genesys-20 spectrophotometer. Subsequent growth curves were done in the same manner, with concentrations of alcohols, fatty acids, or polyamines as reported. Anaerobic growth curves were done in culture tubes capped with rubber stoppers and flushed with Argon for 3 minutes prior to growth in the shaker.

Tolerant strains were streaked out on YPD plates without alcohols weekly for 8 weeks. Single colonies were picked and growth curves were done in 0.12% and 0.15% *n*-hexanol.

Diploid Generation
BY4741 and evolved derivatives and BY4742 were streaked onto fresh YPD plates. After 30 hours, BY4741 derivatives and BY4742 were patched onto a fresh YPD plate and kept at 30°C. After 5 hours, diploids were seen under microscope. Patches were streaked onto selective plates (SD -Lysine -Methionine).

Sporulation
Diploids were resuspended in 1% potassium acetate (Sigma). After 4 days, sporulated diploids were resuspended in 1 M sorbitol (Fisher) + 0.5 mg/ml Zymolyase (from Zymo Research) and cell walls digested for 10 minutes at 30°C. 0.8 mL H_2O was added and cells put on ice, then spores were streaked onto a plate. Tetrads were selected and dissected using dissecting microscope, then gridded onto YPD plates. After 2 days, tetrads were picked into 300 µL YPD in 96-well blocks, including positive and negative controls (sSD021 and BY4741). After 2 days, 2 µL of saturated cultures were diluted into 300 µL YPD or YPD + 0.15% n-hexanol. After 24 hours, OD_{600} was measured for 100 µL using a Molecular Devices SpectraMax M2 plate reader.

Genomic Sequencing
Genomic DNA preparations were done using the YeaStar Genomic DNA kit from Zymo Research Corporation. Sequencing was done on an Illumina platform HiSeq 2000 with Paired-End 100bp reads. Analysis was done using CLC Genomics Workbench 6.

Genetic Methods
His3 and KanMX cassettes amplified and homologous ends added via PCR. Cassettes were transformed into yeast using the LiOAc method [7]. Strains sSD040 and sSD054

were generated by replacing the Gcd7 gene with a His3 cassette in BY4741 containing a plasmids pSD469 (Gcd7^{R56C}) or pSD474 (Gcd7) and confirming by PCR of the junctions. Strains sSD029 and sSD053 were generated by replacing the Gcd1 gene with a KanMX cassette in BY4741 containing plasmids pSD450 (Gcd1^{D85E}) or pSD442 (Gcd1) and confirming by PCR of the junctions. Strains sSD055 and sSD056 were generated by replacing the Sui2 gene with a KanMX cassette in BY4741 containing a plasmids pSD444 (Sui2) or pSD452 (Sui2^{D77Y}) and confirming by PCR of the junctions. Strain sSD060 was generated by replacing the Gcd7 gene with a His3 cassette in strain sSD055 containing a plasmids pSD474 or and confirming by PCR of the junctions. Strain sSD058 was generated by replacing the Gcd7 gene with a His3 cassette in strain sSD056 containing a plasmids pSD469 or and confirming by PCR of the junctions.

Table 4.4. Strains used in this study.

Strain	Parent	Genotype	Reference
BY4741		*MATa his3Δ1 leu2Δ0 met15Δ0 ura3Δ0*	
BY4742		*MATα his3Δ1 leu2Δ0 lys2Δ0 ura3Δ0*	
sSD002	BY4741	*BY4741 GCD1-E85 CIT2-C338*	This Study
sSD003	BY4741	*BY4741 GCD1-E85 CIT2-C338*	This Study
sSD004	BY4741	*BY4741 evolved*	This Study
sSD006	BY4741	*BY4741 GCD7-C56*	This Study
sSD009	BY4741	*BY4741 evolved*	This Study
sSD010	BY4741	*BY4741 evolved*	This Study
sSD017	BY4741	*BY4741 evolved*	This Study
sSD018	BY4741	*BY4741 evolved*	This Study
sSD019	BY4741	*BY4741 GCD1-E85 CIT2-C338 PDR5-*446 UBP13-V135 LSB6-C234 NST1-G662*	This Study
sSD020	BY4741	*BY4741 evolved*	This Study
sSD021	BY4741	*BY4741 GCD7-C56 SUI2-Y77 PDR5-A925 SEY1-529E*	This Study
sSD029	BY4741	*BY4741 Gcd1Δ::KanMX p[GCD1-85E LEU2 CEN6]*	This Study
sSD040	BY4741	*BY4741 Gcd7Δ::His3 p[GCD7-56C URA3 CEN6]*	This Study
pSD053	BY4741	*BY4741 Gcd1Δ::KanMX p[GCD1 LEU2 CEN6]*	This Study
pSD054	BY4741	*BY4741 Gcd7Δ::His3 p[GCD7 URA3 CEN6]*	This Study
pSD055	BY4741	*BY4741 Sui2Δ::KanMX p[SUI2 LEU2 CEN6]*	This Study
pSD056	BY4741	*BY4741 Sui2Δ::KanMX p[SUI2-77Y LEU2 CEN6]*	This Study
pSD058	sSD056	*BY4741 Sui2Δ::KanMX Gcd7Δ::His3 p[SUI2-77Y LEU2 CEN6] p[GCD7-56C URA3 CEN6]*	This Study
pSD060	sSD055	*BY4741 Sui2Δ::KanMX Gcd7Δ::His3 p[SUI2 LEU2 CEN6] p[GCD7 URA3 CEN6]*	This Study

Table 4.5. Plasmids used in this study.

Plasmid	Promoter	Insert	Marker	Reference
pSD442	pGcd1	Gcd1	Leu2	This Study
pSD443	pGcd7	Gcd7	Leu2	This Study
pSD444	pSui2	Sui2	Leu2	This Study
pSD450	pGcd1	$Gcd1^{D85E}$	Leu2	This Study
pSD451	pGcd7	$Gcd7^{R56C}$	Leu2	This Study
pSD452	pSui2	$Sui2^{D77Y}$	Leu2	This Study
pSD469	pGcd7	$Gcd7^{R56C}$	Ura3	This Study
pSD474	pGcd7	Gcd7	Ura3	This Study

REFERENCES

1. Steen E, Chan R, Prasad N, Myers S, Petzold CJ, Redding A, Ouellet M, Keasling JD. Metabolic engineering of Saccharomyces cerevisiae for the production of n-butanol. Microb Cell Fact. 2008, 7:36.

2. Dellomonaco C, Clomburg JM, Miller EN, Gonzalez R. Engineered reversal of the ß-oxidation cycle for the synthesis of fuels and chemicals. Nature. 2011, 476(7360): 355-9.

3. Lamsen EN, Atsumi S. Recent progress in synthetic biology for production of C3-C10 alcohols. Frontiers in Microbiology. 2012, 3(196):1-9.

4. Stanley D, Fraser S, Chambers PJ, Rogers P, Stanley GA. Generation and characterisation of stable ethanol-tolerant mutants of Saccharomyces cerevisiae. J. Ind Microbiol Biotechnol. 2010, 37(2):139-49.

5. Gonzalez-Ramos D, van den Broek M, van Maris AJA, Pronk JT, Daran JMG. Genome-scale analyses of butanol tolerance in Saccharoymces cerevisiae reveal an essential role of protein degradation. Biotechnol Biofuels. 2013, 6(1):48.

6. Ghiaci P, Norbeck J, Larsson C. Physiological adaptations of Saccharomyces cerevisiae evolved for improved butanol tolerance. Biotechnol Biofuels. 2013. 6(1): 101.

7. Geitz D, St Jean A, Woods RA, Schiestl RH. Improved method for high efficiency transformation of intact yeast cells. Nucleic Acids Res. 1992, 20(6):1425.

8. Fischer CR, Klein-Marcuschamer D, Stephanopolous G. Selection and optimization of microbial hosts for biofuels production. Metabol Eng. 2008, 10(6):295-304.

9. Fisher MA, Boyarskiy S, Yamada MR, Kong N, Bauer S, Tullman-Ercek D. Enhancing tolerance to short-chain alcohols by engineering the Escherichia coli AcrB efflux pump to secrete the non-native substrate n-butanol. ACS Synth Biol. 2013, 3(1): 348-54.

10. Bond-Watts BB, Bellerose RJ, Chang MCY. Enzyme mechanism as a kinetic control element for designing synthetic biofuel pathways. Nature Chem Bio. 2011, 7:222-27.

11. Si T, Luo Y, Xiao H, Zhao H. Utilizing an endogenous pathway for 1-butanol production in Saccharomyces cerevisiae. Metab Eng. 2014, 22:60-68.

12. Bowles LK, Ellefson WL. Effects of Butanol on *Clostridum acetobutylicum*. App Env Microbiol. 1985, 50(5):1165-1170.

13. Gaskova D, Plasek J, Zahumensky J, Benesova I, Buriankova L, Sigler K. Alcohols are inhibitors of Saccharomyces cerevisiae multidrug-resistance pumps Pdr5 and Snq2. FEMS Yeast Res. 2013, 13(8):782-95.

14. Golin J, Ambudkar SV, May L. The yeast Pdr5p multidrug transporter: How does it recognize so many substrates? Biochem. Biophys Res. Comm. 2007, 356:1-5.

15. Balzi E, Goffeau A. Yeast Multidrug Resistance: The PDR Network. J Bioenergetics and Biomembranes. 1995, 27(1):71-76.

16. Butamax (Tm) Advanced Biofuels Llc. Yeast with increased butanol tolerance involving a multidrug efflux pump gene. 2010, US patent application: US 12/711,308. Publication number: US20100221801 A1. Filing date: Feb 24, 2010.

Chapter 5
Removing inhibition by medium-chain alcohols

ABSTRACT

Yeast-based chemical production is an environmentally friendly alternative to petroleum-based production or processes that involve harsh chemicals. However, potential products such as isobutanol, *n*-butanol and *n*-hexanol for biochemical applications are toxic to production organisms, making production less efficient and less cost-effective due to reduced yields. Toxicity mechanisms are not well understood, and therefore there have been few successful rational approaches to alleviating toxicity and improving tolerance. We used an evolutionary approach to evolve the laboratory strain of *S. cerevisiae* BY4741 for increased tolerance for *n*-hexanol. We found that the addition of *n*-hexanol inhibits initiation of translation, and evolved mutations in the α subunit of eIF2, Sui2, and the γ subunit of its guanine exchange factor (GEF) eIF2B, Gcd1, rescue this inhibition. Moreover, the translation initiation process is affected by other alcohols including *n*-pentanol, and *n*-heptanol, and the mutations in the eIF2 and eIF2B complexes greatly improve tolerance to these medium-chain alcohols.

INTRODUCTION

S. cerevisiae is used as a production organism for chemicals such as farnesol, *n*-butanol, and isobutanol [1,2,3]. Yeast-based production is desirable because yeasts are genetically tractable and easily maintained, and industrial-scale fermentation processes are well established. A major challenge to this method is that many alcohol compounds have both general and specific toxic effects in the cell. For instance, membrane fluidity and corresponding function are affected by butanol [4]. In addition, solvents increase denaturant sensitivity and decrease thermotolerance of proteins, with effects proportional to carbon chain length [5]. These solvents can also specifically inhibit protein function. For example, *n*-butanol inhibits the ATPase of *Clostridium acetobutylicum* [4] and *n*-butanol and *n*-hexanol inhibit the multidrug resistance pump Pdr5 [6]. Understanding these effects is the first step toward engineering solutions to improve tolerance.

One particularly promising set of studies reveals that the fusel alcohols, including *n*-butanol and isoamyl alcohol, can inhibit translation initiation. Fusel alcohols are by-products of amino acid metabolism in *S. cerevisiae.* Ashe et al. showed that these alcohols inhibit eIF2B and thus translation initiation [7]. To explain this inhibition, Taylor et al. suggest that fusel alcohols are either directly binding eIF2B to inhibit translation, or the alcohols are altering as-yet unidentified post-translational modifications, such as phosphorylation [8]. Moreover, mutations in both eIF2 and its GEF eIF2B can modulate this inhibition [7,8]. Inhibition of translation decreases growth rate and would halt production of enzymes necessary for biofuel production and cell maintenance. It is critical that this inhibition be alleviated for biofuel production organisms.

The eIF2 complex is an important part of translation initiation as it brings the methionine-charged initiator tRNA to the 40S subunit of the ribosome [9,10]. This reaction is powered by GTP, and therefore the GEF eIF2B is required for GDP turnover

[10]. eIF2 is composed of three subunits, α (Sui2), ß (Sui3), and γ. The α subunit, Sui2, is regulated by phosphorylation at serine 51. This phosphorylation inhibits translation initiation. eIF2B is composed of two sub-complexes, one with a regulatory function, and one with catalytic activity. The regulatory subcomplex of eIF2B, composed of the α (Gcn3), ß (Gcd7), and δ (Gcd2) subunits, binds more tightly to phosphorylated Sui2, blocking exchange activity and effectively sequestering the eIF2 [11]. The catalytic subunit, composed of the γ (Gcd1), and ε (Gcd6) subunits, has exchange activity and acts upon phosphorylated and un-phosphorylated Sui2 with equal activity (Hinnebusch 1991). Mutations in the α, ß, and δ subunits ameliorate inhibition by phosphorylated Sui2 [12,13]. For example, S199P, I118T, and D178Y mutations in GCD7, the ß subunit of eIF2B, eliminate translation inhibition by Sui2 phosphorylation, presumably by decreasing binding affinity for Sui2 [12].

	Subunit	Protein	Function
eIF2	α	Sui2	Regulation of eIF2 activity
	ß	Sui3	tRNA binding
	γ	Gcd11	GTP binding
eIF2B	α	Gcn3	Regulatory subunit; eIF2B regulation
	ß	Gcd7	Regulatory subunit, role in eIF2 binding
	γ	Gcd1	Catalytic, non-active, role in eIF2 binding
	δ	Gcd2	Regulatory subunit; eIF2B formation
	ε	Gcd6	GDP to GTP exchange

Table 5.1. eIF2 and eIF2B Subunits.

Several methods have been employed to improve biofuel tolerance of *S. cerevisiae*. Gonzalez-Ramos and colleagues investigated the impact of libraries of overexpressed and knocked-out genes in order to assess butanol stress responses and pinpoint target proteins for tolerance optimization [14]. They discovered that protein degradation pathways are key in minimizing butanol toxicity. Ghiaci *et al*. found that mitochondrial proteins are upregulated under isobutanol stress [15]. Several proteins involved in butanol tolerance have been uncovered through evolution experiments. For example, Ramos *et al.* found that mutations to two transcription factors increased tolerance to butanol [14]. A mutated version of glycerol-3-phosphatase (Gpp2) also improves isobutanol tolerance [15].

We chose to modulate gene function via natural evolution and selection of tolerant strains. This work is fully described in Chapter 4. Briefly, after two 30-day rounds of evolution in *n*-hexanol, the yeasts were significantly more solvent tolerant. We sequenced the genomes of our tolerant strains and noticed several interesting mutations in proteins required for translation initiation, including a D77Y mutation in the eIF2α subunit, Sui2 and a D85E mutation in the γ subunit of eIF2B, Gcd1. With this work, we demonstrate that longer-chain alcohols such as *n*-hexanol also inhibit translation initiation. Previously, only fusel alcohols such as butanol have been shown to be inhibitory [7,8]. This study extends the range of known alcohol inhibitors for the eIF2 and eIF2B complexes, giving insight into the inhibition mechanism. Mutations in several eIF2B subunits are known to modulate fusel alcohol sensitivity [8], yet only tolerance-decreasing mutations have been reported for Gcd1 [7]. Mutations in Sui2 affecting solvent tolerance have not been reported.

REVIEW OF TRANSLATION INITIATION

Pavitt *et al.* propose that the γ (Gcd1) and ε (Gcd6) subunits of eIF2B form a subcomplex that can function independently of the α, ß (Gcd7), and δ subunits [13]. This independent function lacks the regulation provided by the other subunits, so that nucleotide exchange is not inhibited by phosphorylation of the α (Sui2) subunit of eIF2. Thus, translation initiation inhibition by stress responses such as amino acid starvation and fusel alcohols does not occur. The eIF2B α-ß-δ subcomplex preferentially binds to the phosphorylated eIF2 α subunit, preventing nucleotide exchange by the eIF2B γ-ε subcomplex, which binds both forms of eIF2-α equally (Figure 5.1). It is possible that the mutations found in our evolved strains are modulating the binding affinities of the two complexes, and thus removing some regulation. Targeting interactions between these complexes for directed evolution efforts could further eliminate inhibition by alcohols and thus reduce toxicity.

Eukaryotic translation initiation is a tightly regulated process involving multiple heteromeric protein complexes. As detailed in Table 1, the eIF2 complex of *S. cerevisiae* is composed of an α (Sui2), ß (Sui3p), and γ subunit (Gcd11p). The eIF2α subunit, Sui2, brings the methionine-charged initiator tRNA (Met-tRNA$_i^{Met}$) to the 40S subunit of the ribosome and the eIF2γ subunit binds an activating GTP, forming a ternary complex (Figure 5.1) [9,10]. Sui2 can be phosphorylated at S51 by the δ subunit of eIF2B, the guanine exchange factor (GEF) of eIF2 (Table 5.1 and additional details below); this modification generally inhibits translatio [8,16,17] (Figure 5.1). The δ subunit of eIF2B is activated by uncharged tRNAs that accumulate during starvation conditions [9,10], in turn phosphorylating Sui2 and inhibiting translation under these conditions. However, Gcn4p, the transcriptional activator for amino-acid-producing genes, has increased translation under these conditions [11,18,19], allowing the cell to regulate its amino acid availability.

Translation initiation depends on the guanine nucleotide exchange activity of eIF2B. After eIF2 delivers the tRNA$_i^{Met}$, it is left inactive and bound to GDP [11]. eIF2B is the GEF required to re-activate eIF2 after GTP hydrolysis [20] (Figure 5.1). This heteropentameric complex has an α (Gcn3), ß (Gcd7), γ (Gcd1), δ (Gcd2), and ε (Gcd6) subunit (Table 5.1) [11,13,19]. Strains with deletions of the ß, γ, δ, and ε subunits are non-viable [12]. The α, ß, and δ subunits are regulatory and do not have exchange activity. This sub-complex binds more tightly to phosphorylated Sui2 (eIF2α), blocking exchange activity and effectively sequestering the eIF2 [11]. The catalytic subunit, composed of the γ and ε subunits, has exchange activity and acts upon phosphorylated and un-phosphorylated Sui2 with equal activity [11]. Certain mutations in the genes encoding the α, ß, and δ subunits ameliorate inhibition by phosphorylated Sui2. For example, Gcd7^{S199P}, Gcd7^{I118T}, and Gcd7^{D178Y} mutations in the ß subunit of eIF2B, eliminate translation inhibition by Sui2 phosphorylation, presumably by decreasing binding affinity for Sui2 [12]. Additionally, the eIF2Bα subunit, Gcn3p, can be knocked out entirely from the genome without loss of viability and *gcn3Δ* strains are not inhibited by phosphorylation of Sui2 as the wild-type strains are, suggesting a role in Sui2 sequestration [13]. Overexpression of the eIF2B-ß, γ, δ, and ε subunits has the same effect, suppressing translation inhibition by Sui2 phosphoryation [12].

Fusel alcohols inhibit translation initiation. Fusel alcohols are byproducts of amino

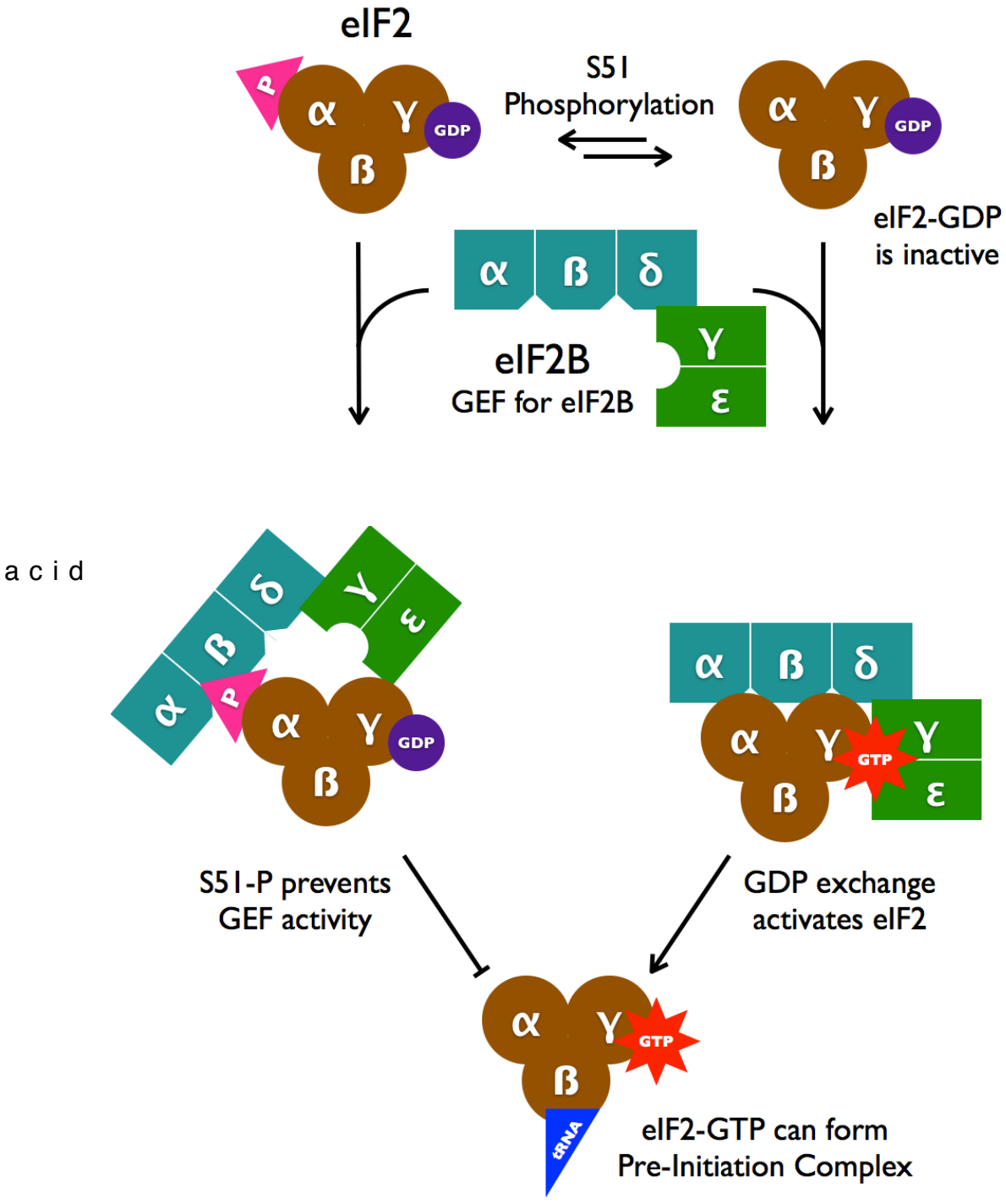

Figure 5.1. eIF2 is regulated by phosphorylation. eIF2 (brown circles) subunit a has a phosphorylation site at S51. When eIF2a is phosphorylated (pink triangle), eIF2B (Green boxes) preferentially binds to the phosphorylated eIF2a. When sequestered, eIF2B cannot exchange GDP for GTP, so eIF2 is inactive.

Evolved Strain Mutations			
sSD003	**sSD019**	**sSD006**	**sSD021**
Gcd1 D85E	Gcd1 D85E	GCD7 R56C	GCD7 R56C
Cit2 G338C	Cit2 G338C		SUI2 D77Y
	Pdr5 Q446*		PDR5 G925A
	Ubp13 G135V		SEY1 A529E
	LSB6 S234C		
	NST1 A662G		
	COX1 silent		

Table 5.2. Evolved Strain Mutations and Gene Descriptions.
- **GCD1** - γ subunit of eIF2B (GEF)
- CIT2 - Citrate Synthase
- PDR5 - ABC drug efflux pump
- UBP13 - Ubiquitin protease
- LSB6 - Type II phosphotidylinositol 4-kinase
- NST1 - unknown, salt sensitivity
- COX1 - Cyotchrome C oxidase
- **GCD7** - ß subunit of eIF2B (GEF)
- **SUI2** - α subunit of eIF2
- SEY1 - role in ER fusion and morphology

catabolism that can accumulate under nitrogen starvation conditions. These alcohols, including butanol and isoamyl alcohol, inhibit translation initiation. Taylor *et al.* showed that increasing concentrations of *n*-butanol leads to increasing inhibition of translation initiation [8]. Overexpression of eIF2B subunits reverses this inhibition, suggesting that the alcohols are inhibiting eIF2B [7]. Several mutations in both eIF2 and eIF2B modulate fusel alcohol inhibition [7,8]. Fusel alcohol inhibition is independent of Sui2 phosphorylation, as an $Sui2^{S51A}$ mutation did not affect inhibition [8]. Butanol inhibits ternary complex levels but without regulation by Sui2 phosphorylation [8]. Isoflurane, an anesthetic, is also known to inhibit translation initiation independently of Sui2 phosphorylation [21]. Taylor et al. suggest that fusel alcohols are either directly binding eIF2 to inhibit translation, or the alcohols are altering as-yet unidentified post-translational modifications, such as phosphorylation [8]. Additionally, a P180S mutation in the Gcd1 subunit of eIF2B was shown to increase *n*-butanol sensitivity [7]. Dev *et al.* show that pairs of Sui2 and Gcd7 mutations can be lethal, or increase or decrease inhibition by Sui2 phosphorylation [22].

RESULTS

Mutations in translation initiation factors confer tolerance phenotype. Previously, we evolved yeast strains with medium-chain alcohol tolerance, as detailed in Chapter 4. Several mutations were found in each of the evolved strains (Table 5.2). Of these mutations, the most striking were the $Gcd1^{D85E}$, $Gcd7^{R56C}$, and $Sui2^{D77Y}$ mutations. Sui2 is a subunit of the eIF2 complex, an essential translation initiation complex. Gcd1 and Gcd7 are subunits of eIF2B, which is the guanine exchange factor for eIF2 (refer to Table 5.1). The evolved strains that carry mutations to these genes grow significantly better than the wild-type strains in the presence of 0.15% *n*-hexanol. We re-created these mutations in wild-type strains by introducing plasmids with the mutated and unmutated gene variants and then knocking out the genomic copies of the genes with a *KANMX* cassette. As these genes are essential, simple knockouts could not be generated. The strains carrying the genes encoding Sui2 and Gcd1 mutations had faster growth rates than strains without these mutations in the presence of 0.15% *n*-hexanol, demonstrating that these mutations indeed give rise to the phenotype observed in the evolved strains (Figure 5.3). Interestingly, the tolerant phenotype is dominant, allowing wild-type strains carrying plasmids encoding $Sui2^{D77Y}$ and $Gcd1^{D85E}$ to outperform strains with control plasmids in the same growth assay (Figure 5.4).

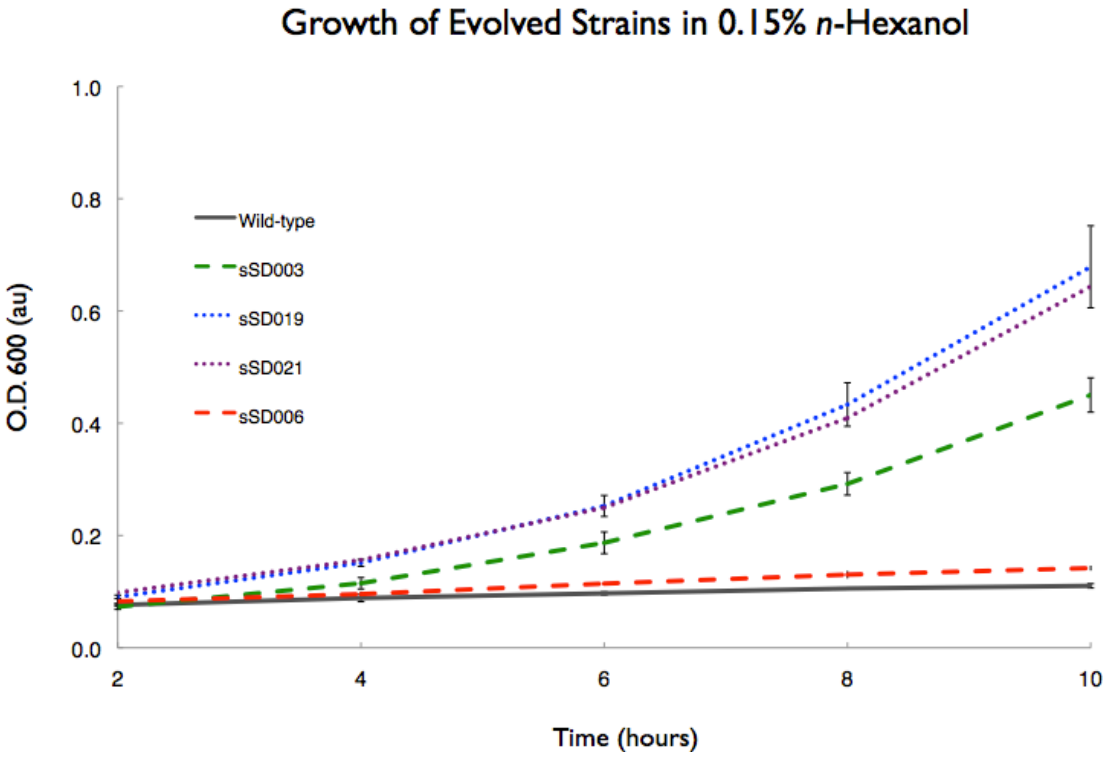

Figure 5.2. Evolved strains show greatly improved growth rates in 0.15% *n*-hexanol when compared to the wild type. Growth was monitored by measuring OD_{600} of cultures grown aerobically in YPD + 0.15% *n*-hexanol v/v. Wild type is shown in a solid black line. Strains from round I evolution are shown in dashed lines. Strains from round II evolution are shown in dotted lines. Samples are run in triplicate and error bars represent standard deviations.

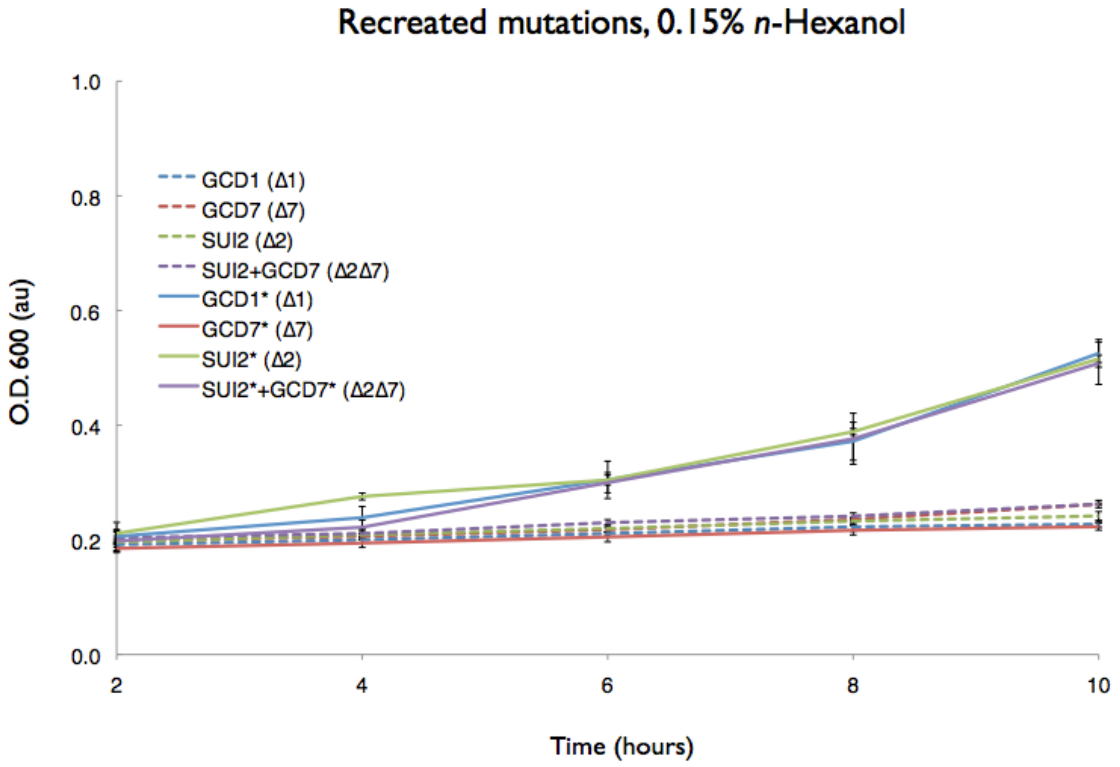

Figure 5.3. Translation initiation mutations Gcd1 D85E and Sui2 D77Y are responsible for alcohol tolerance. Mutated and un-mutated versions of the GCD1, SUI2, and GCD7 genes were expressed in strains with the respective gene knocked out. These strains were grown in YPD plus 0.15% *n*-hexanol and OD_{600} was measured every 2 hours. Samples are run in triplicate and error bars represent standard deviations.

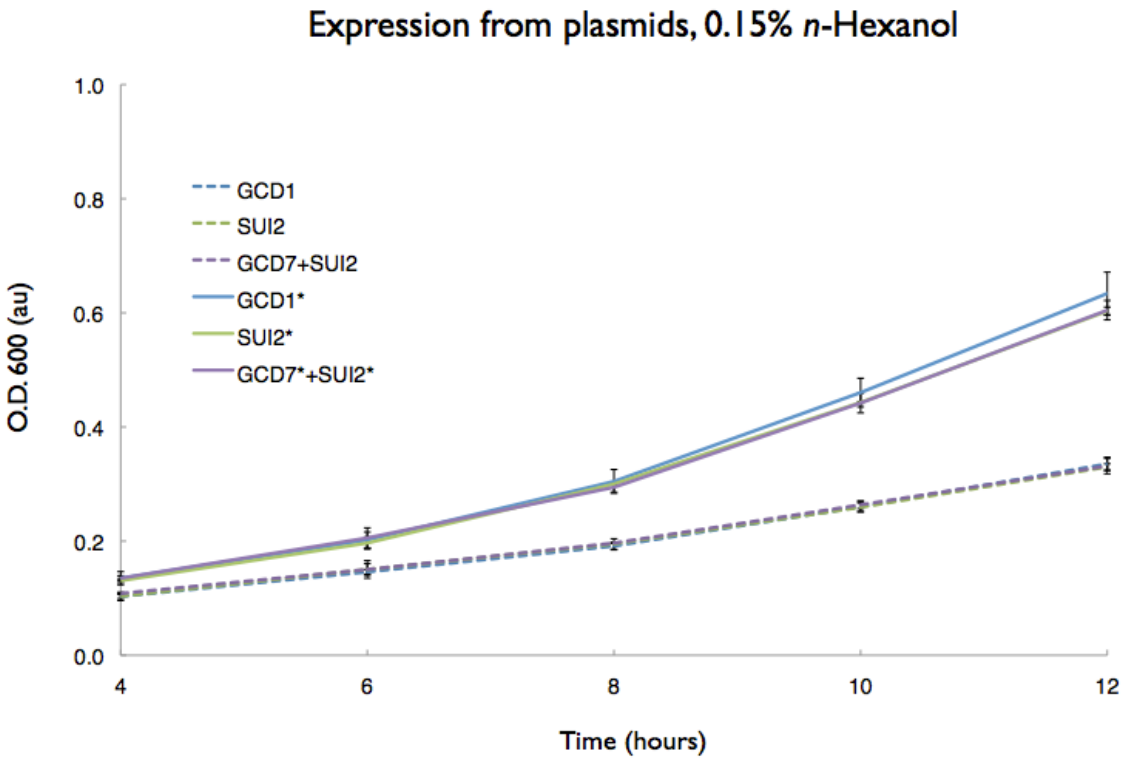

Figure 5.4. The Gcd1 and Sui2 mutations are dominant. Mutated (solid lines) and un-mutated (dashed lines) versions of the GCD1, SUI2, and GCD7 genes were expressed from plasmids in the wild-type strain. These strains were grown in SD-Leu-Ura plus 0.12% *n*-hexanol and OD_{600} was measured every 2 hours. Samples are run in triplicate and error bars represent standard deviations.

Strain	PrOH	BuOH	iBuOH	AOH	iAOH	PtOH	HxOH	HpOH	OcOH
Wild Type	0	0	0	0	0	0	0	0	0
sSD003 Gcd1 D85E	0	+	0	++	++	+++	+++	+++	+++
sSD019 Gcd1 D85E	0	+	+	+++	+++	+++	++++	++++	++
sSD006 Gcd7 R56C	0	0	0	++	++	0	++	++	+
sSD021 Gcd7 R56C Sui2 D77Y	0	0	+	+++	+++	+++	++++	++++	++

Table 5.3. Evolved strains show improved tolerance toward medium-chain alcohols, particularly n-hexanol and n-heptanol. A) Qualitative assessment of evolved strain tolerances based on growth rate improvements in the presence of toxic levels of alcohols. Growth rates (h^{-1}); 0 = 0.0 - 0.03; + = 0.04 - 0.10; ++ = 0.11 - 0.17; +++ = 0.18 - 0.24; ++++ ≥ 0.25. Butanol tolerance is based on final OD_{600} after 48 hrs, rather than growth rate. PrOH: propanol, 3.0%. BuOH: *n*-butanol, 1.2%. iBuOH: isobutanol, 1.0%. AOH: amyl alcohol, 0.5%. iAOH: isoamyl alcohol, 0.5%. PtOH: *n*-pentanol, 0.5%. HxOH: *n*-hexanol, 0.15%. HpOH, 0.05%: *n*-heptanol, 0.05%. OcOH: *3*-octanol, 0.05%.

S. cerevisiae strains evolved increased medium-chain alcohol and fusel alcohol tolerance. The evolved strains exhibit tolerance to C4 to C8 straight-chain alcohols as measured by growth rate in the presence of each solvent. In 0.12% *n*-hexanol, evolved strains have a growth rate of 0.27/hour while the wild-type strain has a growth rate of only 0.12/hour. In higher concentrations of *n*-hexanol, the evolved strains continue to replicate, while the wild-type strain does not noticeably divide. We further characterized these strains with respect to fusel alcohol tolerance. The relative tolerance improvements are summarized in Table 5.3. Of the fusel alcohols, the strains were most tolerant toward amyl alcohol and isoamyl alcohol, which are both five-carbon alcohols. *n*-Butanol and isobutanol tolerance was minimal in these assays. Isobutanol tolerance is likely due to Pdr5 mutations, because it is only seen in strains sSD019 and sSD021, which contained the Pdr5 mutations. In the absence of solvents, the evolved strains and WT strain had equivalent growth in YPD media.

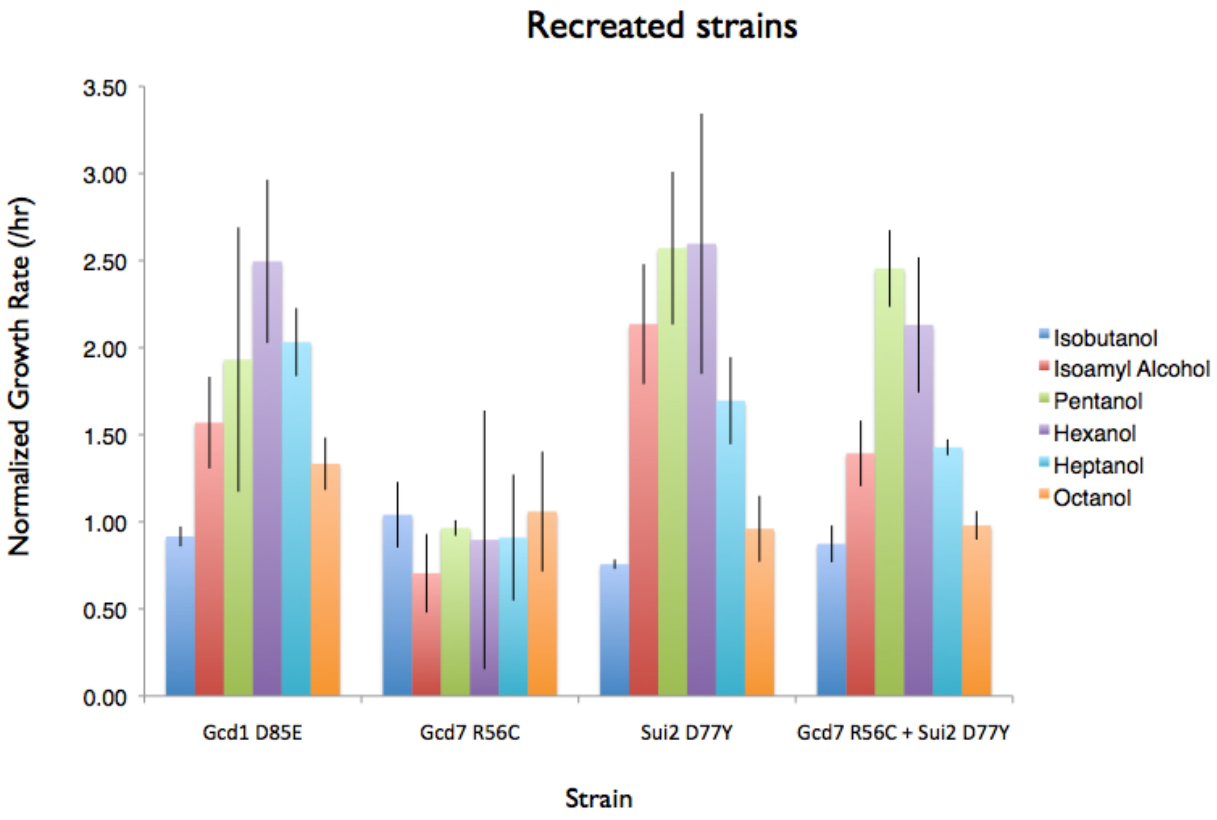

Figure 5.5. Re-created mutation strains show improved tolerance toward medium-chain alcohols, particularly n-pentanol and *n*-hexanol. Strains were grown in YPD + alcohols and OD_{600} measured at 4 and 10 hours. Growth rates were calculated using ln(OD_{600} 10hr/OD_{600} 4 hr)/6 hr. Growth rates were normalized to growth rates of strains expressing wild-type genes. All samples were done in triplicate and error bars represent standard deviations. Isobutanol: 1.0%, Isoamyl Alcohol: 0.5%, *n*-Pentanol: 0.5%, *n*-Hexanol: 0.15%, *n*-Heptanol: 0.05%, *3*-Octanol: 0.05%.

We confirmed that alcohol tolerance is due to the Sui2, Gcd1, and Gcd7 mutations. To do so, we again employed strains harboring a plasmid-borne version of the respective genes and deleted for the genomic version. We grew these strains in YPD supplemented with the various alcohols listed in Table 5.4 and found that the Gcd1 and Sui2 mutations conferred tolerance toward the alcohols with five to eight carbons. Strain sSD006 did not have high tolerance toward any alcohols (Table 5.3), and likewise the mutation in Gcd7 identified in that strain did not confer significantly improved tolerance (Figure 5.5). The Gcd1 and Sui2 mutations confer similar tolerance improvements for all alcohols tested.

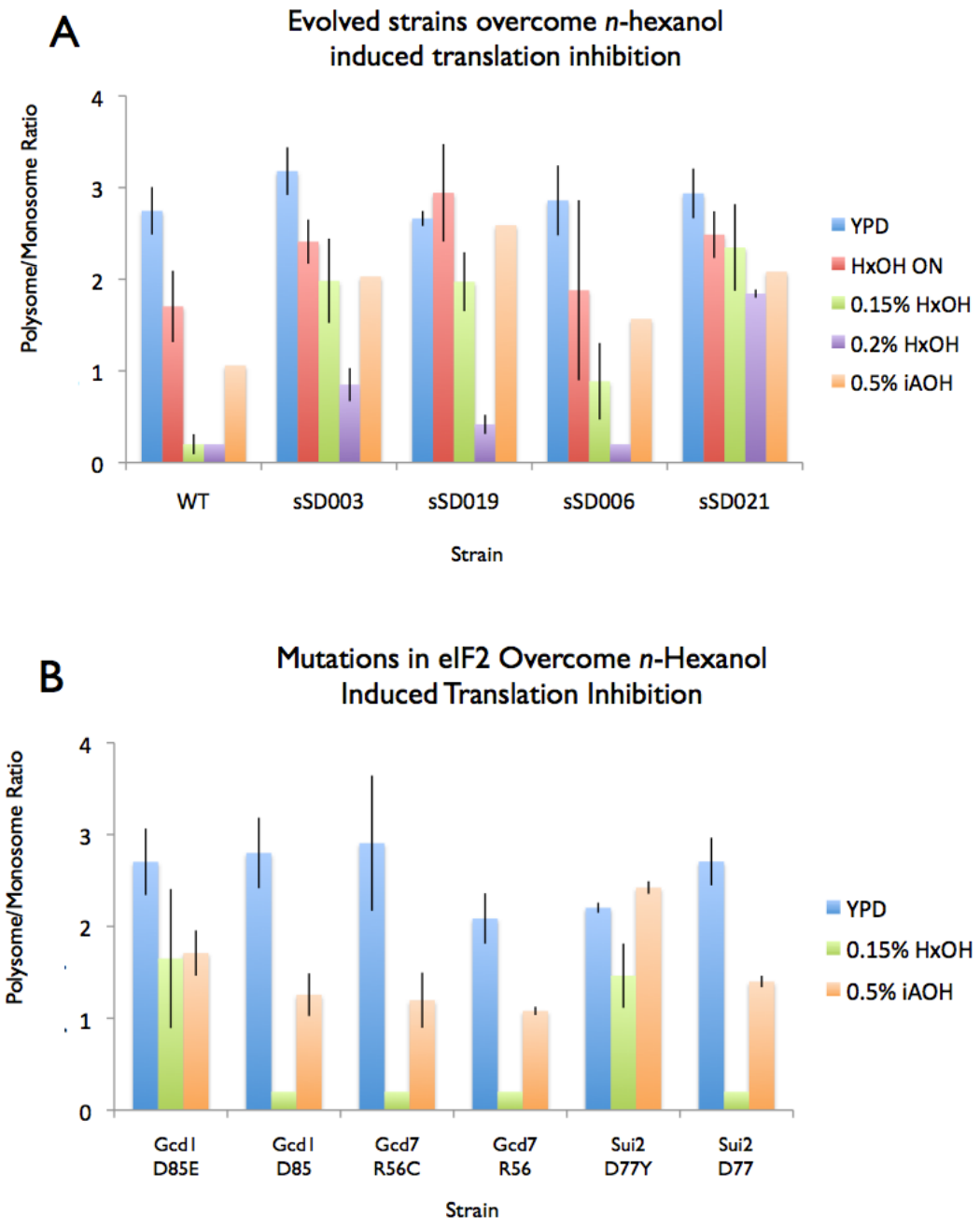

Figure 5.6. The Gcd1 and Sui2 mutations partially rescue the inhibition of translation caused by hexanol and isoamyl alcohol. A) Wild-type and evolved strains were grown in YPD, YPD + 0.15% *n*-hexanol, or YPD + 0.5% isoamyl alcohol, then polysomes were analyzed. Polysome to monosome ratios were calculated and three independent measurements averaged and reported with standard deviations. B) The polysome analysis was repeated on strains generated with single mutations (see Table 3). C) Representative traces of WT, sSD029 (Gcd1 D85E) and sSD056 (Sui2 D77Y).

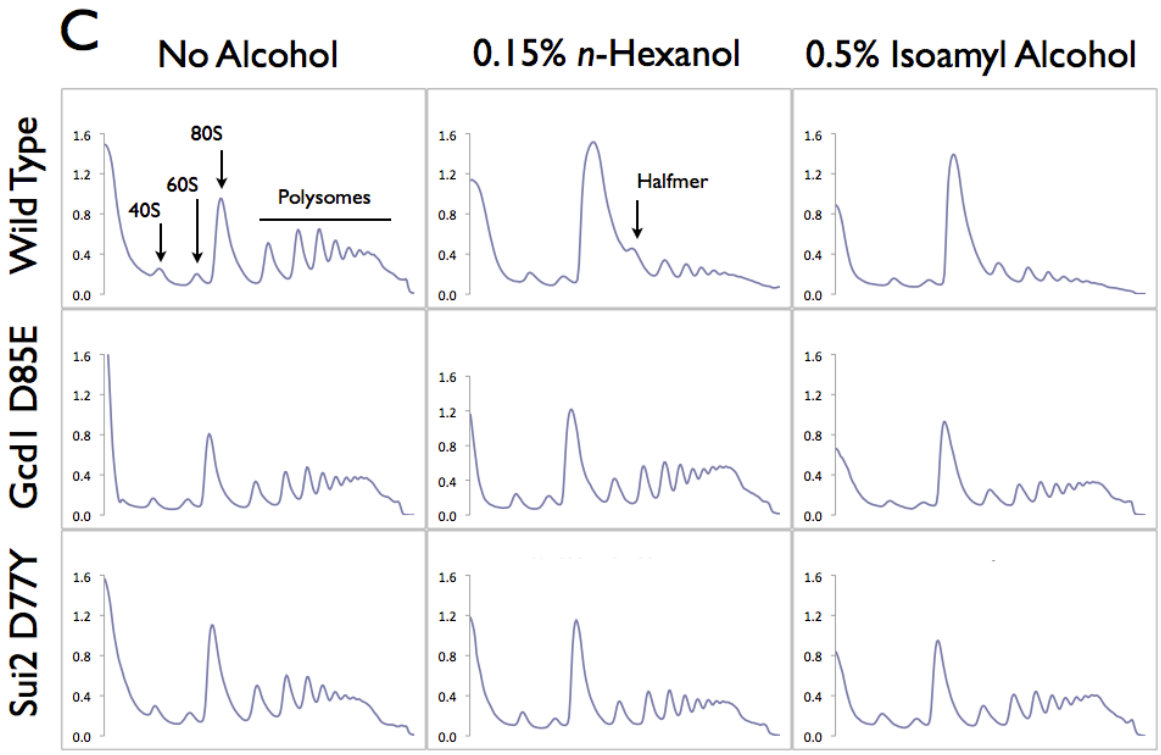

Mutations in Sui2 and Gcd1 decrease inhibition of translation initiation inhibition by alcohols. We investigated the impact of mutations in Gcd1 and Sui2 on translation initiation using polysome analysis. The wild-type strain is notably inhibited by *n*-hexanol and isoamyl alcohols, as seen in Figures 5.6A and C. Halfmers are seen after hexanol exposure (Figure 5.6C), which is indicative of extreme inhibition [28]. The presence of the Gcd1^{D85E} and Sui2^{D77Y} mutations (strains sSD029 and sSD056 respectively) relieve this inhibition, as seen in Figures 5.6B. Strains harboring the Sui2 mutation appear to be more effective at relieving translation initiation inhibition. At 0.2% *n*-hexanol, the polysome to monosome ratio for evolved strain sSD003, containing the Gcd1 mutation, is reduced by a factor of 2, yet the evolved strain sSD021, which contains the Sui2 mutation, is not significantly affected (Figure 5.6A). As expected based on the growth assay results, the Gcd7 mutation (strain sSD040) did not lead to significantly increased polysome to monosome ratios (Figure 5.6B).

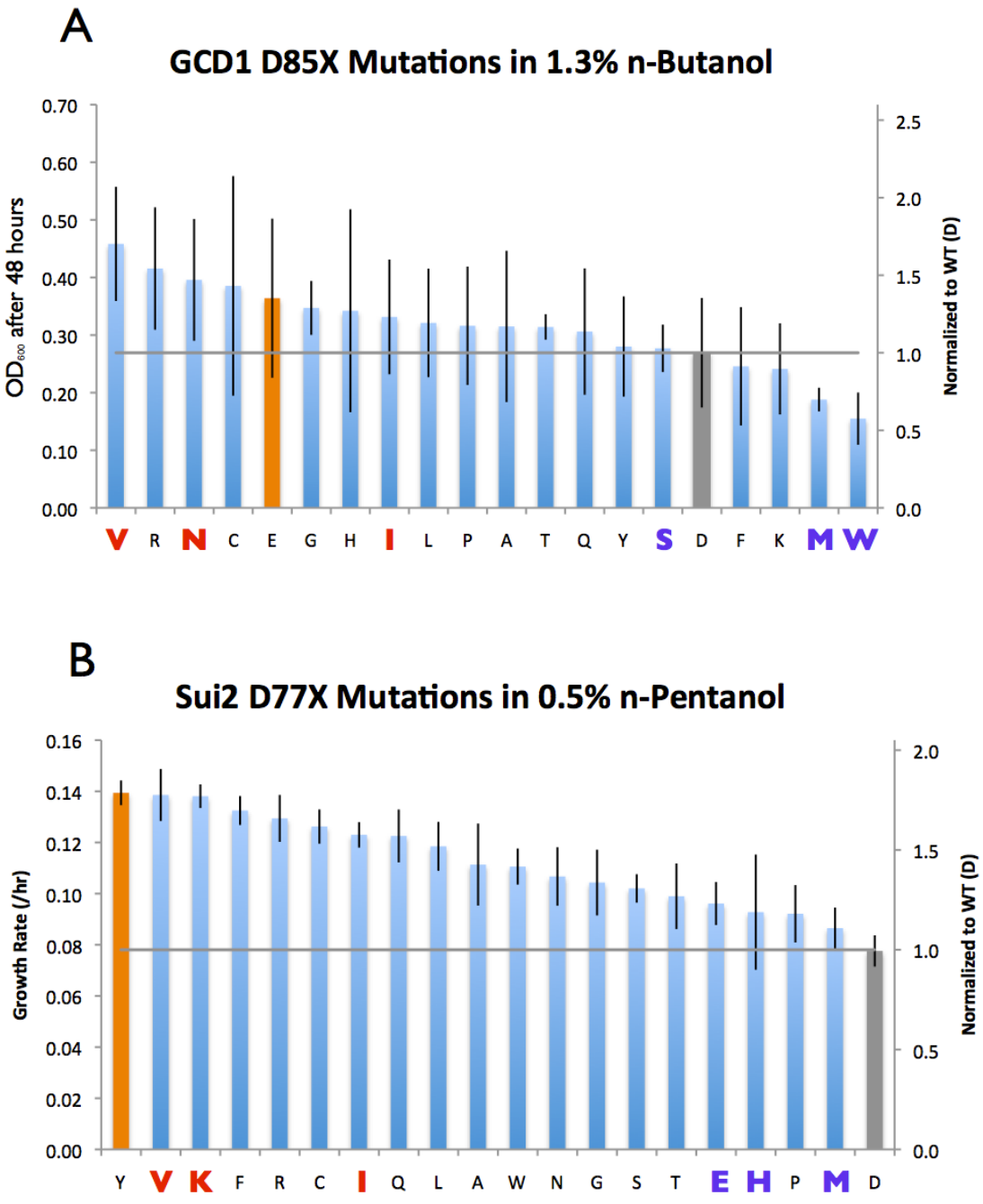

Figure 5.7. Mutations at Gcd1 position 85 and Sui2 position 77 confer a range of tolerance levels. Plasmids containing mutated Sui2 and Gcd1 were transformed into WT strains. Strains were diluted to an OD_{600} of 0.003 in SD-Ura + alcohols and growth rate was calculated using OD_{600} measured at 4 and 12 hours. The grey bar is the WT, the orange bar is the evolved mutation. Samples were run in triplicate three times and error bars represent standard deviations. A, E) Measurements in *n*-butanol represent final OD_{600} after 48 hours of growth in 96-well blocks, rather than growth rate. A-D) Gcd1 D85X mutation strains; WT is D85; evolved is D85E. A) 1.3% *n*-butanol. B) 0.5% *n*-pentanol. C) 0.13% *n*-hexanol. D) 0.05% *n*-heptanol. E-H) Sui2 D77X mutation strains; WT is D77; evolved is D77Y. E) 1.3% *n*-butanol. F) 0.5% *n*-pentanol. G) 0.13% *n*-hexanol. H) 0.05% *n*-heptanol.

C

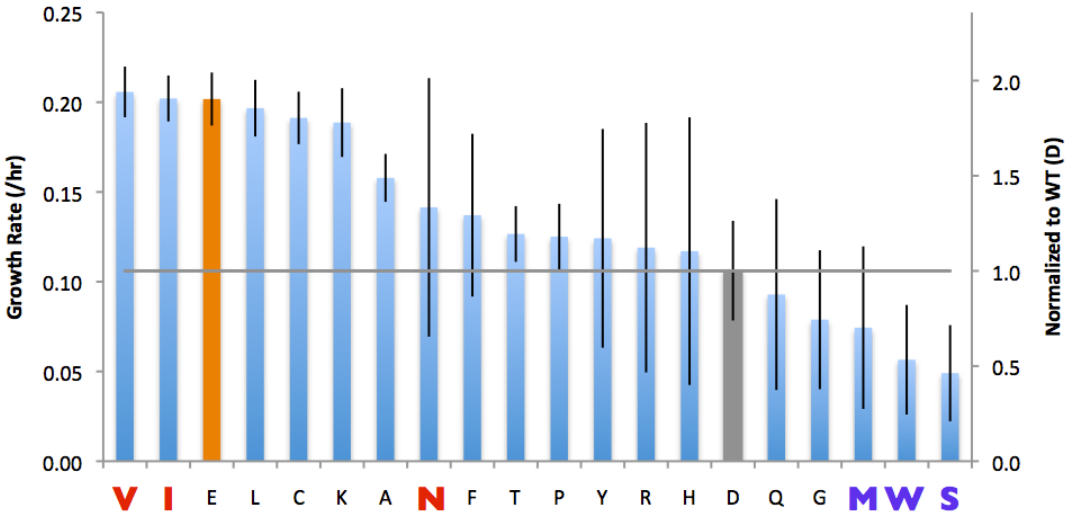
GCD1 D85X Mutations in 0.13% n-Hexanol
Growth Rate (/hr)
0.25
0.20
0.15
0.10
0.05
0.00
Normalized to WT (D)
2.0
1.5
1.0
0.5
0.0
V I E L C K A N F T P Y R H D Q G M W S

D

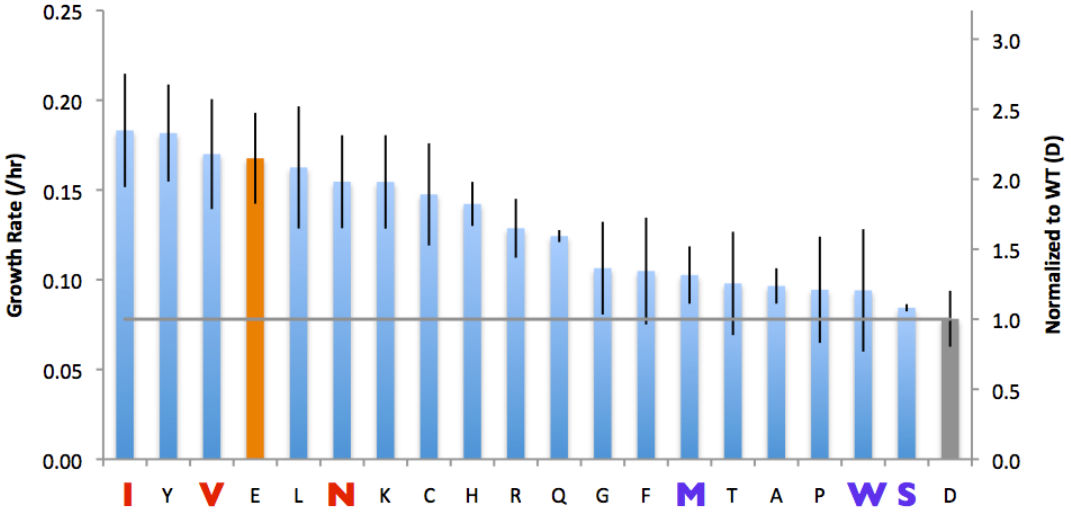
GCD1 D85X Mutations in 0.05% n-Hepanol
Growth Rate (/hr)
0.25
0.20
0.15
0.10
0.05
0.00
Normalized to WT (D)
3.0
2.5
2.0
1.5
1.0
0.5
0.0
I Y V E L N K C H R Q G F M T A P W S D

E

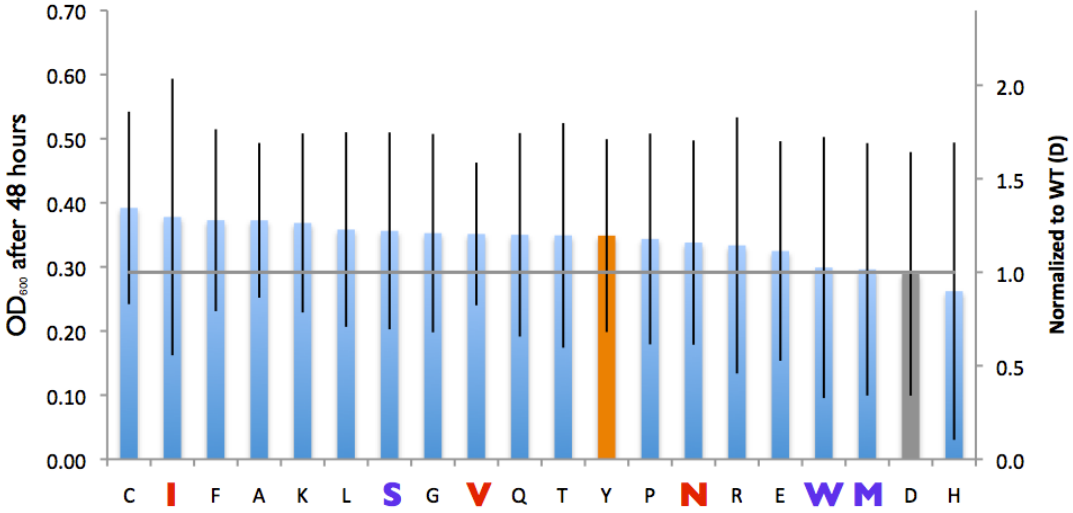
Sui2 D77X Mutations in 1.3% n-Butanol
OD600 after 48 hours
0.70
0.60
0.50
0.40
0.30
0.20
0.10
0.00
2.0
1.5
1.0
0.5
0.0
Normalized to WT (D)
C I F A K L S G V Q T Y P N R E W M D H

F

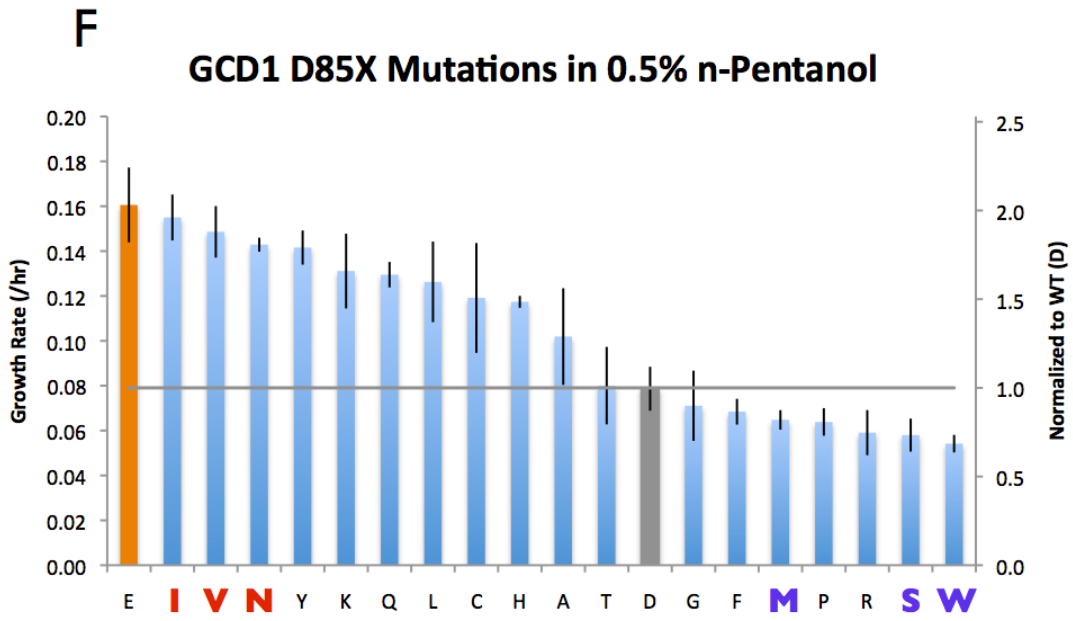
GCD1 D85X Mutations in 0.5% n-Pentanol
Growth Rate (/hr)
0.20
0.18
0.16
0.14
0.12
0.10
0.08
0.06
0.04
0.02
0.00
2.5
2.0
1.5
1.0
0.5
0.0
Normalized to WT (D)
E I V N Y K Q L C H A T D G F M P R S W

G

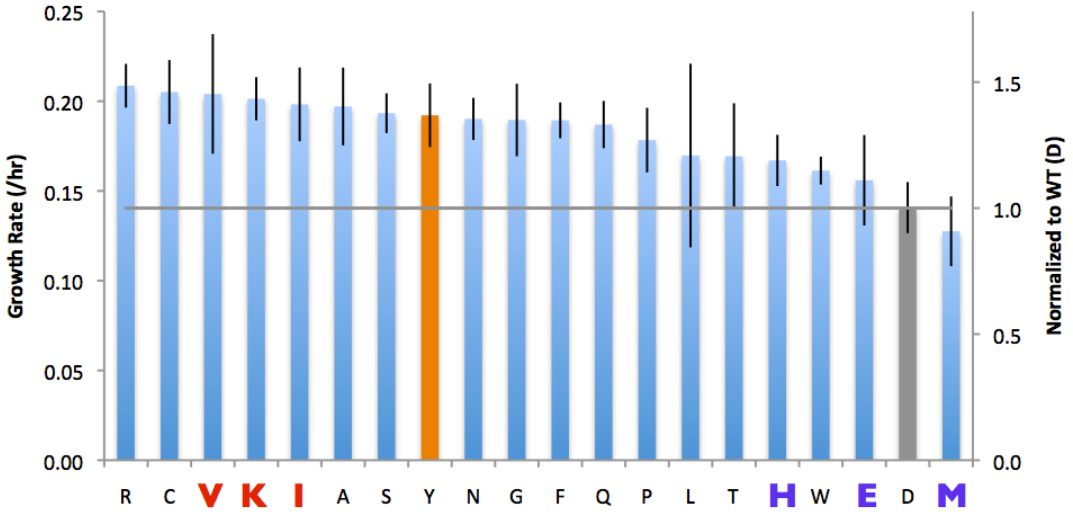
Sui2 D77X Mutations in 0.13% n-Hexanol
Growth Rate (/hr)
0.25
0.20
0.15
0.10
0.05
0.00
Normalized to WT (D)
1.5
1.0
0.5
0.0
R C V K I A S Y N G F Q P L T H W E D M

H

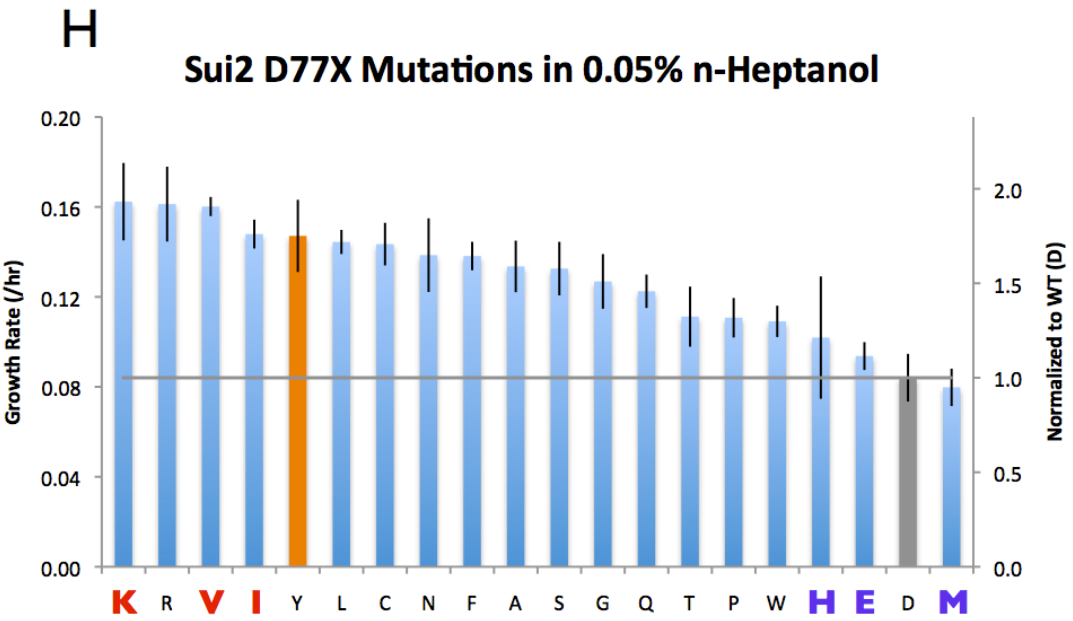
Sui2 D77X Mutations in 0.05% n-Heptanol
Growth Rate (/hr)
0.20
0.16
0.12
0.08
0.04
0.00
Normalized to WT (D)
2.0
1.5
1.0
0.5
0.0
K R V I Y L C N F A S G Q T P W H E D M

Mutations at position 85 of Gcd1 and position 77 of Sui2 give a range of tolerance levels. When plasmid copies of the mutated Sui2 and Gcd1 proteins are expressed from plasmids in wild-type cells such that two copies of the gene are present, the tolerance phenotype is dominant (See Chapter 4). We used this dominant phenotype to our advantage in order to assess the flexibility of the Gcd1 D85 and Sui2 D77 positions with respect to alcohol tolerance. We generated strains with every amino acid at these positions and assessed tolerance levels in C4-C7 straight chain alcohols. Interestingly, we found that there is a range of tolerance levels (Figure 5.7). The relative tolerance levels among the strains expressing proteins with these substitutions were somewhat consistent with respect to the various alcohols. For example, K, R, and V at position 77 in Sui2 usually give rise to tolerance and E, H, and M do not. However, there is not an obvious chemical or structural reason as to why some of the substitutions confer more tolerance than others. Interestingly, several mutations in Gcd1 confer decreased tolerance levels below that of the wild-type strain (Figures 5.7A-D), which we would not have expected in a strain that also carries the wild-type gene. These mutations probably have deleterious effects and we would not anticipate survival of strains carrying only these mutations. The strains with Gcd1^{D85E} mutations (sSD003 and sSD019) showed an increased tolerance to *n*-butanol, while strain sSD021, which has the Sui2^{D77Y} mutation, did not have any *n*-butanol tolerance (Figures 5.3 and 5.4). Saturation mutagenesis at position 85 in Gcd1 resulted in a small range of butanol tolerances (Figure 5.7A), while mutating Sui2 position 77 did not give rise to improved *n*-butanol tolerance (Figure 5.7E).

Sui2 position 77 (Figure 5.8) is highly conserved. The homologous position in human eIF2 α is an aspartate as well (Table 4). Archaea, however, have a range of residues at position 77, including a tyrosine in *Aeropyrum camini* (Table 5.4). The most common residues at this position were aspartate (D) and asparagine (N).. Gcd1 position 85 is fairly well conserved among other yeasts, with either an aspartate (D) or a glutamate (E) appearing in most homologs (Table 5.5). The *Candida* genus had unexpected diversity at this position; notablty a histidine (H) and leucine (L) are known natural variants in this genus.

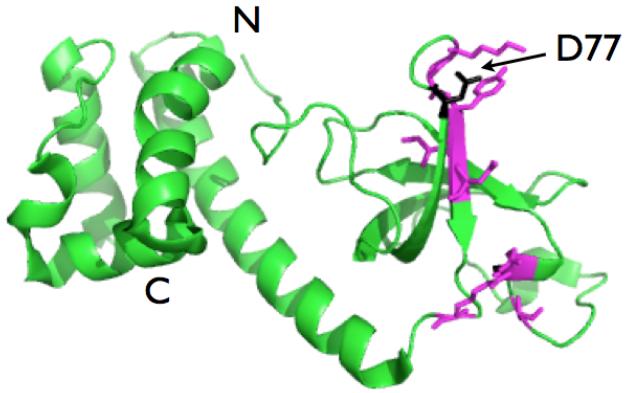

Figure 5.8. Sui2 D77Y mutation is found in the eIF2B and kinase binding domain. *S. cerevisiae* Sui2p structure adapted from Dhaliwal et al. [24], modeled using Pymol [25]. Magenta residues are the eIF2B and kinase binding residues. D77 is shown in black.

Table 5.4. Sui2 Alignments

```
S. cerevisiae      57  RSIQKLIRVGKNDVAVVLRVYKEKGYIDLSKRRVSSEDIIK
S. pombe           57  RSVQKHIRVGRNEVVVVLRVDKEKGYIDLSKRRVSPEDVVK
A. niger ATCC1015  61  RSIQKLIRIGRNEVVIVLRVDKEKGYIDLSKRRVSPEDVVK
H. Sapiens         57  RSINKLIRIGRNECVVVIRVDKEKGYIDLSKRRVSPEEAIK
P. furiosus        52  KNIRDYLREGQKVVAKVIRVDPKKGHIDLSLRRVTQQQRKA
KM3_73_B11         52  RKVNKYVKEGEKKVLLVKKVETGRKEIDLSLKQISKEQRKK
P. fumarii         51  RRIDEVIKEGQKVVVKVIRVHKQRKTVDVSLKRVTEGEKRR
Thaumarchaeota     52  RNINKFVKSGEKKVLLVKRIKEGREEIDLSLKQVSRDQRKR
A. niger            1    MVGKATSGSYFSKFTISMLKSGSYIDLSKRRVSPEDVVK
M. infernus        49  RNIRDHVKVGQRVVAKVLRVNKEKGHIDLSLKRVSDQQRRE
SAT1000_48_A08     52  RKVRRYVKENEKKVLLVKKIQAKRGEIDLSLKQISKEQRKK
Euryarchaeote      53  KNIRAFVREGQRLICKVMRTRKDGTSLELSLKSVSEERRRD
M. maripaludis     49  KNIRDHIKKGQRVVAKVMRVTPHKNQIDLSLKRATDQQKKV
GW2011_AR3         51  RNIRDYVKEGKVVVCKVLRVYLERGNIDLSLRRVTETQKRA
A. camini          62  RNIHAVLKPRQKVVVKVIRVYRNRGQVDVSLKRVMDSEKKR
```

S. cerevisiae: *Saccharomyces cerevisiae*, eIF2 alpha subunit.
S. Pombe: *Schizosaccharomyces pombe* 972h-, eIF2 alpha subunit
H. Sapiens: *Homo Sapiens*, eIF22 subunit 1
A. niger ATCC1015: *Aspergillus niger* ATCC 1015, putative eIF2 alpha subunit
P. furiosus: *Pyrococcus furiosus* DSM 3638, eIF-2
KM3_73_B11: Uncultured marine thaumarchaeote KM3_73_B11, RNA-binding S1 domain-containing protein
P. fumarii: *Pyrolobus fumarii*, eIF-2 subunit alpha
T. archaeon: *Thaumarchaeota archaeon* SCGC AAA007-O23, RNA-binding protein
A. niger: *Aspergillus niger* CBS 513.88, eIF2 subunit alpha
M. infernus: *Methanocaldococcus infernus* ME, eIF2, alpha subunit
SAT1000_48_A08: uncultured marine thaumarchaeote SAT1000_48_A08, RNA-binding S1 domain-containing protein
Euryarchaeote: uncultured marine group II euryarchaeote, eIF-2 subunit alpha
M. maripaludis: *Methanococcus maripaludis* C6, eIF-2 subunit alpha
GW2011_AR3: archaeon GW2011_AR3, eIF2 subunit 1
A. camini: *Aeropyrum camini* SY1 = JCM 12091, eIF-2 subunit alpha

Table 5.5. Gcd1 Alignments.

```
S. cerevisiae      64  PKALLPIGNRPMIEYVLDWCDQADFKEISVVAPVDEIELIE
S. pombe           61  PKALLPIGNKPMLHYPLYWLEAAGFTSAILICMEEAEAHIN
Y. lipolitica      29  PKALLPMANVPVIDYTLKWCETIPNPKVFVCCSTADEAEIS
H. sapien          24  PKPLLPVGNKPLIWYPLNLLERVGFEEVIVVTTRDVQKALC
S. stipitis        26  PKALLPIANKPMLSYVLDWCEKAFFPRVTVVVGTDAESDIQ
L. elongisporus    26  PKALIPVANKSILTYVLDWCFTASFSKILVVTSQESSEQVQ
C. orthopsilosis   26  PKALLPIANEPMINYVLDWCHRAVLSKIVVVTQEETSESVE
A. niger           35  PKCLIPIALRPMVYYPLDWCKRAGINDIVLITPPSALAPLK
C. albicans        26  PKPLLPIANKPMVQYVLDWCLQANFSRIIVLF---EKEDES
S. brasiliensis    34  PKALLPIANRPMVWYPLDFCNRAGITDITLICPPSASEAIK
M. guilliermondii  27  PKALLPVANRPMVEYVLDWCQKAFFPLVTLVCNGEDKLEIA
T. marneffei       35  PKALIPIANRPMVWYPLDWCYRMGITNITLVTPPASQAPLE
```

S. cerevisiae: *Saccharomyces cerevisiae*, eIF2B subunit gamma
S. pombe: *Schizosaccharomyces pombe* 972h-, eIF2B gamma subunit (predicted)
Y. lipolytica: *Yarrowia lipolytica*, eIF-2B gamma N
H. sapiens: *Homo sapiens*, eIF-2B subunit gamma isoform 2
A. niger: *Aspergillus niger* CBS 513.88, eIF2B-gamma
S. stipitis: *Scheffersomyces stipitis* CBS 6054, eIF2B subunit
M. farinosa: *Millerozyma farinosa* CBS 7064, Piso0_002371
L. elongisporus: *Loderomyces elongisporus* NRRLYB-4239 conserved predicted protein
C. orthopsilosis: *Candida orthopsilosis* Co 90-125, Gcd1 translation initiation factor
C. albicans: *Candida albicans* P57072, eIF-2B subunit gamma
S. brasiliensis: *Sporothrix brasiliensis* 5110, eIF-2B subunit gamma
M. guilliermondii: *Meyerozyma guilliermondii*, hypothetical protein PGUG_03826
T. marneffei: *Talaromyces marneffei* ATCC 18224, putative eIF2B-gamma

DISCUSSION

Translation initiation is an intricate and highly choreographed process involving multiple protein complexes. The many layers of regulation for this process are not yet known, as evidenced by the dearth of information on fusel alcohol regulation. We have evolved strains of *S. cerevisiae* with increased tolerance toward medium-chain alcohols owing to mutations in the translation initiation factors Gcd1 and Sui2. These two mutations confer nearly identical tolerance levels. Given the highly similar phenotypes, we expect that these two mutations are alleviating or counteracting the same alcohol toxicity mechanism. The mutations did not affect tolerance toward other non-alcohol compounds such as carboxylic acids or polyamines (Chapter 4). Therefore, it seems likely that the toxicity mechanism is alcohol specific. Since both eIF2 and eIF2B mutations improve translation initiation rates and overall strain tolerance, we hypothesize that the alcohols are interfering with interaction between these two complexes. Sui2 has been crystallized [24], and residues that interact with eIF2B and kinases are known [22,29,30]. Sui2 residue D77 falls in the eIF2B-eIF2 binding interface, as depicted in Figure 5.8. Gcd1 does not have a crystal structure, so it is difficult to interpret how the Gcd1^{D85E} mutation may be affecting eIF2-eIF2B interactions. Further investigation into the Gcd1 and Sui2 mutants will yield valuable information

about the mechanism of translation initiation inhibition by alcohols.

It is interesting to note that both strains sequenced from a second round of evolution (sSD019 and sSD021) acquired mutations in the drug efflux pump Pdr5 (Table 5.2). In Chapter 4 we showed that a *ΔPDR5* strain did not have improved growth in hexanol, though it is known that *ΔPDR5* strains have higher growth rates in butanol [31]. As the only pertinent genomic difference between sSD003 and sSD019 is the *pdr5* truncation which is undoubtedly eliminating Pdr5 function, it is likely that the improvement in growth in isobutanol, amyl alcohol, and isoamyl alcohol is caused by the loss of Pdr5 function. The G925A mutation in strain sSD021 probably has a similar improvement upon tolerance. We ran a polysome analysis on a *ΔPDR5* strain and found that it did not affect translation initiation. The Pdr5 truncation and Pdr5^{G925A} mutation are likely improving tolerance by enhancing overall cell fitness, as Pdr5 utilizes a large amount of energy. In growth-limiting conditions, even slight advantages such as a *ΔPDR5* can help a strain overtake a culture. We did not pursue these mutations further.

Polysome profiling is a standard assay used to assess defects in translation initiation. Polysomes are clusters of ribosomes translating an mRNA [32,33]. Inhibition of translation initiation reduces the number of polysomes inside the cell, while single ribosomes, or monosomes, are comparatively increased. A decrease in the polysome to monosome ratio (P/M) is evidence of defects in translation initiation. Ribosomes that are not translating – "vacant" ribosomes – can be distinguished from single ribosomes by their salt sensitivity [32]. Additionally, defects in elongation can be differentiated with this method. Elongation defects without translation initiation defects will result in a larger P/M ratio, as more ribosomes accumulate on each mRNA [34].

We used polysome profiling to look at how alcohols and the Gcd1 and Sui2 mutants are specifically affecting translation initiation. It is clear that hexanol inhibits translation initiation (Figure 5.6A), and that the Gcd1^{D85E} and Sui2^{D77Y} mutations can rescue the phenotype (Figure 5.6B), though the exact mechanism is as-yet unknown. The Gcd1 and Sui2 mutations confer slightly different polysome profiles, which indicates that they may function through different mechanisms. Strain sSD021, with the Sui2^{D77Y} mutation, continues to exhibit high levels of translation initiation even in 0.2% *n*-hexanol (Figure 5.6A). In the same concentration, strain sSD003, which has the Gcd1^{D85E} mutation, has dramatically reduced translation initiation, and the polysome profiles show halfmers (data not shown). We were unable to identify halfmers in the polysome analysis of strains with the Sui2 mutation. Another hint at multiple mechanisms is the fact that only strains with the Gcd1^{D85E} mutation have *n*-butanol tolerance (Table 5.3).

We wanted to look more deeply at what made these specific mutations give medium-chain alcohol tolerance. Saturation mutagenesis at Gcd1 position 85 and Sui2 position 77 result in a small library with varying tolerance levels (Figure 5.7). Unfortunately, there did not seem to be any pattern for which mutations improved tolerance. I, V, and N at position 85 of Gcd1 confer the most improvement, while M, S, and W give rise to the worst tolerances (Figure 5.7A-D). For Sui2 residue 77, V, I, and K were the most capable mutations, while E, H, and M did not improve tolerances (though butanol tolerance was quite different) (Figure 5.7E-H). It is surprising that so many amino acids were able to improve tolerance levels. Since these positions are very well conserved across species (Table 5.4 and 5.5), we did not expect such a variety of residues to be accommodated. Figure 5.7G shows that nearly all other residues can

improve tolerance over the native aspartate. We anticipate that there is some strong evolutionary pressure toward maintaining these positions. As all of our experiments are done on short timescales and in favorable conditions, the yeasts are not experiencing extreme stress or starvation conditions that would necessitate inhibition of translation initiation for survival. Experiments in amino-acid limited media or over long time-scales would be useful for investigating the mechanisms of both alcohol tolerance and translation initiation regulation.

We anticipate that the Sui2 and Gcd1 mutations will be valuable tools for studying the effects of various alcohols on translation initiation and for probing the mechanism of fusel alcohol inhibition. The mutations, and any further insights into translation initiation inhibition, will be useful for generating medium-chain alcohol production strains with high tolerance and high titers.

MATERIALS AND METHODS

Strains and Media

We used wild-type *Saccharomyces cerevisiae* strain BY4741 (*MAT*a *his3Δ1 leu2Δ0 met15Δ0 ura3Δ0*). Yeast without plasmids were grown in YPD (1% yeast extract, 2% peptone, 2% α-dextrose). Yeast with plasmids were grown in appropriate synthetic dropout media, eg SD-Leu (0.67% Yeast Nitrogen Base (Amresco), 2% α-Dextrose (BD Chemical), 0.2% amino acid mix without leucine from US Biological).

Growth Curves

Single colonies were picked from the post-evolution plates into 5 mL YPD media in culture tubes. Cultures were grown overnight to saturation at 30°C with 280 rpm shaking. Stationary phase cultures were diluted to an OD_{600} of .30-.33 a.u. as measured with a Nanodrop 2000c, 5 mL dilute culture was aliquoted into screw-cap tubes. 5 mL YPD with 0 or 0.24% or 0.30% *n*-hexanol was added. Each sample was run in triplicate. Screw-cap tubes were grown at 30°C with 280 rpm shaking and measurements were taken every 2 hours with Genesys-20 spectrophotometer.

Strain and Plasmid Generation

Plasmids were generated using standard molecular biology cloning techniques and homologous recombination. Transformations were performed using the LiOAc protocol [23]. Knock-outs were generated by replacing the genes of interest with KanMX4 or His3 markers via homologous recombination into strains containing plasmid copies of the selected genes.

Polysome Profiling

Overnight cultures were diluted into 250 mL YPD and grown until an OD_{600} of ~1. Cultures were exposed to solvents for 30 minutes, then 25 mg cycloheximide (Sigma) in DMSO (Sigma) was added to arrest translation. Cells were washed twice and resuspended in buffer {20 mM Tris (Fisher) pH 7.4, 50 mM KCl (Spectrum), 10 mM MgCl2 (EMD), 1 mM DTT (Fisher), 100 µg/mL cycloheximide(Sigma)}. 800 µg of RNA was loaded onto a 10-50% sucrose (Fisher) gradient and centrifuged 3 hours at 35,000 rpm. The gradient was fractionated and absorbance at 254 nm measured. Polysome and monosome peak areas were calculated using Microsoft Excel.

Table 5.6 Plasmids used in this study

Plasmid	Promoter	Insert	Marker	Reference
pSD269	pTdh3	Venus	Ura3	[26]
pSD279	pRev1	Emerald	Leu2	[26]
pSD442	pGcd1	Gcd1	Ura3	This Study
pSD443	pGcd7	Gcd7	Ura3	This Study
pSD444	pSui2	Sui2	Ura3	This Study
pSD450	pGcd1	Gcd1 D85E	Ura3	This Study
pSD451	pGcd7	Gcd7 R56C	Ura3	This Study
pSD452	pSui2	Sui2 D77Y	Ura3	This Study
pSD469	pGcd7	Gcd7 R56C	Leu2	This Study
pSD474	pGcd7	Gcd7	Leu2	This Study
pSD447	pGcd1	KanMX	Ura	This Study
pSD448	pGcd7	KanMX	Ura	This Study
pSD449	pSui2	KanMX	Ura	This Study
pSD463	pHis3	His3	His3	[26]
pSD538	pSui2	Sui2 D77A	Ura3	This Study
pSD539	pSui2	Sui2 D77C	Ura3	This Study
pSD540	pSui2	Sui2 D77E	Ura3	This Study
pSD541	pSui2	Sui2 D77F	Ura3	This Study
pSD542	pSui2	Sui2 D77G	Ura3	This Study
pSD543	pSui2	Sui2 D77H	Ura3	This Study
pSD544	pSui2	Sui2 D77I	Ura3	This Study
pSD545	pSui2	Sui2 D77K	Ura3	This Study
pSD546	pSui2	Sui2 D77L	Ura3	This Study
pSD547	pSui2	Sui2 D77M	Ura3	This Study
pSD548	pSui2	Sui2 D77N	Ura3	This Study
pSD549	pSui2	Sui2 D77P	Ura3	This Study
pSD550	pSui2	Sui2 D77Q	Ura3	This Study
pSD551	pSui2	Sui2 D77R	Ura3	This Study
pSD552	pSui2	Sui2 D77S	Ura3	This Study
pSD553	pSui2	Sui2 D77T	Ura3	This Study
pSD554	pSui2	Sui2 D77V	Ura3	This Study
pSD555	pSui2	Sui2 D77W	Ura3	This Study
pSD557	pGcd	Gcd1 D85A	Ura3	This Study
pSD558	pGcd	Gcd1 D85C	Ura3	This Study
pSD559	pGcd	Gcd1 D85F	Ura3	This Study
pSD560	pGcd	Gcd1 D85G	Ura3	This Study
pSD561	pGcd	Gcd1 D85H	Ura3	This Study
pSD562	pGcd	Gcd1 D85I	Ura3	This Study
pSD563	pGcd	Gcd1 D85K	Ura3	This Study
pSD564	pGcd	Gcd1 D85L	Ura3	This Study
pSD565	pGcd	Gcd1 D85M	Ura3	This Study
pSD566	pGcd	Gcd1 D85N	Ura3	This Study
pSD567	pGcd	Gcd1 D85P	Ura3	This Study
pSD568	pGcd	Gcd1 D85Q	Ura3	This Study

pSD569	pGcd	Gcd1 D85R	Ura3	This Study
pSD570	pGcd	Gcd1 D85S	Ura3	This Study
pSD571	pGcd	Gcd1 D85T	Ura3	This Study
pSD572	pGcd	Gcd1 D85V	Ura3	This Study
pSD573	pGcd	Gcd1 D85W	Ura3	This Study
pSD574	pGcd	Gcd1 D85Y	Ura3	This Study

Table 5.7 Strains used in this study.

Strain	Parent	Genotype	Reference
BY4741		*MATa his3Δ1 leu2Δ0 met15Δ0 ura3Δ0*	
BY4742		*MATα his3Δ1 leu2Δ0 lys2Δ0 ura3Δ0*	
1516	BY4741	*MATa his3Δ1 leu2Δ0 met15Δ0 ura3Δ0 TPO1Δ::KANMX*	[27]
sSD002	BY4741	*BY4741 GCD1-E85 CIT2-C338*	This Study
sSD003	BY4741	*BY4741 GCD1-E85 CIT2-C338*	This Study
sSD004	BY4741	*BY4741 evolved*	This Study
sSD006	BY4741	*BY4741 GCD7-C56*	This Study
sSD009	BY4741	*BY4741 evolved*	This Study
sSD010	BY4741	*BY4741 evolved*	This Study
sSD017	BY4741	*BY4741 evolved*	This Study
sSD018	BY4741	*BY4741 evolved*	This Study
sSD019	BY4741	*BY4741 gcd1-E85 cit2-C338 pdr5-*446 ubp13-V135 lsb6-C234 nst1-G662*	This Study
sSD020	BY4741	*BY4741 evolved*	This Study
sSD021	BY4741	*BY4741 gcd7-C56 sui2-Y77 pdr5-A925 sey1-529E*	This Study
sSD029	BY4741	*BY4741 Gcd1Δ::KANMX p[gcd1-85E LEU2 CEN6]*	This Study
sSD040	BY4741	*BY4741 GCD7Δ::HIS3 p[gcd7-56C URA3 CEN6]*	This Study
pSD053	BY4741	*BY4741 GCD1Δ::KANMX p[GCD1 LEU2 CEN6]*	This Study
pSD054	BY4741	*BY4741 GCD7Δ::HIS3 p[GCD7 URA3 CEN6]*	This Study
pSD055	BY4741	*BY4741 SUI2Δ::KANMX p[SUI2 LEU2 CEN6]*	This Study
pSD056	BY4741	*BY4741 SUI2Δ::KANMX p[sui2-77Y LEU2 CEN6]*	This Study
pSD058	sSD056	*BY4741 SUI2Δ::KANMX GCD7Δ::HIS3 p[sui2-77Y LEU2 CEN6] p[gcd7-56C URA3 CEN6]*	This Study
pSD060	sSD055	*BY4741 SUI2Δ::KANMX GCD7Δ::His3 p[SUI2 LEU2 CEN6] p[GCD7 URA3 CEN6]*	This Study

Table 5.8 Plasmid and strain construction

Plasmid	Insert F/R Primers(Template)	Vector(Restriction Sites)
pSD442	SDc25/SDc26(Genomic)	pSD269(SpeI/BamHI)
pSD443	SDc27/SDc28(Genomic)	pSD269(SpeI/BamHI)
pSD444	SDc29/SDc30(Genomic)	pSD269(SpeI/BamHI)
pSD450	SDc25/SDc26(sSD003)	pSD269(SpeI/BamHI)
pSD451	SDc27/SDc28(sSD006)	pSD269(SpeI/BamHI)
pSD452	SDc29/SDc30(sSD021)	pSD269(SpeI/BamHI)
pSD469	SDc27/SDc28(pSD443)	pSD279(SpeI/BamHI)
pSD474	SDc27/SDc28(pSD451)	pSD279(SpeI/BamHI)
pSD447	SDc31/SDc32(1516)	pSD442(ClaI)
pSD448	SDc33/SDc34(1516)	pSD443(NruI)
pSD449	SDc35/SDc36(1516)	pSD444(BglII)
pSD468	SDc71/SDc72(pSD463)	pSD443(NruI)
pSD538-555	SDc10/SDd72/SDd71/SDc11(pSD444)	pSD449(ClaI)
pSD557-574	SD673/SDe15/SDe06/SDb74(pSD442)	pSD447(ClaI)

Knockout Cassettes	Primers	Template
ΔGcd1Δ::KanMX	SDc25/SDc26	pSD447
ΔGcd7Δ::KanMX	SDc27/SDc28	pSD448
ΔSui2Δ::KanMX	SDc29/SDc30	pSD449
ΔGcd7Δ::His3	SDc27/SDc28	pSD468

Primers	F/R	Sequence
SDc25	F	gggcgaattggagctcactcggaattcagtctactagtgatcacggtcatctcttatg
SDc26	R	atcataaatcataagaaattcgcctcgagttaggatccgaaaacatgaatgaaatgtgta
SDc27	F	gggcgaattggagctcactcggaattcagtctactagttacaactttgaaaagcctttc
SDc28	R	atcataaatcataagaaattcgcctcgagttaggatccagtgcagtatgaataaaagacc
SDc29	F	gggcgaattggagctcactcggaattcagtctactagtattgcgagatgaaatataaacc
SDc30	R	atcataaatcataagaaattcgcctcgagttaggatccaaccatcataggaaataccttc
SDc31	F	aaagttcccaccgttgatagctccccccctattgtcgtagtccgtacgctgcaggtc
SDc32	R	gtctctattaaagagactgaaggaatatacataagtttataatcgatgaattcgagctcg
SDc33	F	gtaaacacaacacgccaactttcgaacttttgcccaacataagcgtacgctgcaggtc
SDc34	R	agatttttatttatttttcatgagtaatgtacaaaagacacaatcgatgaattcgagctcg
SDc35	F	gtcttttctgctgcctcacgcaccttctataatacaccaaatacgtacgctgcaggtc
SDc36	R	tgacacttgaaaacacctagaaaaattaggcgcggcaatgaatcgatgaattcgagctcg
SDc71	F	caacacgccaactttcgaacttttgcccaacataagtaattccgttttaagagcttggtg
SDc72	R	ttttatttatttttcatgagtaatgtacaaaagacacatcatatgatccgtcgagttcaag
SDb73	F	ggtcctgttcttcactcattcttag
SDb74	R	gagtaaaggacaaacaatcaaaagtctc
SDc10	F	tcttacccgcagtcggaga
SDc11	R	gcatgctccactgacaacc
SDd71	F	ccgttgttcttcgtgtcNNNaaagaaaaaggttatattgatttgtcca
SDd72	R	ctttttctttNNNgacacgaagaacaacggcgaca
SDe06	F	cgtcttggattggtgtNNKcaggcagatttc
SDe15	R	gaaatctgcctgNNNacaccaatccaagacg

REFERENCES

1. Ohto C, Muramatsu M, Obata S, Sakuradani E, Shimizu S. Overexpression of the gene encoding HMG-CoA reductase in Saccharomyces cerevisiae for production of prenyl alcohols. Appl Microbiol Biotechnol. 2009, 82(5):837-45.

2. Steen E, Chan R, Prasad N, Myers S, Petzold CJ, Redding A, Ouellet M, Keasling JD. Metabolic engineering of Saccharomyces cerevisiae for the production of n-butanol. Microb Cell Fact. 2008, 7:36.

3. Avalos JL, Fink GR, Stephanopoulos G. Compartmentalization of metabolic pathways in yeast mitochondria improves the production of branched-chain alcohols. Nat Biotechnol. 2013, 31(4):335-41.

4. Bowles LK, Ellefson WL. Effects of Butanol on *Clostridum acetobutylicum*. App Env Microbiol. 1985, 50(5):1165-70.

5. Miyawaki O, Tatsuno Michiko. Thermodynamic analysis of alcohol effect on thermal stability of proteins. J Biosci Bioeng. 2011, 111(2):198-203.

6. Gaskova D, Plasek J, Zahumensky J, Benesova I, Buriankova L, Sigler K. Alcohols are inhibitors of Saccharomyces cerevisiae multidrug-resistance pumps Pdr5 and Snq2. FEMS Yeast Res. 2013, 13(8):782-95.

7. Ashe MP, Slaven JW, DeLong SK, Ibrahimo S, Sachs AB. A novel eIF2B-dependent mechanism of translational control in yeast as a response to fusel alcohols. EMBO J. 2001, 20(22):6464-74.

8. Taylor EJ, Campbell SG, Griffiths CD, Reid PJ, Slaven JW, Harrison RJ, Simps PF, Pavitt GD, Delneri D, Ashe MP. Fusel Alcohols Regulate Translation Initiation by Inhibiting eIF2B to reduce ternary complex in a mechanism that my involve altering the Integrity and Dynamics of the eIF2B Body. Mol Biol Cell. 2010, 21(13):2202-16.

9. Merrick WC. Eukaryotic Protein Synthesis: Still a Mystery. J Biol Chem. 2010, 285(28):21197-201.

10. Hinnebusch AG. Translational regulation of GCN4 and the general amino acid control of yeast. Annu Rev Microbiol 2005, 59:407-50.

11. Hinnebusch AG, Liebman SW. Protein synthesis and Translational Control in S. cerevisiae. V.1. The Molecular and Cellular Biology of the Yeast Saccharomyces: Genome Dynamics, Protein Synthesis, and Energetics, 1991. Cold Spring Harbor Laboratory Press.

12. Pavitt GD, Yang W, Hinnebusch AG. Homologous segments in three subunits of the guanine nucleotide exchange factor eIF2B mediate translational regulation by phosphorylation of eIF2. Mol Cell Biol. 1997, 17(3):1298-313.

13. Pavitt GD, Ramaiah KVA, Kimball SR, Hinebusch AG. eIF2 independently binds two distinct eIF2B subcomplexes that catalyze and regulate guanine-nucleotide exchange. Genes Dev. 1998, 12:514-26.

14. Gonzalez-Ramos D, van den Broek M, van Maris AJA, Pronk JT, Daran JMG. Genome-scale analyses of butanol tolerance in Saccharoymces cerevisiae reveal an essential role of protein degradation. Biotechnol Biofuels. 2013, 6(1):48.

15. Ghiaci P, Norbeck J, Larsson C. Physiological adaptations of Saccharomyces cerevisiae evolved for improved butanol tolerance. Biotechnol Biofuels. 2013, 6(1): 101.

16. Ezeji T, Milne C, Price ND, Blaschek HP. Achievements and perspectives to overcome the poor solvent resistance in acetone and butanol-producing microorganisms. Appl Microbiol Biotechnol. 2010, 85:1697–712.

17. Knoshaug EP, and Ming Z. Butanol Tolerance in a Selection of Microorganisms. Appl Biochem Biotechnol. 2009, 153:13-20.

18. Dever TE. Using GCN4 as a reporter of eIF2a phosphorylation and translational regulation in yeast. Methods. 1997, 11:403-17.

19. Yoon H, Donahue TF. Control of translation initiation in S. cerevisiae. Mol Microbio. 1992, 6(11):1413-19.

20. Preiss T, Hentze MW. Starting the protein synthesis machine: eukaryotic translation initiation. BioEssays. 2000, ;25:1201-11.

21. Palmer LK, Shoemaker JL, Baptiste BA, Wolfe D, Keil RL. Inhibition of translation initiation by volatile anesthetics involves nutrient-sensitive GCN-independent and -dependent processes in yeast. Mol Cell Biol. 2005, 16:3727-39.

22. Dev K, Qiu H, Dong J, Zhang F, Barthlme D, Hinnebusch AG. The ß/Gcd7 Subunit of Eukaryotic Translation Initiation Factor 2B (eIF2B), a Guanine Nucleotide Exchange Factor, Is Crucial for Binding eIF2 *In vivo*. Mol Cell Biol. 2010, 30(21): 5218-33.

23. Geitz D, St Jean A, Woods RA, Schiestl RH. Improved method for high efficiency transformation of intact yeast cells. Nucleic Acids Res. 1992, 20(6):1425.

24. Dhaliwal S, Hoffman DW. The crystal structure of the N-terminal region of the alpha subunit of translation initiation factor 2 (eIF2alpha) from Saccharomyces cerevisiae provides a view of the loop containing serine 51, the target of the eIF2alpha-specific kinases. J Mol Biol. 2003, 334:187-95.

25. The PyMOL Molecular Graphics System, Version 1.7.4 Schrödinger, LLC.

26. Lee ME, Aswani A, Han AS, Tomlin CJ, Dueber JE. Expression level optimization of a multi-enzyme pathway in the absence of a high-throughput assay. Nucleic Acids Res. 2013, 41(22):10668-78.

27. Giaever G, Chu AM, Ni L, Connelly C, Riles L, Véronneau S, Dow S, Lucau-Danila A, Anderson K, André B, Arkin AP, et al. Functional Profiling of the *Saccharomyces cerevisiae* Genome. Nature. 2002, 418(6896):387-91.

28. Helser TL, Baan RA, Dahlberg AE. Characterization of a 40S ribosomal subunit complex in polyribosomes of *Saccharomyces cerevisiae* treated with cycloheximide. Mol Cell Biol. 1981, 1(1):51.

29. Dar AC, Dever TE, Sicheri F. Higher-Order Substrate Recognition of eIF2alpha by the RNA-Dependent Protein Kinase PKR. Cell. 2005, 122:887-900.

30. Dey M, Trieselmann B, Locke EG, Lu J, Cao C, Dar AC, Krishnamoorthy T, Dong J, Sicheri F, Dever TE. PKR and GCN2 Kinases and Guanine Nucleotide Exchange Factor Eukaryotic Translation Initiation Factor 2B (eIF2B) Recognize Overlapping Surfaces of eIF2B a. Mol Cell Biol. 2005, 25(8):3063-75.

31. Butamax (Tm) Advanced Biofuels Llc. Yeast with increased butanol tolerance involving a multidrug efflux pump gene. 2010, US patent application: US 12/711,308. Publication number: US20100221801 A1. Filing date: Feb 24, 2010.

32. Lee AS, Burdeinick-Kerr R, Whelan SP. A ribosome-specialized translation initiation pathway is required for cap-dependent translation of vesicular stomatitis virus mRNAs. Proc Natl Acad Sci USA. 2013, ;110(1):324-29.

33. Yoon H, Donahue TF. The sui1 supressor locus in Saccharomyces cerevisiae encodes a translation factor that functions during $tRNA^{Met}_i$ Recognition of the Start Codon. Mol Cell Biol. 1992, ;12(1):248-60.

34. Ortiz PA, Kinzy TG. Dominant-negative mutant phenotypes and the regulation of translation elongation factor 2 levels in yeast. Nuc Acid Res. 2005, 33(18):5740-48.

Chapter 6
Improving yields by optimizing AcCoA flux

ABSTRACT

Many commercial products, including biofuels and specialty compounds, are produced cytosolically in *Saccharomyces cerevisiae* from acetyl-CoA (AcCoA). Increasing available AcCoA can improve titers of these bioproducts. One mechanism to increase cytosolic AcCoA is to use a transporter to direct AcCoA from organelles such as the mitochondria into the cytoplasm. There is no direct AcCoA transport between these regions. However, AcCoA transporters exist. The human AT-1 transporter acts directly on AcCoA to move AcCoA from the cytosol to the endoplasmic reticulum (ER) lumen [1]. Additionally, there is a homolog found in *S. cerevisiae*, YBR220C. We are re-engineering these transporters to control AcCoA flux between the mitochondria and cytoplasm.

INTRODUCTION

Acetyl Coenzyme A (AcCoA) is important for production of many compounds, including industrially useful molecules such as pharmaceuticals and biofuels. One such compound is amorphodiene, a precursor to the drug artemisinin [2]. High value products such as α-santalene [3] and flavenoids such as naringenin [4] are also produced from AcCoA. AcCoA is the building block for cellular lipids, and lipid-like products such as linolenic acid [5], sterols [6], and omega-3-fatty acids [6]. AcCoA can be built up to butyryl-CoA and then converted to *n*-butanol via alcohol dehydrogenase [7,8]. A potential limitation in the production of such compounds is the level of cytosolic AcCoA.

Many groups have used metabolic engineering approaches to improve cytoplasmic acetyl CoA levels. The strategy of deleting competing AcCoA-utilizing enzymes and pathways, including malate and citrate synthases, has been used to improve *n*-butanol production [7]. Another example involves what was coined the "pyruvate dehydrogenase bypass," in which Shiba and colleagues expressed a *Salmonella* AcCoA synthetase in *S. cerevisiae* and overexpressed acetaldehyde dehydrogenase to increase cellular acetyl-CoA levels [2]. This technique resulted in two-fold higher titers of amorphodiene [2]. A combination of these approaches was used to increase α-santalene production by four-fold [3]. It is also possible to engineer pyruvate dehydrogenase overproduction to increase cytoplasmic AcCoA; this approach conferred a 12-fold increase in *n*-butanol production [9].

AcCoA is found in significant concentrations within the cytosol, peroxisomes, and mitochondria, but there is no direct transport of AcCoA between these locations in yeast [10]. Additionally, AcCoA pools are not constant, and vary depending on cell state and carbon source [10]. Increasing overall AcCoA certainly helps to improve cytoplasmic concentrations, but there is still room for improvement. Controlling flux of AcCoA among the cellular pools can help stabilize AcCoA levels and direct AcCoA to the cytoplasm where it is needed for bioproduction. In an interesting study, Matsuda *et al*. simulated a merging of cytoplasmic and mitochondrial spaces, which allowed for transport of cofactors such as $NADP^+$ and acetyl-CoA between the two spaces. The merged

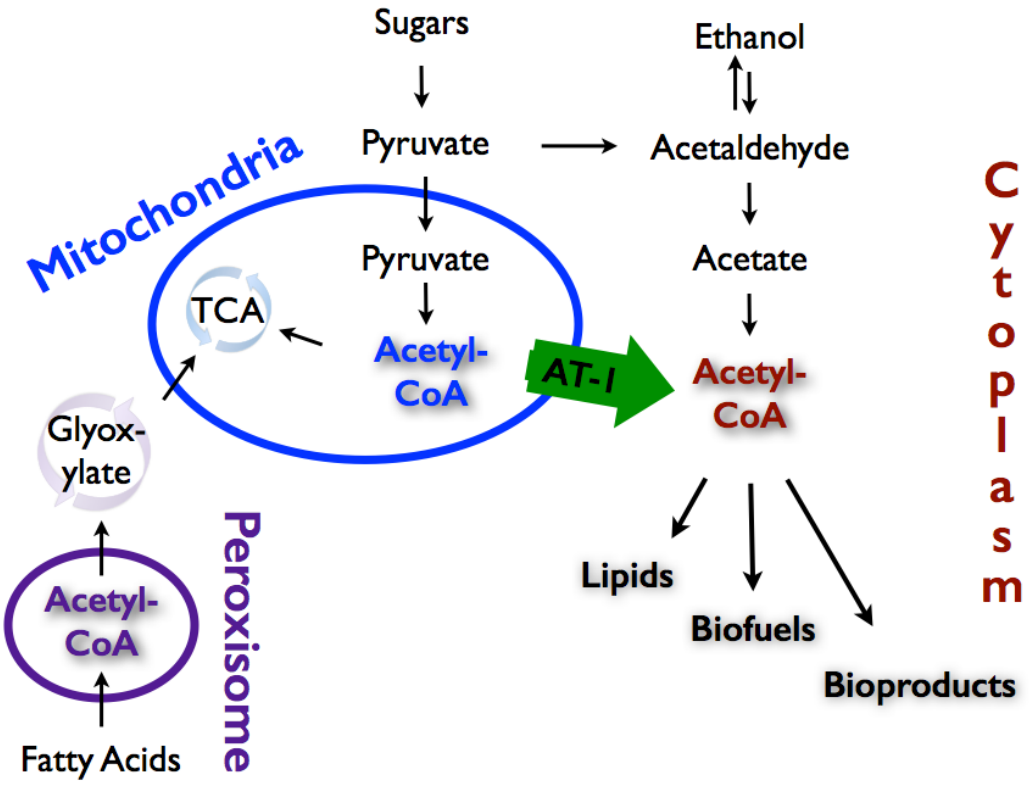

Figure 6.1. Acetyl CoA metabolism is important for production of many bioproducts. The purple circle indicates the peroxisome and the blue circle indicates the mitochondria. Cytosolic AcCoA is shown in red. The AcCoA pools are linked indirectly via metabolism. We intend to directly link the mitochondrial and cytoplasmic AcCoA pools via the AT-1 transporter.

cytoplasm-mitochondria model improved theoretical yields of *n*-butanol production [11]. Implementing this "sharing" of acetyl-CoA among the mitochondria and cytoplasm in conjunction with the metabolic strategies for increasing AcCoA will improve strains for AcCoA-based bioproduction.

AcCoA cannot passively diffuse through membranes at appreciable rates, so an alternate transport mechanism is required to move it between intracellular compartments. There are several indirect methods that control AcCoA levels in intracellular compartments (Figure 6.1) [3]. In yeast, the glyoxylate cycle depletes peroxisomal and cytoplasmic AcCoA levels. AcCoA is enzymatically converted into malate and succinate, which are transported to the mitochondrial lumen, in which they enter the TCA cycle [12-13]. In the peroxisome, AcCoA is converted to citrate, which readily leaves the compartment [14]. Another mechanism is the carnitine shuttle, which eukaryotic cells use to deliver AcCoA from the cytoplasm to the mitochondrial matrix [15]. In this process, an enzyme transfers the acetyl group from AcCoA to carnitine, which is than transported into the mitochondria via the Crc1 transporter [12,14]. Inside

the mitochondria, the carnitine is de-acetylated by the enzyme Cat1 and AcCoA is regenerated. Yeast cannot synthesize carnitine, and media supplementation would be cost-prohibitive, which limits implementation of the carnitine shuttle for high-level production. Interestingly, the peroxisome lacks the carnitine transporter Crc1, despite the presence of the Cat1 enzyme [14], so there may be other undiscovered carnitine and AcCoA transport mechanisms. As targets for metabolic engineering, both the glyoxylate shunt and carnitine shuttle have some disadvantages, as they are multi-step processes with low energy efficiency.

A more efficient way to control AcCoA flux is to directly transport AcCoA between compartments. An AcCoA transporter has been identified in humans [16]. Jonas *et al.* identified and characterized the AT-1 transporter as an endoplasmic reticulum (ER)-localized transporter that brings AcCoA from the cytoplasm into the ER lumen [1]. Acetyl-CoA is needed in the ER for protein acetylation. There is a homolog in *S. cerevisiae*, YBR220C, though to date no studies have been published on this transporter. AT-1 is a Major Facilitator Superfamily transporter, so it does not use ATP [1]. These proteins are excellent candidates for engineering increased cytosolic AcCoA concentrations.

With this work, we set out to direct AcCoA flux toward the cytosol using membrane-based transporters. Our first goal was to secrete AcCoA from the mitochondria into the cytosol. We identified and tested several targeting sequences predicted to localize proteins to the mitochondrial membrane. We are now assessing how cytoplasmic AcCoA concentrations are affected by engineered transporters in the mitochondria.

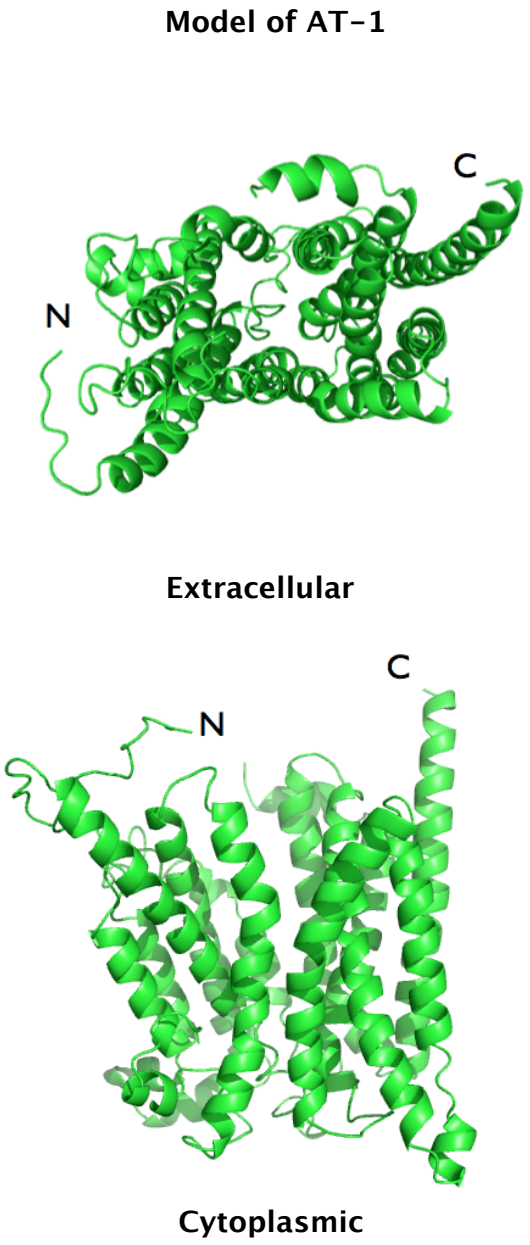

Figure 6.2. AT-1 is an Acetyl-CoA Transporter from H. sapiens. AT-1 is modeled on GlpT using Phyre [25].

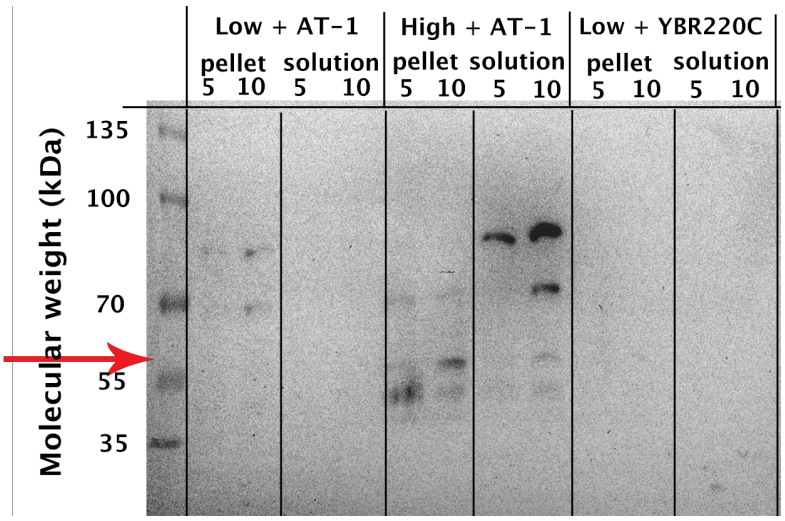

Figure 6.3. The protein transporter AT-1 successfully expresses within the yeast cell. FLAG-tagged AT-1 and YBR220C were expressed under high (pTdh3) and low (pRev1) strength constituitive promoters. Whole cell extracts were run on 15% SDS polyacrylamide gels and transferred to PVDF membranes. Mouse anti-FLAG primary and HRP-conjugated anti-Mouse secondary antibodies were used.

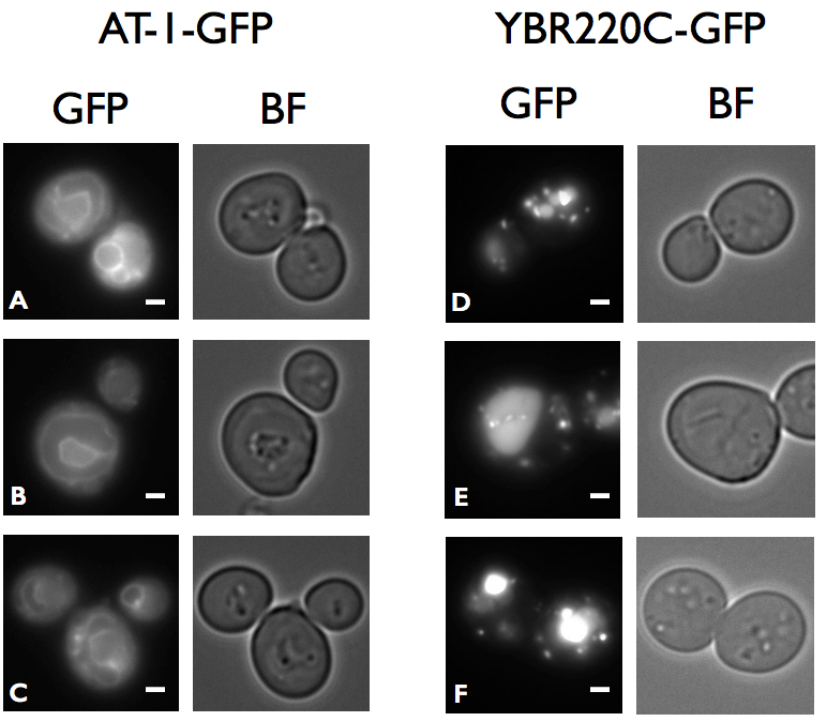

Figure 6.4. AT-1 localizes to the ER while overexpressed YBR220C aggregates. Fluorescent (GFP) and bright field (BF) images of A-C) Strains expressing AT-1 with a C-terminal GFP fusion, D-F) Strains expressing YBR220C with a C-terminal GFP fusion. Scale bar represents 1 μm.

RESULTS

The H. sapiens transporter AT-1 expresses in S. cerevisiae. We cloned the gene encoding the AT-1 transporter with a C-terminal FLAG tag into plasmids under the control of the low-strength pRev1 promoter or the high-strength pTdh3 promoter. Expression was confirmed using a western blot (Figure 6.3). The AT-1-FLAG construct is 64.0 kDa. In the insoluble pellets from strains containing either the low- or high-expression plasmids, we observe bands near the correct size, with some apparent degradation products as well. There is also a larger-sized band, which we attribute to aggregation of degradation products because it is not large enough to be a dimerization of the full protein. Additionally, microscopic analysis of AT-1-GFP fusions show that the transporter is localizing to intracellular membranes, likely the endoplasmic reticulum (Figure 6.4A-C).

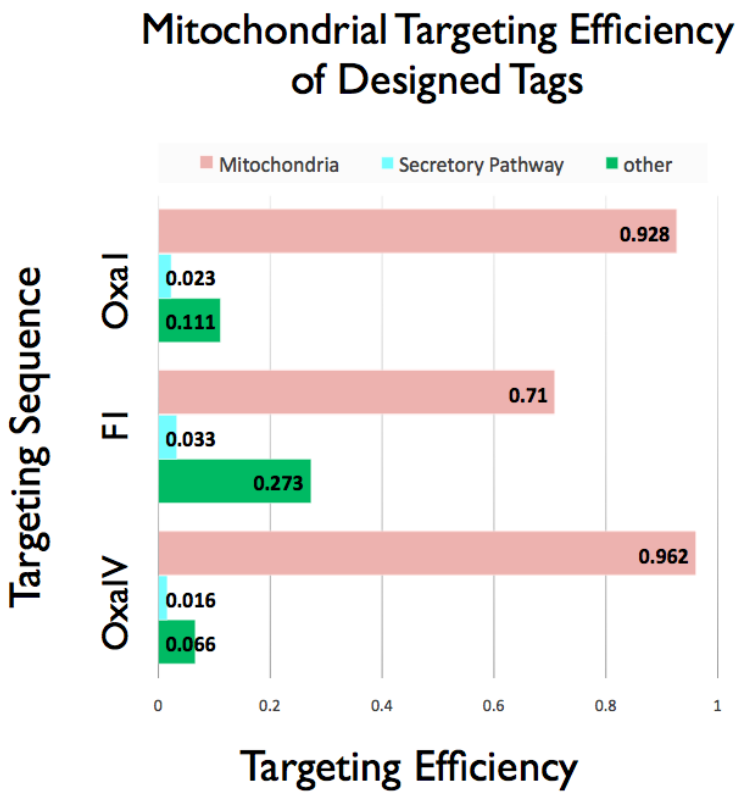

Figure 6.5. Targeting Sequences with high efficiencies are derived from mitochondrial proteins. N-terminal targeting sequences were taken from three mitochondrial proteins: Mitochondrial Oxidase Assembly protein 1 (Oxa1), ATPase F-1 β-subunit (F-1), and Cytochrome Oxidase IV (OxaIV). Targeting efficiencies were calculated with TargetP [20].

Designed tags direct proteins to the mitochondrial inner membrane. Mitochondrial-targeting tags were designed from the N-terminal region of mitochondrial inner membrane proteins. The sequences were taken from the mitochondrial proteins Oxa1, ß-subunit of the F1-ATPase (F1), and cytochrome oxidase IV (OxaIV) (Table 6.2). We used the online program TargetP [20] to predict ability of these designed tags to target proteins to the mitochondria (Figure 6.5). When fused to GFP, the Oxa1 and OxaIV tags appear to localize to the mitochondria, as evidenced by co-localization of tagged GFP and the mitochondrial stain in Figures 6.6A and 6.6C. The F1 tag has a lower targeting efficiency, which much of the GFP remaining in the cytoplasm (Figure 6.6B).

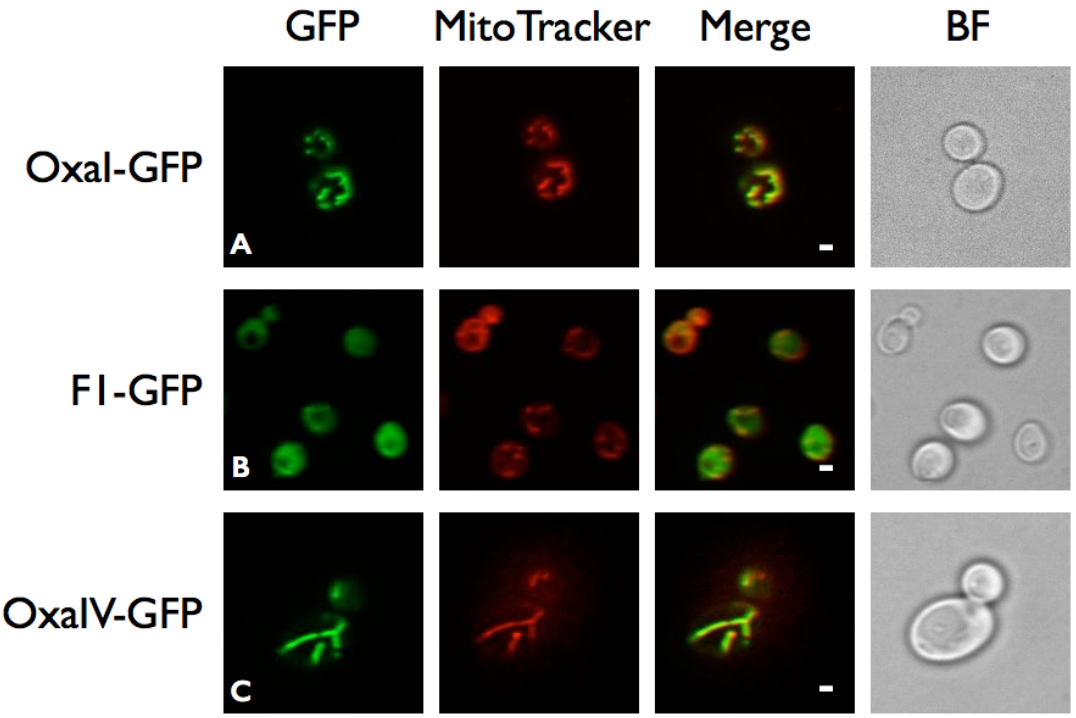

Figure 6.6. Mitochondrial localization of GFP using designed tags. Fluorescent and bright field (BF) images were taken with a confocal microscope. Cells were stained with MitoTracker mitochondrial dye. Images are of strains expressing GFP tagged with targeting sequences A) Oxa1, B) F1, C) Oxa1V. Scale bar represents 1 μm.

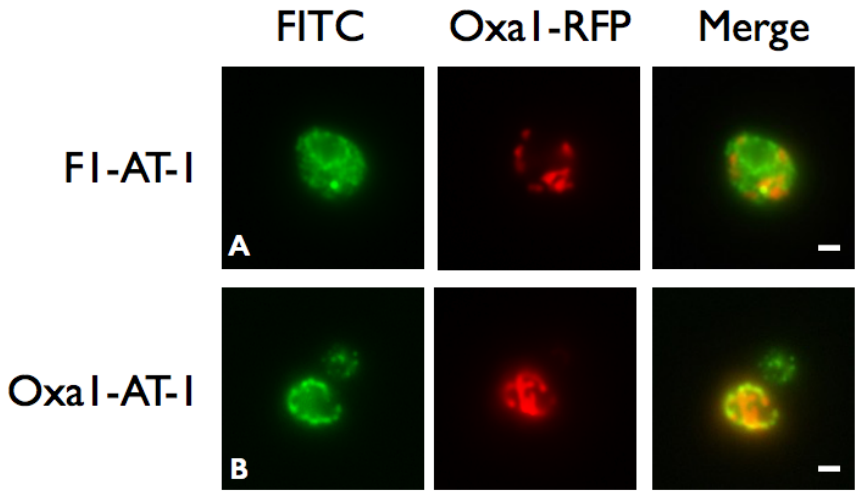

Figure 6.7. Oxa1-tagged AT-1 localizes to the mitochondria, but the F1-tag does not move AT-1 from the ER. Cells expressing Oxa1-RFP and A) Oxa1-AT-1-FLAG or B) F1-AT-1-FLAG were fixed and FLAG tags were labeled with mouse anti-FLAG and goat anti-mouse FITC conjugated antibodies. Scale bar represents 1 µm.

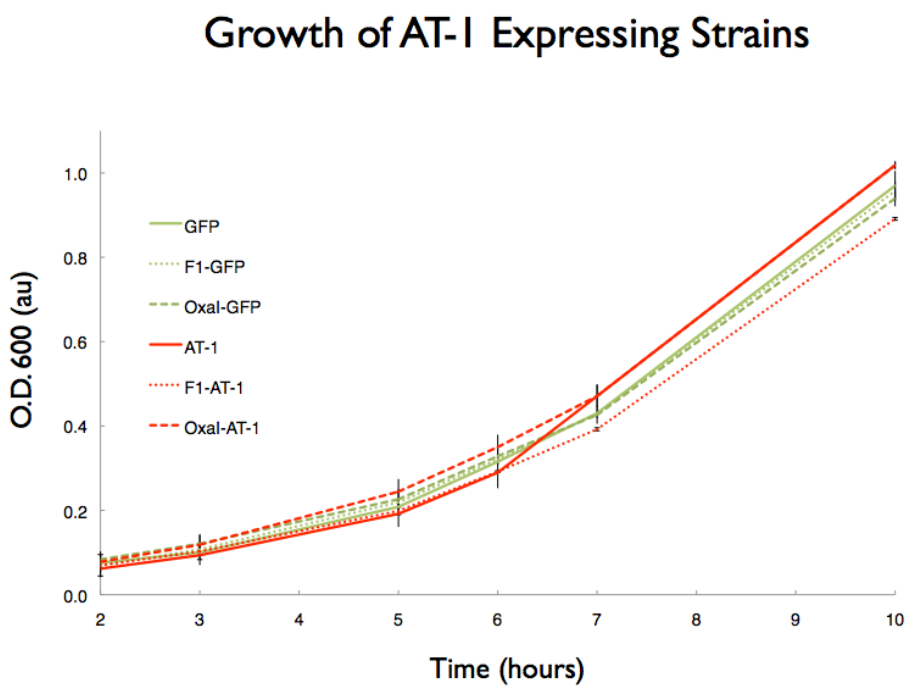

Figure 6.8. AT-1 does not cause a growth defect in *S. cerevisiae*. Strains expressing AT-1 (solid red line), F1-tagged AT-1 (dotted red line) and Oxa1-tagged AT-1 (dashed red line) were grown in SD-Leu and OD_{600} measured periodically. Strains expressing GFP (solid green line), F1-tagged GFP (dotted green line) and Oxa1-tagged GFP (dashed green line) were grown as controls. Samples were run in triplicate and error bars represent standard deviations.

The AT-1 transporter can be targeted to the mitochondria. We similarly generated fusions of the Oxa1 and F1 tags to the AT-1 transporter along with a C-terminal GFP, but were unable to detect any fluorescence. Thus, we next generated fusions of the Oxa1 and F1 tags to the AT-1 transporter along with a C-terminal FLAG tag. We then used immunofluorescence to assess localization. The MitoTracker dye does not work with fixed cells, so we employed an Oxa1-tagged RFP as a mitochondrial control. The Oxa1-tagged AT-1 co-localizes with an Oxa1-tagged RFP, so it is likely that the transporter is in the mitochondria (Figure 6.7B). Conversely, the F1-tagged AT-1 appears to be minimally co-localized with the Oxa1-tagged RFP (Figure 6.7A). The variation in fluorescence patterns is likely because the images were collected on a standard fluorescence microscope.

Mitochondrially targeted AT-1 does not affect growth rates. Growth rates for strains expressing mitochondrial-targeted AT-1 were monitored for 10 hours (Figure 6.8). Control strains expressing GFP, mitochondrially targeted GFP, and untargeted AT-1 were also monitored for growth. There does not appear to be any growth defect for strains expressing AT-1 or mitochondrially-targeted AT-1 or GFP.

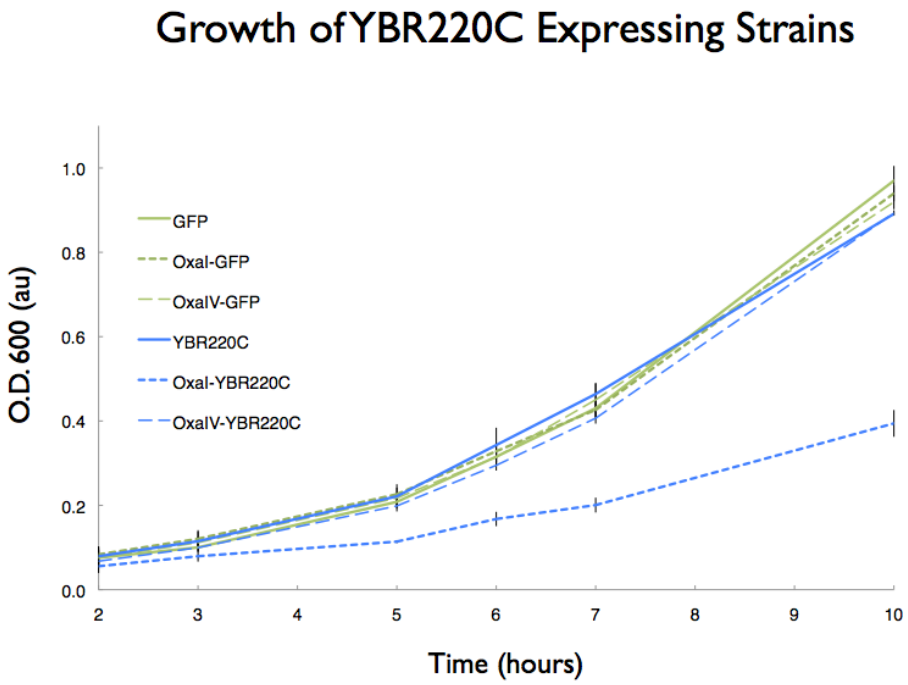

Figure 6.9. Overexpressed YBR220C can disrupt the the mitochondria when tagged with the OxaI tag. Strains expressing YBR220C (solid blue line), OxaI-tagged YBR220C (short dashed blue line) and OxaIV-tagged YBR220C (long dashed blue line) were grown in SD-Leu and OD_{600} measured periodically. Strains expressing GFP (solid green line), OxaI-tagged GFP (short dashed green line) and OxaIV-tagged GFP (long dashed green line) were grown as controls. Samples were run in triplicate and error bars represent standard deviations.

AT-1 reduces cytosolic levels of Acetyl-CoA. Intracellular AcCoA was extracted and LC-MS used to quantify AcCoA levels. Strains expressing a GFP control or the AT-1 transporter have approximately the same amounts of intracellular AcCoA (Figure 6.10A). Localizing the transporter to the mitochondria with the OxaI and F1 tags decreases total AcCoA levels. Cytoplasmic fractions were isolated to examine AcCoA levels in each relevant organelle. Cytoplasmic AcCoA levels decrease when the AT-1 transporter is expressed as compared to cells expressing only GFP (Figure 6.10B). Results from strains expressing F1-tagged AT-1 were variable, while OxaI-tagged AT-1 may confer decreased cytoplasmic AcCoA levels.

The yeast homologue, YBR220C requires different expression conditions than AT-1. Expression of a YBR220C-GFP fusion from the high-strength promoter pTdh3 leads to aggregation (Figure 6.4D-F). Additionally, OxaI-tagged YBR220C confers a decreased growth rate compared to control strains as well as OxaIV-tagged YBR220C (Figure 6.9). Interestingly, overexpression of YBR220C without modifications does not decrease growth rates, so we anticipate that optimization of the expression conditions for each fusion will result in minimally affected growth rates as observed with AT-1.

DISCUSSION

In order to direct a transporter to the mitochondria, we first needed to design some mitochondrial targeting tags. Several published studies on the characterization of mitochondrial targeting peptides [20-22] simplified tag design for this work. We chose the N-terminal sequences from known mitochondrial proteins cytochrome oxidase activity I (Oxa1) [21], cytochrome oxidase IV (OxaIV) [22], and ATPase F1 ß-subunit (F1) [22] to target proteins to the mitochondrial membrane. Using the TargetP program [20], we optimized the three tags for high targeting efficiency but short sequence, to reduce the chance of including a domain that would fold separately or disrupt folding for the targeted proteins. As longer tags gave a higher targeting efficiency, the designed tags have a range of sizes, from 28 to 80 residues, with a concomitant range of targeting efficiency (Figure 6.5). We fused these tags to GFP to confirm mitochondrial targeting via microscopy. The Oxa1 and OxaIV tags direct the majority of GFP into the mitochondria, as seen in Figure 6.6A and 6.6C. The tagged GFP co-localizes significantly with the MitoTracker dye. However, the F1 tag has a low efficiency, and minimal co-localization of F1-GFP and the MitoTracker dye is seen (Figure 6.6B). The majority of the F1-GFP appears to be cytoplasmic. The F1 tag may serve as a relevant negative control for future studies.

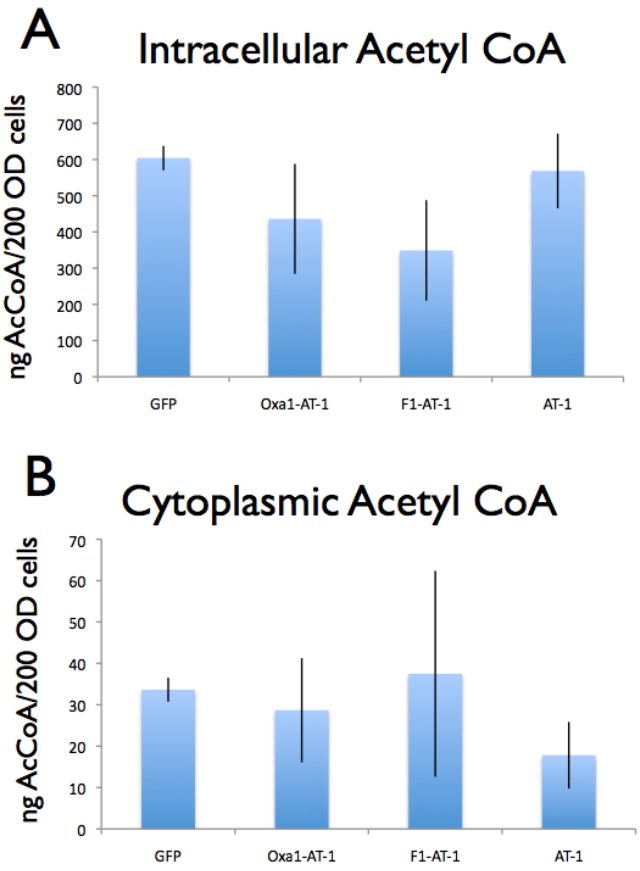

Figure 6.10. ER-targeted AT-1 decreases cytoplasmic Acetyl-CoA concentrations. Acetyl-CoA was extracted from 200 OD of stationary phase cells grown in SD-Leu. Concentrations were measured using GC-MS. Error bars represent standard deviations, n=3. A) Intracellular AcCoA was extracted from sonicated cells. B) Cytoplasmic AcCoA was extracted from osmotically lysed spheroplasts.

The heterologous AT-1 transporter is functional and properly localized in *S. cerevisiae*. In human cells, the AT-1 transporter localizes to the endoplasmic reticulum [1]. When expressed in yeast, it appears to also localize to the ER, as assessed by microscopy of AT-1-GFP fusions (Figure 6.4A-C). Analysis of cytoplasmic AcCoA concentrations shows a decrease in strains expressing AT-1 (Figure 6.9). This is likely due to the AT-1 transporting AcCoA from the cytoplasm into the ER. Additionally, the AT-1 transporter does not confer any growth rate defect when expressed in yeast (Figure 6.8). Together, these data show that AT-1 is a promising target for engineering

AcCoA concentrations within various organelles of *S. cerevisiae*.

The mitochondrial targeting tag OxaI is able to direct AT-1 to the mitochondria (Figure 6.7B). The F1 tag is not particularly effective, though some AT-1 is likely in the mitochondria (Figure 6.7A); the majority of the AT-1 is localized to the ER. Neither of these tagged transporters cause a growth defect (Figure 6.8). Unfortunately, our preliminary data suggests the mitochondrially targeted AT-1 does not improve cytoplasmic AcCoA levels (Figure 6.10B). The error for these experiments is high, which may be obscuring any improvements. We are currently refining the extraction method and expect to reduce the errors with further experimentation. We will also try several tag variations, including tags with an added transmembrane domain, in order to test whether orientation of the AT-1 transporter is reversed with the current tags. If the transporter is not oriented correctly, it will not efflux AcCoA from the mitochondria.

The homologous YBR220C has not been as amenable to study as the AT-1 transporter. Expression of a YBR220C-FLAG fusion under control of the low-strength pRev1 promoter is not detectable by western blot (Figure 6.3). Moreover, overexpression of a YBR220C-GFP fusion under the control of the high-strength pTdh3 promoter causes what structures that appear to be aggregates to form (Figure 6.4B). When directed into the mitochondria with the OxaI tag, these YBR220C aggregates cause a significant growth defect (Figure 6.9). Surprisingly, the OxaIV-targeted YBR220C did not cause a growth defect. We suspect that altering the promoter will improve growth rates upon overexpression of YBR220C. In Chapter 2, we showed that promoter strengths are important for proper function of the transporter Tpo1. Again, in Chapter 5, we found that promoter strength was critical for the essential translation initiation proteins. The high-strength pTdh3 promoter, which was developed for high expression levels of heterologous cytosolic enzymes [23], may not be appropriate for expression of native yeast proteins and particularly membrane proteins. Thus we will optimize YBR220C expression using its native promoter as well as other transporter promoters such as pTpo1 and pPdr5 (See Chapter 2). Optimizing the promoter will allow us to move forward with engineering YBR220C for AcCoA efflux from the mitochondria.

MATERIALS AND METHODS

Strains and Media

We used wild-type *Saccharomyces cerevisiae* strain BY4741 (*MAT*a *his3Δ1 leu2Δ0 met15Δ0 ura3Δ0*). Yeast without plasmids were grown in YPD (1% yeast extract, 2% peptone, 2% α-dextrose). Yeast with plasmids were grown in appropriate synthetic dropout media, eg SD-Leu (0.67% Yeast Nitrogen Base (Amresco), 2% α-Dextrose (BD Chemical), 0.2% amino acid mix without leucine from US Biological).

Plasmid Generation

Plasmids were generated using standard molecular biology cloning techniques and homologous recombination. Transformations were performed using the LiOAc protocol [17]. The AT-1 gene was cloned from MGC Human AT-1 sequence-verified cDNA from Thermo Scientific.

Westerns

Whole cell lysates were prepared by resuspending 2 mL of stationary phase cells in 200 uL Homogenization Buffer (50 mM Tris, pH 7.5, 1 mM EDTA, 1 mM BME, 10% glycerol, 17.4 ug/ml PMSF). Cells were lysed by vortexing 2 minutes with glass beads. Lysed cells were pelleted by spinning at 10,000 xg for 2 minutes. Supernatants were separated and pellets resuspended in 200 uL Homogenization buffer. 4X SDS running buffer (200 mM Tris, 4% ß-mercaptoethanol, 8% SDS, 0.04% bromophenol blue, 40% glycerol pH 6.8) was added and samples were boiled 95°C for 5 minutes. 10 uL of sample were run through a 15% SDS-PAGE gel. Proteins were transferred to PVDF membrane using a semi-dry blotting protocol. Membranes were blocked in 5% milk in TBST (50 mM Tris, 150 mM NaCl, 0.05% Tween-20, pH 7.5) for 30 minutes at room temperature. Membrane was incubated in a 1:7,000 dilution of mouse anti-FLAG antibody in TBST + 1% milk (Sigma) overnight, washed 3X 5 minutes with 10 mL TBST, then incubated 2 hours at room temperature in a 1:1000 dilution of HRP-conjugated goat anti-mouse antibody in TBST. Membranes were imaged using the SuperSignal West Pico Chemiluminescent substrate (Pierce) and Chemidoc Imager.

Confocal Microscopy

Confocal images were taken using a Leica SD600 confocal microscope with a Yokogawa CSU-X1 spinning disk head and a 100X, 1.4 n.a. oil immersion objective. Images were captured using Metamorph software from Molecular devices and 488 and 561 nm lasers. Mitochondria were stained using MitoTracker Red MXRos dye from Molecular Probes. Images were processed using ImageJ.

Immunofluorescence

Images were taken using an Andor Clara-Lite digital camera and a Nikon Ni-U upright microscope with a 100x, 1.45 n.a. plan apochromat oil immersion objective. Images were taken at room temperature. Fluorescence images were collected using a C-FL Endow GFP HYQ band pass filter and the Y-2E/C bandpass filter. Images were captured using the Nikon NIS Elements software. Images were processed using ImageJ.

Growth Curves

Single colonies were picked from the post-evolution plates into 5 mL SD-Leu media in culture tubes. Cultures were grown overnight to saturation at 30°C with 280 rpm shaking. Stationary phase cultures were diluted to an OD_{600} of 0.30-0.33 a.u. as measured with a Nanodrop 2000c, 10 mL dilute culture was aliquoted into screw-cap tubes. Each sample was run in triplicate. Screw-cap tubes were grown at 30°C with 280 rpm shaking and measurements were taken every hour with Genesys-20 spectrophotometer.

Acetyl CoA Measurement

Single colonies were innoculated into 12 mL SD-Leu media and grown at 30°C, 280 rpm shaking for 24 hours. 200 OD_{600} was pelletted and washed with 2 mL sterile H_2O. For whole-cell AcCoA measurments, pellets were resuspended in 1 mL 2 Methanol (Fisher): 2Acetonitrile (Fisher):1H_2O + 0.1% formic acid. Samples were sonicated for a total of 7 minutes with a cycle of 20” on, 40” off at 50% power. Samples were

centrifuged for 20 minutes at 5,000 rpm, 4°C. Supernatants were removed and vacuum centrifuged for 1 hour at 45°C to remove solvents. Method was adapted from [18].

For cytoplasmic AcCoA measurements, pellets were resuspended in 800 uL Buffer A (1.2 M sorbitol (Fisher), 50 mM K_2PO_4 (Fisher), 1 mM EDTA (Fisher), 1 mM KCl(Spectrum), 10 mM DTT (OmniPur), pH 7.5). 1 mg Zymolyase (Zymo Research) was added and solution was incubated for 1 hour at 30°C. Samples were centrifuged 4,000 xg for 5 minutes at RT. Spheroplasts were resuspended in 1 mL Buffer B (1.2 M Sorbitol, 5 mM MES (Fisher), 1 mM EDTA, 1 mM KCl, pH 5.5). Spheroplasts were again centrifuged and resuspended in 200 uL Buffer C (5 mM MES, 1 mM EDTA, 1 mM KCl, pH 5.5). Lysed cells were spun at 20,000 xg for 20 minutes at 4°C. Spheroplast method was adapted from [19]. Supernatant was removed and 2V Methanol and 2V Acetonitrile was added. Precipitates were removed via centrifugation at 5,000 rpm for 20 minutes at 4°C. Supernatant was removed and vacuum centrifuged for 1 hour at 45°C to remove solvents.

Analysis of AcCoA was conducted with a reverse-phase C18 column using a Shimadzu LC-MS system. Mobile phase was 20 mM ammonium acetate in water (Solvent A), and 20 mM ammonium acetate in methanol (Solvent B). separated with the following gradient: 10% to 22.5% B for 15 min, 22.5% to 100% B for 5 min, 100% to 10% B for 0.1 min, held at 10% B for 24.9 min. A flow rate of 0.14 mL/min was used throughout. A 1 mg/mL AcCoA standard (Sigma) in 50% methanol: 50% water was diluted for the standard curve. Analysis method was adapted from [18].

Table 6.1. Strains and Plasmids used in this study

Strain	Parent	Genotype	Reference
BY4741		*MATa his3Δ1 leu2Δ0 met15Δ0 ura3Δ0*	

Plasmid	Promoter	Insert	Marker	Reference
pSD476	pRev1	YBR220C	Leu2	This Study
pSD477	pTdh3	YBR220C-link-Emerald	Leu2	This Study
pSD478	pTdh3	YBR220C	Leu2	This Study
pSD508	pRev1	AT-1	Leu2	This Study
pSD509	pTdh3	AT-1	Leu2	This Study
pSD510	pRev1	AT-1-link-Emerald	Leu2	This Study
pSD511	pTdh3	AT1-link-Emerald	Leu2	This Study
pSD527	pRev1	AT-1-4XFLAG	Leu2	This Study
pSD528	pTdh3	AT-1-4XFLAG	Leu2	This Study
pSD529	pRev1	YBR220C-4XFLAG	Leu2	This Study
pSD616	pRev1	Emerald-link-YBR220C	Leu2	This Study
pSD617	pTdh3	Emerald-link-YBR220C	Leu2	This Study
pSD619	pTdh3	F1tag-Emerald-link-AT-1	Leu2	This Study
pSD620	pTdh3	Oxa1tag-Emerald	Leu2	This Study
pSD621	pTdh3	F1tag-Emerald	Leu2	This Study
pSD627	pTdh3	OxaIVtag-Emerald	Leu2	This Study
pSD635	pTdh3	Oxa1tag-AT-1	Leu2	This Study
pSD636	pTdh3	F1tag-AT-1	Leu2	This Study

pSD638	pTdh3	Oxa1tag-AT-1-4XFLAG	Leu2	This Study
pSD639	pTdh3	F1tag-AT-1-4XFLAG	Leu2	This Study
pSD668	pTdh3	Oxa1tag-mKate	Ura3	This Study
pSD669	pTdh3	F1tag-mKate	Leu2	This Study
pSD670	pTdh3	OxaIVtag-mKate	Leu2	This Study
pSD671	pTdh3	OxaItag-YBR220C	Leu2	This Study
pSD672	pTdh3	OxaIVtag-YBR220C	Leu2	This Study

Table 6.2. Mitochondrial Targeting Tags
OxaI: 60 amino acids
MFKLTSRLVTSRFAASSRLATARTIVLPRPHPSWISFQAKRFNSTGPNANDVSEIQTQLP

F1: 28 amino acids
MVLPRLYTATSRAAFKAAKQSAPLLSTS

OxaIV: 80 amino acids
MLSLRQSIRFFKPATRTLCSSRYLLQQKPVVKTAQNLAEVNGPETLIGPGAKEGTVPTD
LDQETGLARLELLGKLEGIDV

REFERENCES

1. Jonas MC, Pehar M, Puglielli L. AT-1 is the ER membrane acetyl-CoA transporter and is essential for cell viability. J Cell Sci. 2010, 123: 3378-88.

2. Shiba Y, Paradise EM, Kirby J, Ro DK, Keasling JD. Engineering of the pyruvate dehydrogenase bypass in Saccharomyces cerevisiae for the high-level production of isoprenoids. Metab Eng. 2007, 9(2):160-68.

3. Chen Y, Daviet L, Schalk M, Siewers V, Nielsen J. Establishing a platform cell factory through engineering of yeast acetyl-CoA metabolism. Metab Eng. 2013, 15:48-54.

4. Koopman F, Beekwilder J, Cimi B, van Houwelingen A, Hall RD, Bosch D, van Maris AJ, Pronk JT, Daran JM. De novo production of the flavenoid naringenin in engineered Saccharomyces cerevisiae. Microb Cell Fact. 2012, 11:155-160.

5. Dyer J, Chapital D, Juan J, Mullen R, Pepperman A. Metabolic engineering of Saccharomyces cerevisiae for production of novel lipid compounds. App Microbiol Biotechnol. 2002, 59(2-3):224-230.

6. Veen M, Lang C. Production of lipid compounds in the yeast Saccharomyces cerevisiae. App Microbiol Biotechnol. 2004, 63(6):635-46.

7. Krivorucho A, Serrano-Amatriain C, Chen Y, Siewers V, Nielsen J. Improving biobutanol production in engineered Saccharomyces cerevisiae by manipulation of

acetyl-CoA metabolism. J Ind Microbiol Biotechnol. 2013, 40:1051-56.

8. Steen E, Chan R, Prasad N, Myers S, Petzold CJ, Redding A, Ouellet M, Keasling JD. Metabolic engineering of Saccharomyces cerevisiae for the production of n-butanol. Microb Cell Fact. 2008, 7:36.

9. Lian J, Si T, Nair NU, Zhao H. Design and construction of acetyl-CoA overproducing Saccharomyces cerevisiae strains. Metab Eng. 2014, 24:139-49.

10. Chen Y, Siewers V, Nielsen J. (2012) Profiling of cytosolic and peroxisomal acetyl-CoA metabolism in Saccharomyces cerevisiae. PLOS One, 7(8): e42475.

11. Matsuda F, Furusawa C, Kondo T, Ishii J, Shimizu H, Kondo A. Engineering strategy of yeast metabolism for higher alcohol production. Microbial Cell Fact. 2011, 10:70.

12. Lee YJ, Jang JW, Kim J, Maeng PJ. TCA cycle-independent acetate metabolism via the glyoxylate cycle in Saccharomyces cerevisiae. Yeast. 2011, 28:153-166.

13. Kunze M, Pracharoenwattana I, Smith SM, Hartig A. A central role for the peroxisomal membrane in glyoxylate cycle function. Biochim Biophys Acta. 2006, 1763:1441-52.

14. Rottensteiner H, Theodoulou FL. The ins and outs of peroxisomes: Co-ordination of membrane transport and peroxisomal metabolism. BBA Molecular Cell Research. 2006, 1763(12):1527-40.

15. van Roermund CWT, Hettema EH, van den Berg M, Tabak HF, Wanders RJA. Molecular characterization of carnitine-dependent transport of acetyl-CoA from peroxisomes to mitochondria in Saccharomyces cerevisiae and identification of a plasma membrane carnitine transporter, Agp2p. EMBO J. 1999, 18(21):5843-52.

16. Kanamori A, Nakayama J, Fukuda MN, Stallcup WB, Sasaki K, Fukuda M, Hirabayashi Y. Expression cloning and characterization of a cDNA encoding a novel membrane protein required for the formation of O-acetylated ganglioside: a putative acetyl-CoA transporter. Proc Natl Acad Sci USA. 1997, 94: 2897-902.

17. Geitz D, St Jean A, Woods RA, Schiestl RH. Improved method for high efficiency transformation of intact yeast cells. Nucleic Acids Res. 1992, 20(6):1425.

18. Yuzawa S, Chiba N, Katz L, Keasling J. Construction of a part of a 3-hydroxypropionate cycle for heterologous polyketide biosynthesis in Escherichia coli. Biochemistry. 2012, 51:9779-81.

19. Distel B, Kragt A. Purification of yeast peroxisomes. Methods Mol Biol. 2006, 312:21-26.

20. Emanuelsson O, Brunak S, von Hejne G, Nielsen H. Locating proteins in the cell using TargetP, SignalP, and related tols. Nature Protocol. 2007, 2:953-71.

21. Herrmann JM, Neupert W, Stuart RA. Insertion into the mitochondrial inner membrane of a polytopic protein, the nuclear-encoded Oxa1p. EMBO J. 1997, 16(9): 2217-26.

22. vonHeijne G, Steppuhn J, Herrmann RG. Domain structure of mitochondrial and chloroplast targeting peptides. Eur J Biochem. 1989, 180:535-45.

23. Lee ME, Aswani A, Han AS, Tomlin CJ, Dueber JE. Expression level optimization of a multi-enzyme pathway in the absence of a high-throughput assay. Nucleic Acids Res. 2013, 41(22):10668-10678.

24. Kelley LA, Mezulis S, Yates CM, Wass MN, Sternberg MJE. The Phyre2 web portal for protein modeling, prediction and analysis. Nat Protocol. 2015, 10:845-858.

Conclusions

The potential for manipulating cellular small-molecule transport

As more transporters are discovered for small molecules such as alkanes [1], it becomes clear how crucial transporters are to biotechnology. Transporters are essential for both native cell processes such ethanol production and engineered processes such as butanol production. Transporters drive production by importing sugars for energy [2], pathway substrates [3], and even water [4] into the cell. Excreting products to the extracellular space removes toxic products from the cell and simplifies downstream extraction processes.

A common problem with using transporters is that expression level is a critical parameter. In Chapter 2, we showed that the native Tpo1 promoter gives the optimal expression level, even in the presence of toxic levels of MCFAs. Low-strength promoters expressed insufficient Tpo1 levels to efflux the MCFAs while high-strength promoters expressed so much Tpo1 that the transporter itself became toxic. Proper expression of the native acetyl-CoA transporter YBR220C in *S. cerevisiae* was also dependent on the promoter, as showed in Chapter 6. Other transporters, such as AcrB in *E. coli* [5], have the same optimization issue. Since negative results are not often reported, it is likely that many other groups struggle with optimizing expression levels of transporters.

In moving forward with transport-related projects in *S. cerevisiae*, developing a library of transporter-specific promoters would be beneficial. Since the membrane area is significantly smaller than the cytoplasm and already crowded with other membrane proteins, expression levels need to be lower than that of cytoplasmic enzymes. Overexpressed transporters can oversaturate the membrane, disrupting membrane fluidity and function. Additionally, many transporters are constitutively active, using large amounts of ATP or depleting the proton gradient. This basal activity increases energy demand on the cell and may reduce growth rate. Having a suite of constitutive promoters tailored to the parameters of transporter proteins would simplify implementation of heterologous transporters, as well as streamline optimization of native transporters for novel applications.

Protein engineering perspectives

The *Saccharomyces cerevisiae* transporter of polyamines (Tpo1) is known for its activity on polyamines such as spermine and spermidine, and our work with this transporter indicates it would make a particularly advantageous engineering target. We characterized Tpo1 for its activity on medium-chain fatty acids (MCFAs), which are promising potential biofuels. Surprisingly, we found that distinct sets of binding residues are utilized for MCFAs as compared to polyamines. These dual sets of substrate-binding residues in Tpo1 are interesting from a protein design perspective.

Currently, random non-active site mutations generated by directed evolution are often more effective than rational design [6]. However, these random mutations are limited to small steps in the energy landscape [7]. On the other hand, well-designed mutations can confer exactly the desired phenotype [8-9]. As modeling and computer

design technology improve [10], we can better target mutations for effective protein engineering. Developing a rigorous understanding of how proteins interact with small molecules and other proteins at the amino acid level could help inform computer models and enable the design of novel and desired features.

As a rational design challenge, it would be intriguing to attempt to engineer Tpo1 to bind new substrates while maintaining activity on a subset of native substrates. For example, it might be useful to engineer specificity for alcohol substrates using the fatty acid-binding residues, while maintaining native polyamine activity. Such efforts, if successful, would be a step toward more complex, multi-functional protein designs and would provide elegant solutions for effluxing biofuels and toxic feedstock impurities from production cells.

REFERENCES

1. Grant C, Deszcz D, Wei YC, Martínez-Torres RJ, Morris P, Folliard T, Sreenivasan R, Ward J, Dalby P, Woodley JM, Baganz F. Identification and use of an alkane transporter plug-in for applications in biocatalysis and whole-cell biosensing of alkanes. Sci Rep. 2014, 4:5844.

2. Celenza JL, Marshall-Carlson L, Carlson M. The yeast SNF3 gene encodes a glucose transporter homologous to the mammalian protein. Proc Natl Acad Sci USA. 1988, 85(7):2130–34.

3. Penrod JT, Mace CC, Roth JR. A pH-sensitive function and phenotype: evidence that EutH facilitates diffusion of uncharged ethanolamine in Salmonella enterica. J Bacteriol. 2004, 186(20):6885–90.

4. Day RE, Kitchen P, Owen DS, Bland C, Marshall L, Conner AC, Bill RM, Conner MT. Human aquaporins: regulators of transcellular water flow. Biochim Biophys Acta. 2014, 1840(5):1492–506.

5. Fisher MA, Boyarskiy S, Yamada MR, Kong N, Bauer S, Tullman-Ercek D. Enhancing tolerance to short-chain alcohols by engineering the Escherichia coli AcrB efflux pump to secrete the non-native substrate n-butanol. ACS Synth Biol. 2013, 3(1): 348-54.

6. Giger L, Caner S, Obexer R, Kast P, Baker D, Ban N, Hilvert D. Evolution of a designed retro-aldolase leads to complete active site remodeling. Nat Chem Biol. 2013, 9(8):494-98.

7. Romero PA, Arnold FH. Exploring protein fitness landscapes by directed evolution. Nat Rev Mol Cell Biol. 2009, 10(12):886-76.

8. Graf L, Craik CS, Patthy A, Roczniak S, Fletterick RJ, Rutter WJ. Selective alteration of substrate specificity by replacement of aspartic acid-189 with lysine in the binding pocket of trypsin. Biochemistry.1987, 26:2616–23.

9. Rana S, Pozzi N, Pelc LA, Di Cera E. Redesigning allosteric activation in an enzyme. Proc Natl Acad Sci USA. 2011, 108(13):5221-25.

10. Rajagopalan S, Wang C, Yu K, Kuzin AP, Richter F, Lew S, Miklos AE, Matthews ML, Seetharaman J, Su M, Hunt JF, Cravatt BF, Baker D. Design of activated serine-containing catalytic triads with atomic level accuracy. Nat Chem Biol. 2014, 10(5): 386-91.